# System Dynamics and Agent-Based Models Applied to Public Health Problems

by

Sen Lin

A dissertation submitted to The Johns Hopkins University in conformity with the requirements for the degree of Doctor of Philosophy.

Baltimore, Maryland

February, 2017

# Abstract

During the past decades, there has been a growing body of research on the development of new methodologies in system sciences in public health. While systems thinking is prevalent in the practice of public health, there is a need for tools to quantify the multidimensional and multidisciplinary aspects of such thinking. In this thesis, we focus on two system science methods: Agent-Based Modeling (ABM) and System Dynamics (SD).

We begin with an ABM to simulate the effects of an urban food desert environment on school-aged children. The data that was used to inform this model is based on children in low-income neighborhoods of Baltimore City. The baseline model was used to predict changes in body mass index due to eating behaviors of simulated children interacting with their food environment. The model was then used as a virtual social laboratory by introducing interventions into the environment and assessing their effects on child behaviors and weight gains.

For our second application of systems science, we developed an SD model to study the stability of community functioning (CF) after a natural disaster. We define CF

ABSTRACT

as a measure of a broad range of community activities in providing services to its residents. We studied the dynamic response of CF post-disaster from two different aspects: resilience, which indicates the speed of recovery after event, and resistance, which measures the degree to which a community can continue to function during the event. Key components that support or reduce CF were identified and were quantified as variables in a system of ordinary differential equations. The data for the model was obtained at the county level for 3143 United States counties, and the model results for resilience and resistance ratings were presented in a series of maps so that the regional patterns of our findings could be visualized.

Finally, our last application was an SD model applied in a different public health context: an analysis of the mechanisms underlying the health system in Afghanistan between 2010 and 2012. We were interested in the Pay-for-Performance (P4P) intervention, in which relatively small health facilities were given bonus payments as a reward for year-to-year improvements in quality and quantity of health services. A recently published data analysis of the P4P intervention showed no improvement in health services. By working with some of the researchers who participated in this intervention, we were able to develop causal loops in the system associated with some of the key interactions that were generated within the health facilities. We then synthesized these loops into a model of differential equations with delays. We were able to generate several scenarios that indicate that the failure of P4P may be caused by poor implementation processes and gaming within the system.

ABSTRACT

In summary, we demonstrate how ABM and SD can naturally embody systems thinking into a quantitative form, and can produce a wide array of numerical and visual results that capture the complex processes that characterize public health.

Primary Reader: Professor Takeru Igusa

Secondary Reader: Professor Benjamin Schafer and Professor James Guest

# Acknowledgments

It has been my privilege to work with two excellent professors at Hopkins and I would like to take this opportunity to express my sincere gratitude: Prof. James K. Guest encouraged me to build a solid and broad understanding on this research field and industry; Prof. Takeru Igusa gave me enormous support on my education, research and life. Their deep knowledge and great enthusiasm will keep inspiring me after my graduation.

I also would like to thank Prof. Robert A. Dalrymple, Judith Mitrani-Reiser, Benjamin W. Schafer, Sauleh Siddiqui, and Lori Graham-Brady, from the Whiting School of Engineering, and Jonathan M. Links, Norma Kanarek, Olakunle O. Alonge, Brian S. Schwartz, and David Peters from the Bloomberg School of Public Health, Johns Hopkins University, for the guidance and encouragement that they gave me during the past years, Dr. Longyu Zhao in the Department of Materials Science & Engineering for his help in conducting experiments on the fluid diode research, my lab-mates Gary Lin, Xilei Zhao and Zhaohao Fu for their inspiring discussion, with me about research, and Prof. Zhenyu Liu and Dr. Yongbo Deng in CIOMP of the

Chinese Academy of Sciences for their support, and valuable insights at the early stages of my research education.

Last, but not least, I would like to thank my parents for their continuous encouragement about my education.

Research reported in Chapter 2 was supported by the Global Obesity Prevention Center (GOPC) at Johns Hopkins and the Eunice Kennedy Shriver National Institute of Child Health and Human Development (NICHD) and the Office of the Director (OD) of the National Institutes of Health under award number U54HD070725. The content is solely the responsibility of the author and does not necessarily represent the official views of the National Institutes of Health.

Research reported in Chapter 3 was supported by the Centers for Disease Control and Prevention (CDC) through grant 5P01TP000288 and research contract 200-2014-60654. The content is solely the responsibility of the authors and does not necessarily represent the official views of the Centers for Disease Control and Prevention.

# Dedication

To Prof. Tak Igusa, who made everything possible.

# Contents

# List of Tables

# List of Figures

# Chapter 1

# Introduction

## 1.1 Motivation and Background

The mission and scope of public health has been evolving at an ever increasing pace. Traditionally, public health was considered as a discipline that studies the control of contagious diseases by means of sanitation and vaccination.[1] Nowadays, public health studies large-scale solutions to promote the welfare of communities and populations by using multidisciplinary approaches, involving applied science, education, economics, social sciences, and management.[1] For example, while a physician would work on medical methods to treat obesity patients, public health researchers would explore the links between obesity and food environment, social network influences and inactivity, and then propose systematic strategies to reduce the prevalence of obesity.

By nature, many public health problems can be characterized as dynamic complex systems. The methodologies of system sciences are well suited to study such problems, and have recently been gaining acceptance in academics and in practice. System science is an interdisciplinary field that studies integrated components with the following properties:[2]

1. The components are heterogeneous.

2. Multiple patterns of interaction exist among the components.

3. High-level emergent features are generated from these components and their interactions; these emergent features cannot be found by separate analyses of the individual components.

4. Behaviors of an isolated component are relatively straightforward to study, while the emergent behaviors may be complex.

In this thesis we demonstrate the applications of two modeling methods of system science, System Dynamics (SD) and Agent Based Modeling (ABM), on the analysis of several public health systems. In the remainder of this chapter, we briefly summarize these methods.

## 1.2 System Dynamics (SD)

There are three types of components involved in SD models and they are explained as below.

**Stock** Stocks are continuous variables that represent the time-dependent state of a system. Stocks change with respect to time or other independent variables, and their rates of change are influenced by other components of the system.

**Flow** Stocks are often described as quantities of water in tanks; in this analogy, flows are the movements of this water through pipes connecting these tanks. Mathematically, flows are the time derivatives of stocks that result in time-varying stocks.

**Causal loop** The value of a flow can be affected by other variables in the system, and these relationships are indicated by causal arrows. If the affecting variable is a stock that is the origin or destination of the flow, then the corresponding causal arrow and associated flow form a feedback loop. There is an important distinction between flow and feedback loop: flow involves a depletion of the originating stock and an accumulation of the destination stock, while a feedback loop involves a connected sequence of influences between variables that may involve stocks, flows and other interacting variables.

SD models are suitable to solve problems with these properties:

1. Each individual component is relatively simple to understand and quantify.
2. The system behaviors are determined by interactions of component behaviors.
3. Behaviors of the components are dynamic, with changes with respect to time or other independent variable.

## 1.3 Agent Based Modeling (ABM)

Agent based modeling (ABM) is a simulation technique that builds the model from bottom up by capturing the properties and behaviors of abstract entities known as "agents."[3] Similar to the concept of "class" in many object-oriented programming languages, each agent in an ABM possesses properties and behaviors, and can autonomously act according to the environment and other agents in the model. In many ABMs, the interactions between agents generate emergent behaviors that can only be described at the system level. No single agent exhibits these emergent behaviors. An example would be the flock formation of birds,[4] in which the bird flock exhibits properties as if it is a self-governing organism. Usually the emergent behaviors are difficult to study directly as compared with individual behaviors of a single agent; ABMs are well-suited to analyze these types of complex systems.

An agent in an ABM is a simplification of its counterpart in the real world. If given unlimited computation resources and data that can be used to describe agent behaviors no simplification would be necessary. While the simplification should be sufficient to make the model computationally viable, there is always a risk of over-simplification, in which we lose important properties or behaviors that the real world counterpart possesses and an accurate model requires.

## 1.4 Thesis overview

In Chapter 2 we develop an agent-based model to simulate the effects of the food environment on childhood obesity in a low-income urban area. In Chapter 3 we study the factors affecting community resilience and develop a model to predict the time-course of community functioning in response to a hypothetical event for every county in the United States. In Chapter 4 we develop an SD model to study a Pay-For-Performance intervention for improving health care at the facility level in Afghanistan and to explain why expected outcomes did not occur and suggest how it can be improved.

# Chapter 2

# Agent-Based Models for Childhood Obesity Simulation

## Notation

**ABM** Agent Based Model

**BLIFE** Baltimore Low-Income Food Environment model

**BM** Body Mass

**BMI** Body Mass Index

**CDC** Centers for Disease Control and Prevention

**CO** Carryout store

**CS** Corner Store

**EI** Energy Intake

**EX** Energy Expenditure

**GIS** Geographic Information System

**GUI** Graphic User Interface

**SD** System Dynamics

**SU** Supermarket

**UML** Unified Modeling Language

## 2.1 Introduction

Childhood obesity has increased dramatically in the United States over the past three decades.[5–8] Although overweight children from all backgrounds are more likely to become obese in adulthood compared to their thinner counterparts,[9,10] this pattern is most pronounced in racial/ethnic minority groups such as African Americans and groups of lower socioeconomic status.[11,12] The etiology of the disparities in childhood obesity is complex and multi-faceted, but research indicates that environmental factors including the "food environment" may shape eating preferences particularly in low-income and minority urban communities. In these communities, the "food environment" may contain fewer locations that offer healthy food and beverages leading to fewer healthy choices for both adults and children.[13]

An increasing number of studies aim to understand the impact of the food environments on "child dietary behaviors or dietary patterns," meaning the choices children make about what to eat and drink throughout the course of a day.[14] While a large body of evidence demonstrates the impact of the home and school environments on child dietary behaviors,[15–17] much less is known about the impact of after-school food environments. Food and beverage choices made outside of school are important to assess as they may contribute to excess calories, particularly in urban low-income neighborhoods where high-calorie, energy-dense foods are readily available.[18] There have also been efforts to characterize child dietary behaviors in a given neighborhood food environment,[14,19–22] but these types of traditional epidemiological studies are limited in their ability to account for the complex factors that drive dietary behaviors.[23]

Computational modeling approaches have previously been used to study the obesity epidemic. Fallah-Fini et al[24] developed a system dynamics (SD) model to estimate the energy gap for each gender-race-BMI group, and found out that intervention should be specially designed for each sub-population. Finegood et al used simplified versions of the Foresight Obesity System Map to build SD models.[25] Other researches include.[26,27] However, SD based models lack the ability to assess the interaction between food environment and people.

ABM has found its applications in game theory,[28,29] social science,[30–32] computational economics,[33] urban planning,[34,35] and public health.[36] ABMs simulate the complex behavior of a given system composed of agents with relatively simple properties and behavioral rules. Agents respond to other agents and the modeled environment, and this autonomous and dynamic nature allows for the study of emergent outcomes or higher-order properties (i.e., properties that arise from agents' interactions).

Just as environment shapes human behavior, the obesogenic environment shapes obesity prevalence. Edwards and Clarke demonstrated that the important obesogenic variables are age, gender, deprivation, ethnicity, qualification, and tenure.[37] It is also essential to incorporate spatial heterogeneity in obesity ABM, since the food environment, physical activities, and outcomes of intervention policies are all determined largely by geographical information. The ABM built by Widener, et al[38] simulated effects of multiple policies on healthy food purchasing of low-income households in Buffalo, NY. This study confirms that it is important to consider spatial as well as non-spatial factors when analyzing the impact of healthy food availability on purchasing behaviors in low-income neighborhoods.

The goal of this chapter is to describe the design and structure of an agent-based model (ABM) that simulates the after-school dietary behaviors of children aged 10 to 14 years old and their obesity risk in an urban food desert environment. The developed ABM can be employed to conduct experiments in a controlled environment to better understand and evaluate the dynamic interactions of child food-foraging among various food sources encountered after school hours.

## 2.2 Modeling obesity

### 2.2.1 Overview

The Baltimore Low Income Food Environment (BLIFE) 1.0 model was built using the NetLogo platform. NetLogo is a general-purpose coding language with an Integrated Development Environment (IDE) for agent based modeling.[39] In the BLIFE ABM, agents move and interact with the food environment, which is modeled with GIS (Geographic Information System). Agents representing children are programmed to interact with GIS-specified streets, homes, schools, recreation centers, and food sources. These agents travel the streets between their homes and schools, and they visit recreation centers and food sources mainly according to proximity to their commuting paths. Each agent contains a set of sub-models that compute weight changes associated with caloric intake and energy expenditure. Height growth trends are simulated by tracking the CDC growth charts[40] and assume continued growth along the starting trajectory. The ABM also incorporates the effects of quality (varieties of different healthy foods) of each food source in the environment on agents' outcomes. The energy intake of each agent is affected by the quality of the food at the food source. For example, increasing the quality of the food source may result in healthier food consumption, which in turn reflected by reduced caloric intake.

The current version of the ABM is a relatively small-size model. The detailed information concerning size and scale is available in Table 2.1.

**Table 2.1:** Size and scale of BLIFE AMB 1.0

| Item | Number Contained within the Model |
|---:|---|
| Number of children | 200 (106 female and 94 male) |
| Number of food sources | 313 (CO: 94; CS: 274; SU: 17) |
| Number of schools | 51 |
| Number of recreation centers | 7 |
| Spatial resolution | 121 by 81 patches |
| Number of iterations | 1825 (days; total 5 years) |

### 2.2.2 Agent mode of child

Each agent is an autonomous individual or collective entity that can act and interact with the other agents. Child agents are considered to be simulated humans that have memory and exhibit some aspects of intelligent behaviors. The UML (Unified Modeling Language) diagram of a child agent is shown in Figure 2.1.

#### 2.2.2.1 State variables

A list of state variables is shown in Figure 2.1. The model uses baseline data collected from a sample of Baltimore City youth 10-14 years old in 2013-2014.[41] At the beginning of the simulation, all of the properties of the child agents are set to the status (same height, weight, age and gender) of the Baltimore City youth at the initial point of the survey. To protect the identities of the youths, the ages were

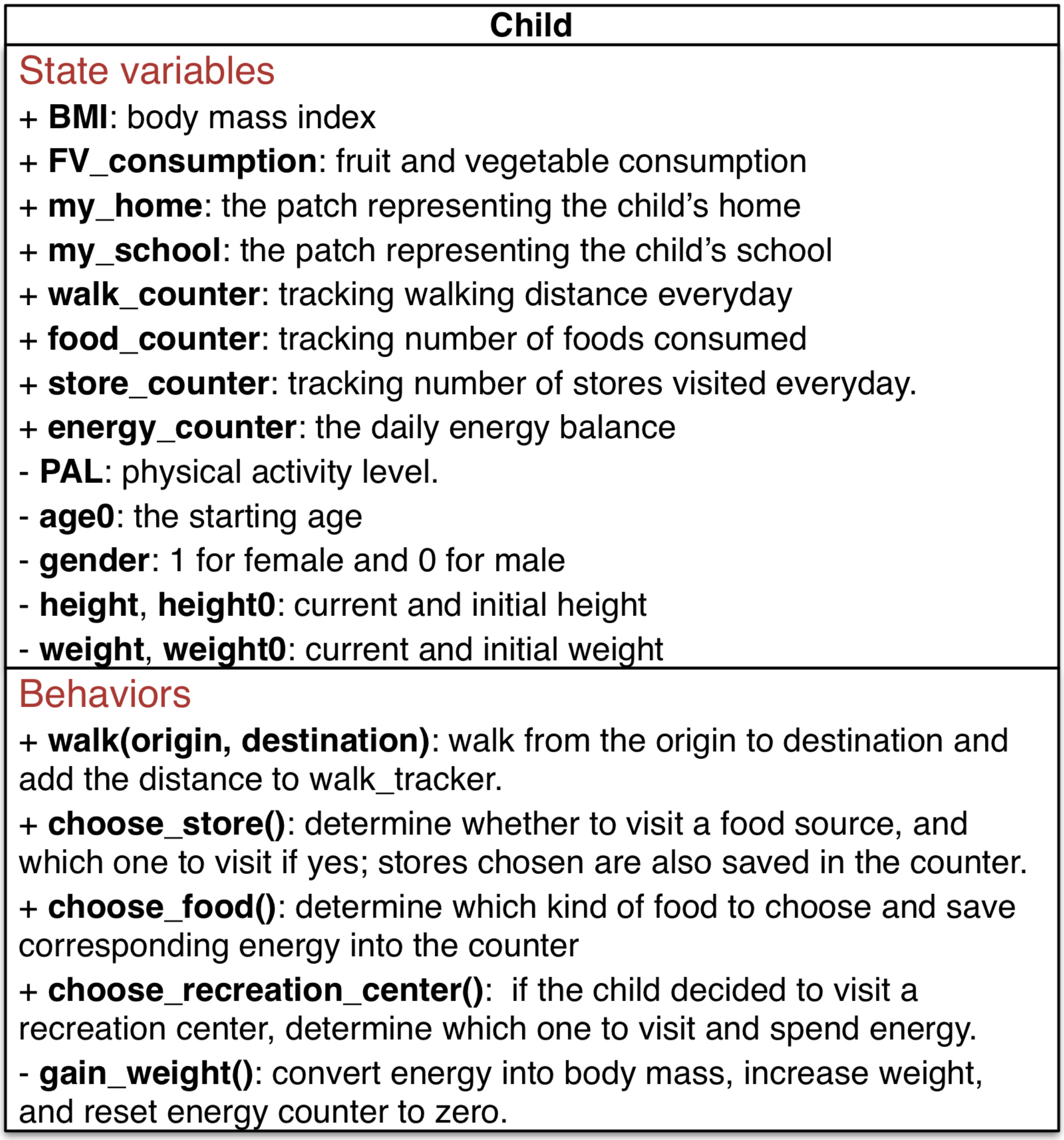


**Figure 2.1:** UML diagram of a child agent

rounded to years, and the home locations were randomly generated. Schools were assigned according to the placement of the randomly generated home locations with respect to the school catchment regions.

#### 2.2.2.2 Daily activities

The model simulates obesity iteratively, in which a cycle is one simulated day. Each day, the child agents walk from home to their respective schools. On the way back home, they decide whether or not to stop at one or more food sources and/or recreation centers according to their preference parameters. These parameters, measured by the survey of Baltimore City youth and de-identified as noted in the end of Section 2.2.2.1, are shown in Figure 2.2. At the beginning of each day, the children reset their counters of walking distance and calorie intake to zero and proceed to gain weight and height cumulatively until the end of the day.

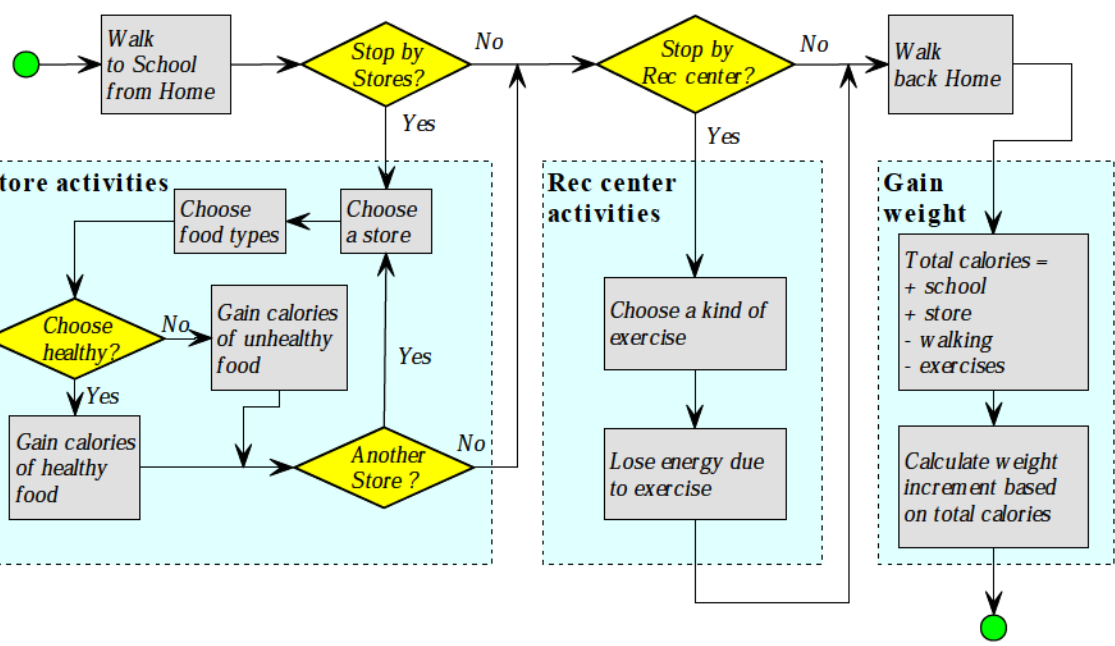


**Figure 2.2:** Diagram of a child's daily activities

#### 2.2.2.3 Behavioral rules

The location of the agent's school is based on age and school catchment. The model assumes that children only attend schools within walking distance (0.5 mile) of their homes. In the current version of the ABM children attend schools of the same type. Due to lack of data on recreation center visits, we assume that all children go to a recreation center with the same constant probability (20%). If a child decides to visit a recreation center, then he or she will choose the one closest to their home.

Agents select a food source based on proximity and preferences that were collected through child interviews, including a food-frequency questionnaire and child-impact questionnaire.[41] We used these data to calculate preference factors for each food source type for each agent. Based on the preference factors and proximity, each agent gets a list of food sources to visit. Foods options at each food source are scored based upon food availability, price, training, and promotion. The child agent decides what to eat by calculating a score for each healthy or unhealthy option and then chooses the items that receive the most points.

### 2.2.3 Patch model of the environment

The simulation region is uniformly discretized as a grid. In the context of NetLogo, each rectangle in the grid is called a patch, which is identified by its horizontal and vertical coordinates. As for child agents, patches also have individual memory and can make decisions; the only difference is that patches do not move. Some spatial functions have been pre-defined for patches in NetLogo, including identification of neighbors (adjacent patches), smoothing a variable of all patches over neighbors, and searching for movable agents currently located on a specific patch. These features make patches inherently suitable for modeling geographic or environmental agents. In this paper, all streets and buildings (including stores, homes, schools, and recreation centers) are modeled as patches. Figure 2.3 provides an overview of all the environment entities.

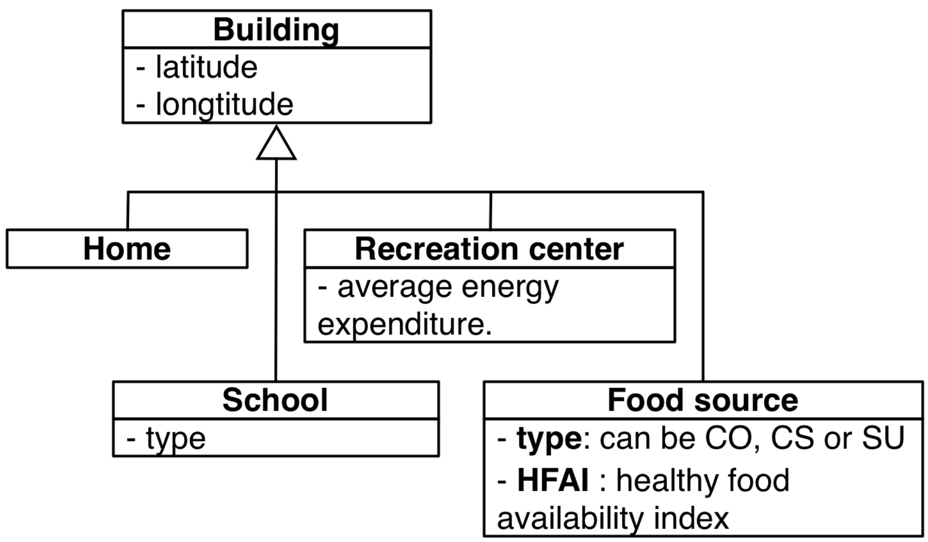


**Figure 2.3:** UML diagram of schools, homes, recreation centers and food sources

Schools are geo-located based on data provided by the Center for a Livable Future at the Johns Hopkins Bloomberg School of Public Health. Latitude and longitude of schools can be obtained from their street addresses, and then they are mapped to patch coordinates to integrate them into the model environment. In school, each child agent consumes the standard meal plan provided by Baltimore City Public Schools and spends a fixed amount of energy.

The model places the child agent homes on the grid based upon their actual street address. Children's eating habits at home are strongly affected by their parents and the household food supply. However, in this version of the model, we did not incorporate parents. For the purpose of simplicity, we assume the amount of energy intake at home is also fixed. On the way back home from school or a food source, the child agent may decide to stop by a recreation center and engage in physical activity. We assume no calorie intake in recreation centers. Energy expenditures of both walking and exercise at the recreation centers are considered.

Food sources are categorized as Carryouts (CO), Corner Stores (CS), and Supermarkets (SU). In Baltimore City, the primary local sources of food are corner stores and carryouts, which are predominantly small, family-owned businesses. These food outlets are a common source of calories associated with unhealthy foods, in which most products sold are typically high in fat, salt, and sugar.[42–44] Corner stores and supermarkets are assigned a base healthy food availability index score, based on Baltimore neighborhood in-store assessments.[45] Corner stores and carryout restaurants are also characterized by level of infrastructure (e.g., availability of a produce refrigerator), level of training in selection, promotion and preparation of healthy foods, and pricing of these foods. Locations of all food sources are specified by latitude and longitude. During initialization of the model, NetLogo determines the patch corresponding to each food source and creates patch agents with properties associated with the food source.

Geographic information on the location of roads is imported into NetLogo from GIS shape files. NetLogo then translates the location of each road into a grid of patches. Each patch has a binary mobility variable which is set to 1 if a road intersects the patch and 0 otherwise. Agents can find the locations of the roads by examining the mobility variable at each patch. At the beginning of the simulation, prior to the first simulated day, the shortest paths connecting the child agents' homes, schools, stores, and recreation centers are calculated and stored so that the ABM can reuse this information during the simulation of daily activities.

### 2.2.4 Modeling child agent growth

We cannot calculate the total calories consumed during the whole day because we have not incorporated data about school and home meals into the current version of the ABM. Instead, we assume that the baseline trajectory of body mass follow CDC growth curves,[40] with perturbations from this baseline determined according to after-school food foraging behaviors. The CDC growth curves are generated mainly from five national health examination surveys of the United States. These curves are based on growth data of infants, children and adolescents in clinical practice and research.[40] Examples of the CDC growth curves are shown in Figure 6. The figure gives growth curves of height and weight for girls aged between 2 and 20. The curves with different colors represent different percentiles. In our ABM we assume that the children's baseline trajectories will follow a constant percentile. While the CDC curves are used for the baseline trajectories, the ABM is used to determine the deviation from these trajectories.

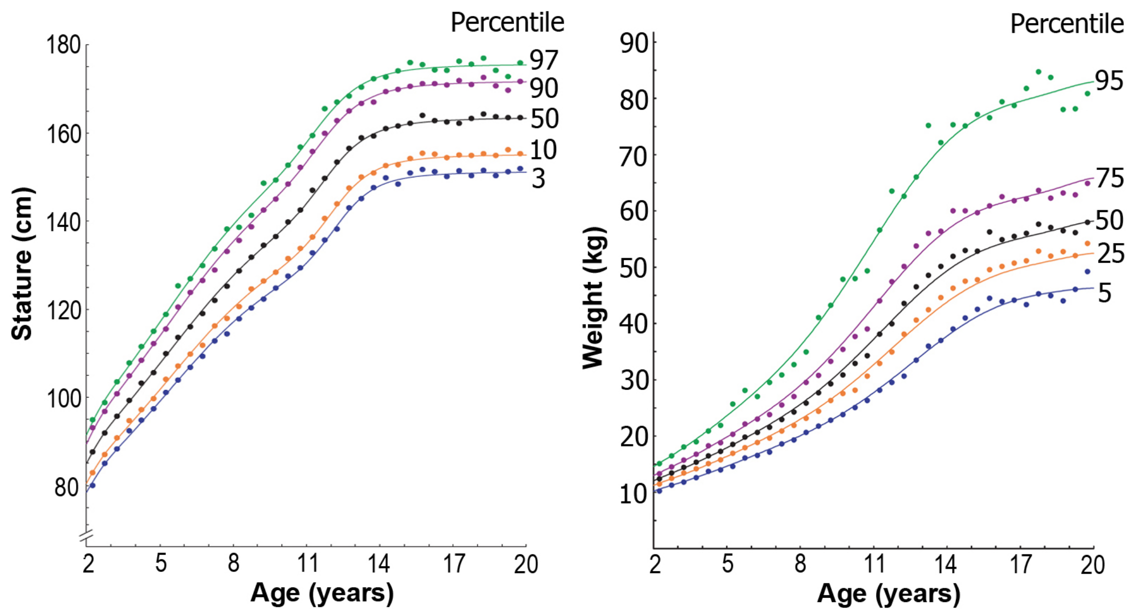


**Figure 2.4:** CDC growth curves for girls aged between 2 and 20 (Left: height-for-age; right: weight-for-age)

For height growth, we assume the children follow the CDC height growth curves strictly; we assume that weight growth will not perturb the CDC heights curves. At the beginning of the simulation, initial gender, height and age are used to find the height percentile. In the case that height and age do not fall on an existing percentile curve, two-dimensional interpolation is employed to approximate the percentile. Afterwards, we use the interpolated percentile curve to predict height for subsequent time. A similar approach is used in predicting weight, except that we perturb the percentile based on calories intake and energy expenditure: if a child has an above-average energy balance, then his or her percentile is shifted higher using calculations for added body weight, described in the following.

We utilized the methodology suggested by Butte et al[46] to estimate the body mass (BM) increment that arises from the difference between caloric intake and energy expenditure. BM increment is obtained by using the following equation:[46]

$$\Delta \mathrm{BM} = \frac{1}{c}(0.9 \cdot \mathrm{EI} - \mathrm{EE}) \tag{2.1}$$

In the above equation, EI is the energy intake and EE is the energy expenditure due to basal metabolism, daily activity, and exercise. The constant $c$ is defined as below:

$$c = \mathrm{cf} \cdot \frac{\mathrm{fr}}{\mathrm{ef}} + \mathrm{cff} \cdot \frac{1 - \mathrm{fr}}{\mathrm{eff}} \tag{2.2}$$

where cf is the energy density stored in fat mass; cff is the energy density stored in fat-free mass; fr is the fraction of fat mass in the total body mass; and ef and eff are efficiencies in the conversion of energy to fat and fat-free masses.

Children consume energy when they walk. According to Rose et al,[47] walking energy expenditure can be estimated via

$$\mathrm{EE}_{\mathrm{walk}} = \mathrm{distance} \cdot 65(\mathrm{kcal/mile}) \tag{2.3}$$

### 2.2.5 GUI to support policy making

The GUI (Graphic User Interface) is almost as important as the computational part of the model. Not only does the GUI make the model more understandable for policy makers and stakeholders, but it also facilitates model development and simulation analysis.

The GUI of the BLIFE1.0 ABM can be separated into four regions. As shown in Figure 7, Region 1 is the visualization of agents and the surrounding environment; Region 2 contains several buttons to start, pause, stop, or reset the simulation. Region 3 consists of buttons, sliders, and switches to modify simulation parameters such as agents and environment properties. In Region 4, results are gathered during simulation; curves are plotted to show the system-level behaviors of the model. Ideally the developed GUI can be used to assist food policy making. Before proceeding with a candidate policy, the GUI serves to communicate estimates of the policy's intended impact and any potential unintended consequences.

## 2.3 Results and Discussions

### 2.3.1 BMI percentile prediction

At the beginning of the simulation, all children properties (e.g., height, weight, age, and gender) are initialized using survey data conducted in Baltimore with de-

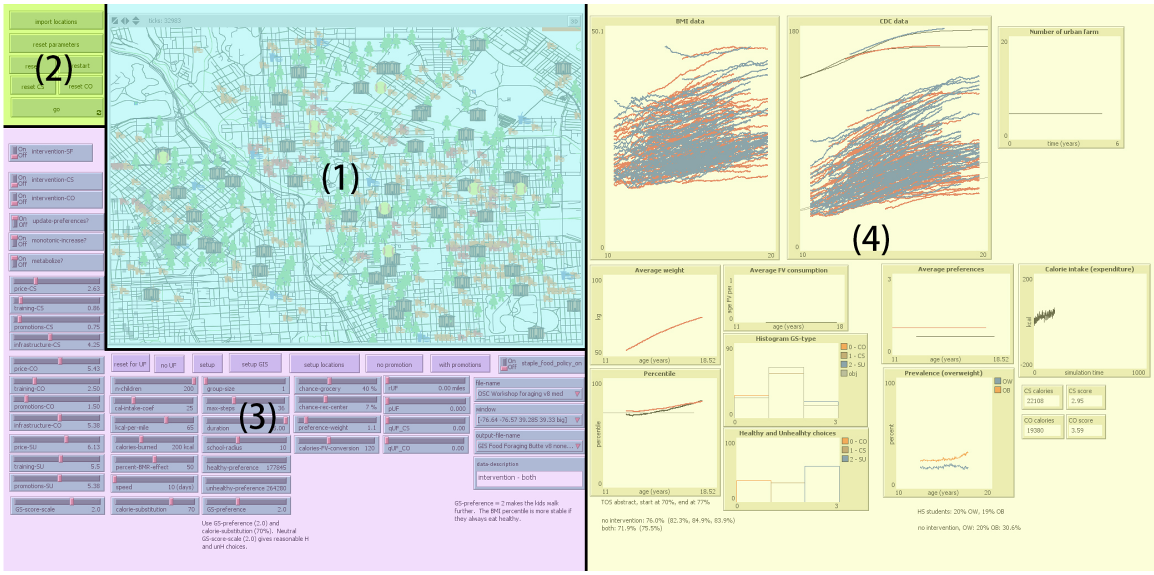


**Figure 2.5:** Demonstration of the graphical user interface. Region 1: visualization of children movement and food environment; Region 2: simulation controller; Region 3: model parameters controller; Region 4: model outputs

identification procedures noted earlier. The model then uses the starting data to predict children growth during the following five years. Using the method established by Butte et al. (as described in Section 2.2.4), we calculate the body mass change for each child. BMI is calculated using the formula

$$\text{BMI} = \frac{(\text{mass in kg})}{(\text{height in m})^2} \tag{2.4}$$

Upon obtaining the average BMI for boys and girls, we use the CDC percentile data in Figure 2.4 to interpolate the mean BMI percentile for these groups. The results, plotted in Figure 2.6, indicate a substantial increase in mean BMI percentile among low-income African-American children in Baltimore over a 5-year period associated with after-school eating behavior.

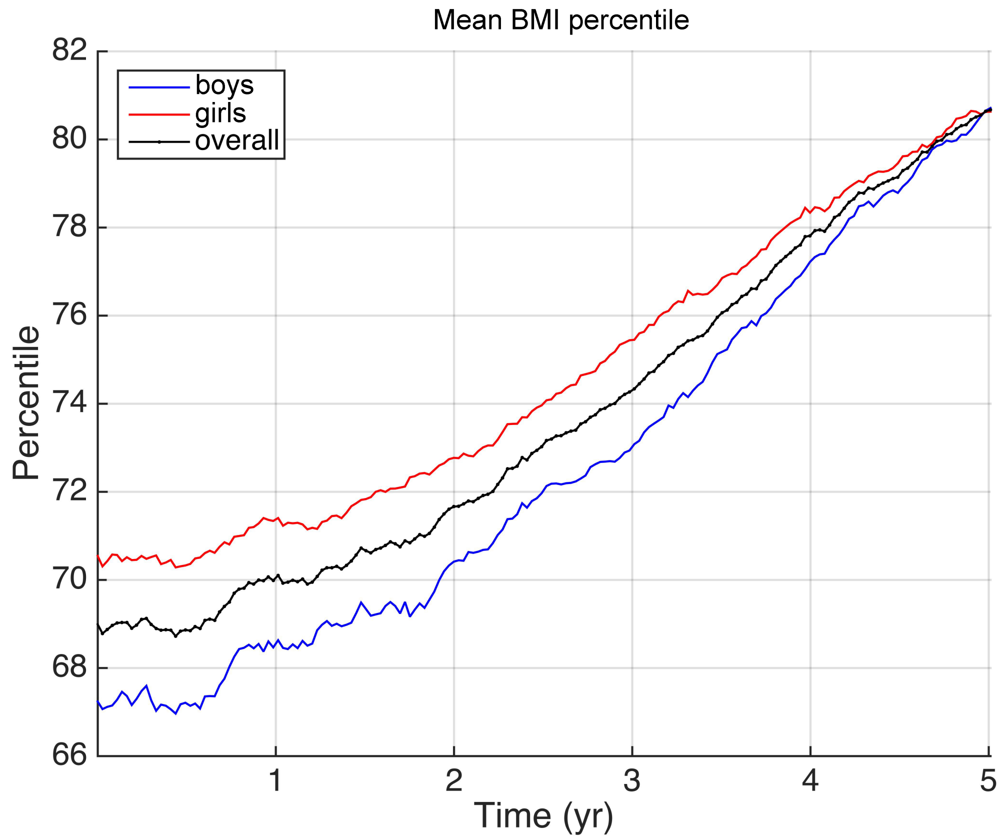


**Figure 2.6:** BMI percentile prediction for boys, girls and overall

## 2.3.2 Results validation

We validated our findings by comparing the predicted BMI trajectories with data from 3 prospective cohorts of children and adolescents enrolled by Project HeartBeat, which was a study of cardiovascular risk factors. Project HeartBeat collected weight, height, and other anthropometric measurements for 678 children in Texas and estimated growth of body fat across 5 commonly used indices. The majority of data collected by Project HeartBeat were for white (74.6%) and black (20.1%) children. In Figure 2.7 we compare our predicted mean BMI with BMI trajectories observed for

African-American males and females in the Project HeartBeat cohorts.[48] It can be seen that the children in Baltimore started with higher initial BMI for both genders, so here we only compare the rate of increment of BMI increase (i.e., the slope of the trajectories). Figure 2.7 shows a good agreement between the BMI growth rates.

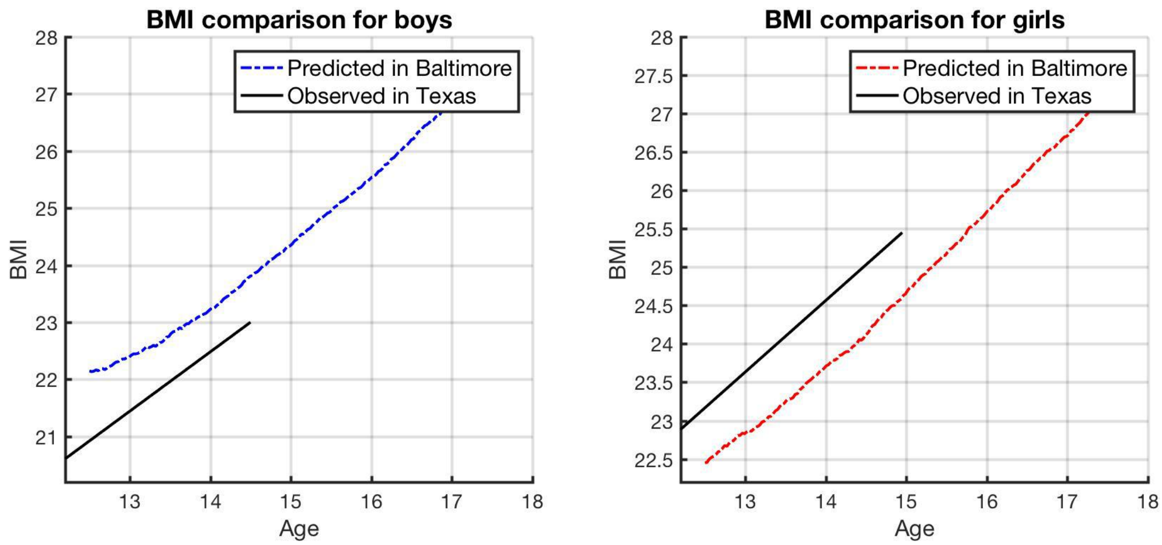


**Figure 2.7:** Validation of predicted BMI

### 2.3.3 Advances and innovations of the model

To our knowledge, this was the first use of an ABM to simulate after-school child dietary behaviors and obesity risk of urban children in a low-income food environment. Compared with SD (System Dynamics) modeling and Discrete Event Simulations, ABM is capable of capturing more real-world phenomena.[49] SD models only capture properties of the whole system, while ABM simulates systems-level (or emergent) properties by modeling many individual agents, none of whom have the systems-level properties. Each agent can be quite different from the others, which enables a realistic modeling of heterogeneity. For example, food sources are distributed non-uniformly in the simulated space, and the same food policy (e.g., requiring small stores to stock a range of healthy foods) could influence different areas in quite variable ways.

# Chapter 3

# System Dynamics Model for Community Resilience Research

## 3.1 Introduction

This study is about community resilience, i.e., a community's capacity for resisting and recovering from adverse natural or man-made events. The performance of a community can be measured by a broad range of community activities in providing services to its residents, which we denote as Community Functioning (CF). The concept of resilience can be found in many disciplines, such as psychology, ecology and physics. In a general sense, there are two concepts that describe resilience from different points of view: **resistance**, which quantifies the abilities to counteract an event's potential to inflict damage, and **recovery**, which quantifies the ability of the system to recover to its original level after the event.

In this research, we adopted the same notions. **Community resistance** is defined as the proportion of CF that is sustained during a disaster event, and **community recovery** is defined in terms of the speed at which a community recovers after the event. Additionally, **community resilience** is defined as the combination of resistance and recovery, quantified by the area under the CF curve, as described in detail in Section 3.4.2. It is important to note that community resistance, recovery and resilience are related with the dynamic changes of CF during and after an event, and thus cannot be directly measured before the event. Community resistance, recovery and resilience capture the stability of CF, and should not be confused with the baseline CF. It is entirely possible for a community to have poor CF but strong resilience and/or resistance, while another community to have excellent CF before an event that is reduced quickly during a disaster and restored slowly thereafter.

Community recovery, resilience and resistance represent behaviors of a complex and dynamic system, and we demonstrate herein that they can be analyzed using an SD model. In the SD model, survey data is used to quantify the initial values of the model. Resilience, recovery and resistance will be derived from the resulting time-dependent fluctuations of CF using the equations of the SD model.

The geographical resolution is selected to be at the county level for two reasons. First of all, residents in a county usually share a common government, culture and laws. Many public health and emergency management activities are organized at this level, and thus a county can be treated as a community. Another important reason is that relatively more data are available at the county level in United States, compared with finer scales such as census tracts. Although even more data is available at the state level, we believe a state is too large to be considered as a "community."

# Notation

**CF** Community Functioning

**ES** Engineered Systems

**NS** Natural Systems

**ODE** Ordinary Differential Equation

**PM** Prevention and Mitigation

**PR** Preparedness and Response

**PVID** Population Vulnerability, Inequality and Deprivation

**SC** Social Cohesion

**FIPS code** Federal Information Processing Standards code (unique identifiers for all counties in the United States)

$c_v$ Coefficient of variation

$\sigma$ Standard deviation

$\mu$ Mean

$\nu$ Median

$\gamma_1$ 3rd standardized moment

$\lambda$ Coefficient in the Box-Cox transformation

# 3.2 The SD model

## 3.2.1 Essential components

We first identified the key components in the model in Table 3.1.

## 3.2.2 Event

The event is defined as an independent, external input function to the model of a community. A natural event is mathematically specified as a mono-exponential function with respect to time:

$$\text{Event}_t = \text{Event}_0 \cdot k \cdot \exp(-kt) \tag{3.1}$$

**Table 3.1:** Essential components of the community stability model

| Symbol | Component | Definition |
|---|---|---|
| CF | Community Functioning | CF is a measure of a broad range of community activities in providing services to its residents. The activities include these areas: communication, economy, education, food and water, government, housing, medicine and public health, nurturing and care, transportation and well-being. |
| PM | Prevention Mitigation | PM is a combination of the influences of natural and engineered systems and preventive activities that mitigate damage from an event. |
| PVID | Population Vulnerability Inequality Deprivation | PVID is the social, political and economic conditions that can potentially harm a community's capability of responding to and recovering from a hazardous event. |
| SC | Social Cohesion | This is the sense among county residents of social connection and belongingness that effectively supports the rise of community functioning after an event. |
| PR | Preparedness Response | PR is the set of activities before and during events that includes planning, organizing, training, equipping, exercising, evaluating and taking corrective actions to ensure effective coordination in the event of a disaster. |
| ER | External Resource | ER is the stock of resources that is brought into a community after an event that originates from outside the affected county. |

where $k$ is a parameter controlling the time scale of the event, quantified by the rate of time decay, and $\text{Event}_0$ is the total overall magnitude of the event, given by the integral of event magnitude over time.

$$\text{Event}_0 = \int_0^{+\infty} \text{Event}_t \,\mathrm{d}\,t \tag{3.2}$$

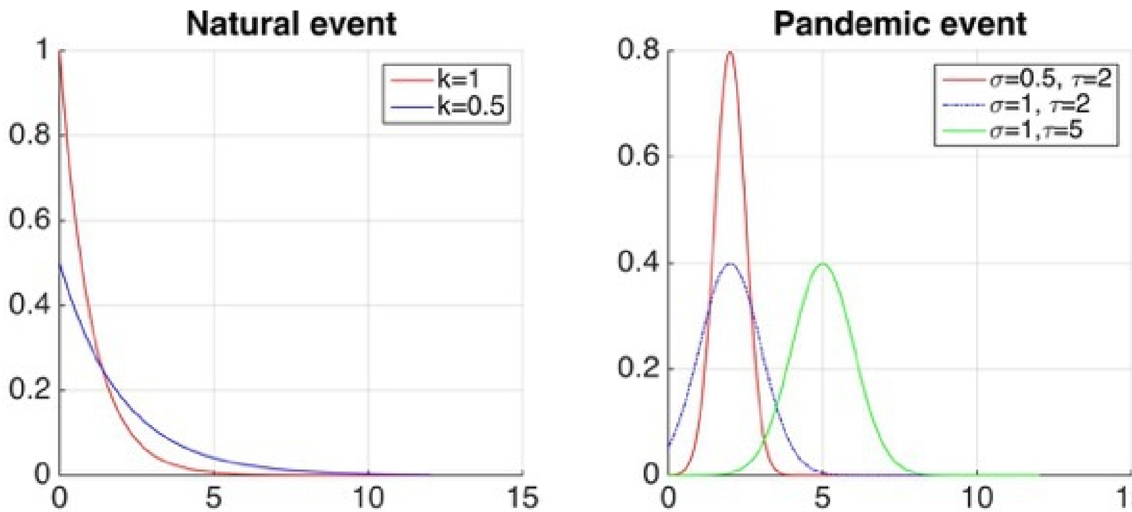


**Figure 3.1:** Functions that model natural and pandemic events

For a pandemic event, which has a gradual ramp-up period before the peak and is followed by gradual decline in severity, the magnitude at time $t$ is defined in terms of a Gaussian function,

$$\text{Event}_t = \text{Event}_0 \cdot \frac{1}{\sqrt{2\pi\sigma^2}} \cdot \exp\left(-\frac{(t-\tau)^2}{2\sigma^2}\right) \tag{3.3}$$

where $\text{Event}_0$ is defined as before, $\tau$ is the time of the peak of the pandemic, and $\sigma$ is the measure of the spread of the event in time.

### 3.2.3 Mathematical formulations

As shown in the stock-flow diagram in Figure 3.2, the CF stock is drained by an event as it occurs, and the three stocks, SC, PR, and ER, replenish CF as the event subsides. The rate at which the event damages CF is regulated by PVID and

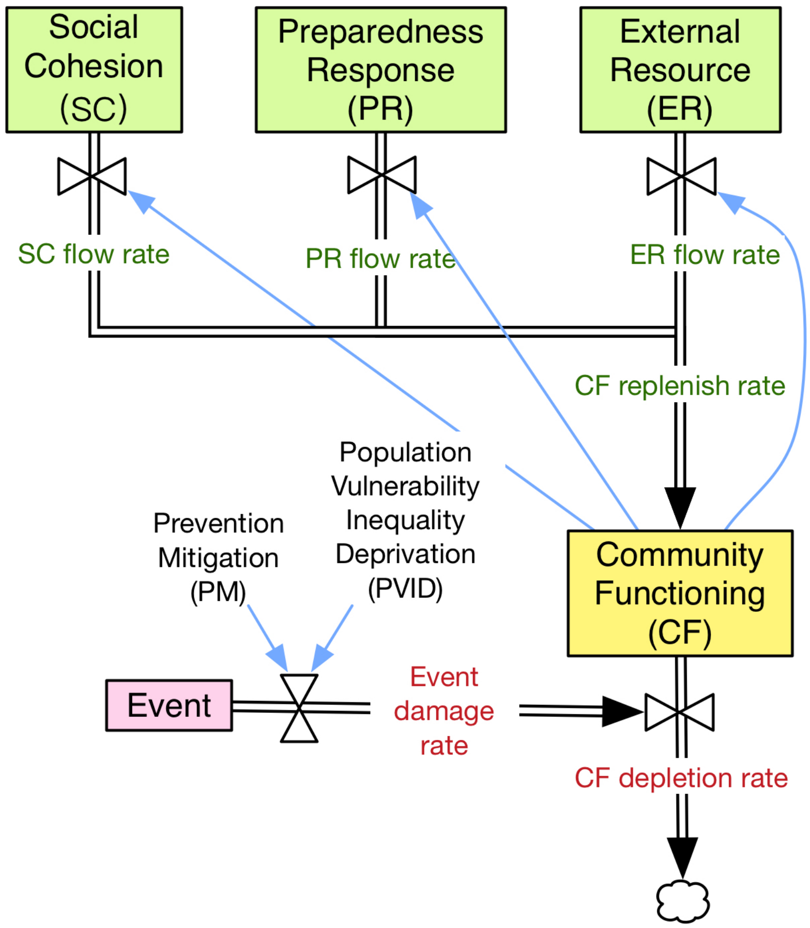


**Figure 3.2:** Flow diagram of the ODE model

PM, while the rate of CF replenishment is controlled by all three stocks and by CF itself. As noted earlier, the phenomena in which the rate of change of a stock is regulated by its own value is called feedback. The dynamic value of CF is determined by the combined effects of flows and feedback loops. Below we give the corresponding ordinary differential equations that mathematically describe these actions.

$$\frac{\mathrm{d}\,\mathrm{SC}}{\mathrm{d}\,t} = -\mathrm{CF}_t \cdot \mathrm{ER}_t \cdot (\mathrm{CF}_0 - \mathrm{CF}) \tag{3.4}$$

$$\frac{\mathrm{d}\,\mathrm{PR}}{\mathrm{d}\,t} = -\mathrm{PR}_t \cdot (\mathrm{CF}_0 - \mathrm{CF}) \tag{3.5}$$

$$\frac{\mathrm{d}\,\mathrm{ER}}{\mathrm{d}\,t} = -\mathrm{ER}_t \cdot (\mathrm{CF}_0 - \mathrm{CF}) \tag{3.6}$$

$$\frac{\mathrm{d}\,\mathrm{CF}}{\mathrm{d}\,t} = -\alpha \cdot \mathrm{CF}_t \frac{\mathrm{d}\,\mathrm{Event}}{\mathrm{d}\,t} \frac{\mathrm{PM}_0 + \mathrm{PVID}_0}{2} - \frac{\mathrm{d}\,\mathrm{ER}}{\mathrm{d}\,t} - \frac{\mathrm{d}\,\mathrm{PR}}{\mathrm{d}\,t} - \frac{\mathrm{d}\,\mathrm{SC}}{\mathrm{d}\,t} \tag{3.7}$$

The rates of change of SC, PR and ER are defined by equations (3.4) to (3.7) and the rate of change of CF is the combination of the damage caused by the event and the combined replenishment of the three blocks as shown in Equation (3.7). In the above equations $\alpha$ is a parameter that determines the time scale of the CF curve. In future work, $\alpha$ will be calibrated using data from observed CF changes after historical events. In this thesis we set $\alpha = 5$ so that CF recovers within one year. The Runge-Kutta method[50] is used to numerically solve the above ODEs.

## 3.3 Measures and data

### 3.3.1 Measure hierarchy

All measures used in this research are categorized into a hierarchy with 3 levels.

**Domain** Domains are the top-level conceptualized components that play important roles in determining community resilience. There are 6 domains in total as shown in Table 3.1.

**Suddomain** Each domain is divided into multiple subdomains, which are closely related but represent different aspects of the domain. For some domains like SC and PR, only one subdomain is used.

**Measure** Measures are the specific indicators at the bottom level that are aggregated to characterize a subdomain.

### 3.3.2 Selection of measures

Several criteria were applied when we selected the measures for each component of the model.

1. The measure should have face validity as judged by public health and social science experts.

2. Data for the measure should be available for the majority of the counties in the United States, preferably with multiple years.

3. The data should exhibit a reasonable amount of variation across all counties. As we discussed in detail later in Section 3.3.3, we will transform the data to amplify the variation if necessary.

4. The data should be easy for others to acquire and implement; no significant computation or GIS processing should be needed.

5. The measure should capture a single aspect of the concept, rather than being synthesized outcomes, because the latter type of indicator tends to characterize multiple domains of the model. There is an exception for the subdomain "Population Well Being," in which we used a standard health indicator, "Average life expectancy."

The essential component of the model is community functioning. Based on the aforementioned requirements and data availability, we selected measures for community functioning as below. Each measure could contribute positively or negatively to the subdomain and their directions are labeled using "+" or "-", respectively.

- Communication
  - \+ Percentage of households with Internet service over 200 kbps.
- Economy
  - \+ Number of finance and insurance companies per 10k population.
  - \+ Median household income.
  - \+ Number of employers per 10k population.
- Education
  - − Pupil/teacher ratio (public school).

+ High school graduation rate.

- Food and water
  + Number of grocery stores per 10k population.
  + Number of grocery stores per 100 square miles.
  + Percentage of population on public water.
  − Low access to grocery store.
- Government
  + Per capita federal government spending
- Housing
  − Percentage of household with severe problems
  + Number of house units per capita
- Healthcare delivery and public health services
  + Number of mental health care providers per 10k population
  + Number of primary care physicians per 10k population
  + Number of hospital beds per 10k population
  + Percentage of female Medicare enrollees aged 67 to 69 that receive mammography screening

    + Percentage of diabetic Medicare enrollees ages 65 to 75 that receive HbA1c monitoring
    − Percentage of uninsured adults in age group 16 to 64
    − Percentage of adults who are current smokers
    − Percentage of leisure-time physical inactivity prevalence

- Nurturing and care
    + Number of nursing care facilities per 10k population
- Transportation
    + Percentage of population who walk or cycle to work
- Population well being
    + Average life expectancy
    − All-cause mortality per 100k population
    + Percentage of self-reported excellent or very good health
    − Percentage of adults with frequent mental distress

In the case of a natural event, Prevention Mitigation consists of natural systems and engineered systems. In the event of a pandemic disaster, a different set of counter-measures are required and will be one of the future works of this thesis.

- Natural systems

  + Distance to the nearest coast.

- Engineered systems
  − Percentage of bridges with structural deficiencies.
  − Average age of housing stock.
  + Percentage of housing units that are not mobile homes.
  − Percentage of population affected by water violation of those served by public water system.

PVID is composed of three subdomains:

- Vulnerability
  − Percentage of children in population (below 18).
  − Percentage of elderlies in population (65 and older).
  − Percentage of population in institutions.
  − Percentage of civilian noninstitutionalized population with a disability.
- Inequality
  − Gini index of income inequality.
- Deprivation
  − Percentage of population (18 to 24 years) with less than high school education.

- − Percentage of population (16 years and over) not in the labor force.
- − Percentage of children in poverty.
- − Percentage of civilian in labor force but unemployed.
- − Percentage of household on public assistance and food stamps.

SC has one subdomain, Social Capital and Cohesion,

- Social Capital and Cohesion
  - \+ Percentage of population who use carpool to work
  - \+ Percentage of population affiliated with religious group
  - \+ Number of religious organizations per 100 square mile
  - \+ Number of social advocacy organizations per 10k population

We currently have no optimal measure for PR, and use FEMA events temporarily. The logic behind this is that if a county has experienced multiple events in recent history, then it will tend to have better emergency policies and will be better prepared for future events.

- Preparedness
  - \+ Number of social advocacy organizations per 10k population

### 3.3.3 Transformation

The data at the measure level will be scaled and aggregated to subdomain and domain levels. Table 3.2 summarizes the procedure; the details are discussed in this section. The details of the data, including the mathematical operations need to scale the data and maps of the scaled results can be found in Appendix B.1.2.

In our data transformations, we perform the same mathematical operation on each measure. In practical statistics analysis, data transformations are frequently required to improve interpretability of the data or to bring the distribution closer to the assumptions of the model. In this research, data transformation is indispensable because of the skewness of much of the raw data. This is to be expected because many phenomena in economics described by variables which follow the log-normal distribution,[51] with large values that may exceed the average by several orders of magnitude.

#### 3.3.3.1 Skewness

Skewness describes asymmetry in the data distribution. It can be measured by several statistical properties. It is worthwhile to mention that each property only describes one aspect of skewness, and in practice we need to look at several skewness properties in combination.

- Coefficient of variation $c_v$, also known as the relative standard deviation, defined as the ratio between the standard deviation $\sigma$ and the mean $\mu$. It measures the

**Table 3.2:** Procedures of data transformation and aggregation

| **Operation** | **Motivation** |
|---|---|
| 1. Treat negatives as missing value. | Due to the nature of this research, all measures should have a positive value. Negative and zero values should not occur and should be treated as invalid data. We do allow zero values because it implies that the information for the measure of interest is nonexistent. |
| 2. Transform each measure using Box-Cox transformation. | Much of the original data is extremely skewed. Transforming the data towards the normal distribution increases their differentiating power and interpretability. |
| 3. Take Z-score of each measure. | This is important because in the aggregation stage all measures will be summed together. |
| 4. Truncate with $\pm 3.5$ at the measure level. Data after this step is called **scaled** data. | It is noted that some values still stay quite large after the Box-Cox transformation. To control the effect of outliers, the Z scores are truncated at 3.5, namely 3.5 times the standard deviation of the transformed data. |
| 5. Adjust for direction. | The polarity of some measures are in the opposite direction of that of the corresponding domain. |
| 6. Scale the data from range $[-3.5, 3.5]$ to $[0, 1]$. | The scale from 0 to 1 is easier to interpret. |
| 7. For each county, take the average of available measures in each subdomain as the value for the subdomain | Missing data are simply ignored in calculating the aggregated values. |
| 8. For each county, take the average of subdomain values as the domain value | Subdomains are aggregated into domains. |
| 9. Fill in missing values of any domain with the average of that domain for all counties in the same state. | The state average is a good, simple estimate of missing values. |

amount of variability relative to the mean.

$$c_v = \frac{\sigma}{\mu} \tag{3.8}$$

- The 3rd standardized moment, defined as below

$$\gamma_1 = E\left[\left(\frac{X-\mu}{\sigma}\right)^3\right] \tag{3.9}$$

- Ratio of mean and median. In symmetric distributions such as the normal distribution, the mean is equal to the median and thus this ratio is 1.

**Table 3.3:** Statistics of the original data for the measure: Number of grocery stores per 100 square miles (Appendix A.1.4.2)

| Item | Value |
|---:|---|
| Minimum value | 0 |
| Maximum value | 5839.06 |
| Mean $\mu$ | 9.0 |
| Median $\nu$ | 0.87 |
| Standard deviation $\sigma$ | 130.90 |
| Mean-to-median ratio $\mu/\nu$ | 10.36 |
| Coefficient of variation $c_v$ | 14.47 |
| 3rd standardized moment $\gamma_1$ | 34.96 |

As an example, grocery store density (Number of grocery stores per 100 square miles (Appendix A.1.4.2)) is a measure of economical activities, and it roughly follows the lognormal distribution. According to the USDA Food Environment Atlas, in 2011 the maximum value of this measure is 5839 stores/100 sq.mi., while its mean is only 9.0 stores/100 sq.mi. More detailed statistics are shown in Table 3.3. As shown in Figure 3.3, the majority of the data entries falls within the leftmost bin in the histogram plot, and large values are so infrequent such that they are not discernible in the histogram plot. In the color coded map, almost all counties are blue (minimum value) and the map provides almost no information.

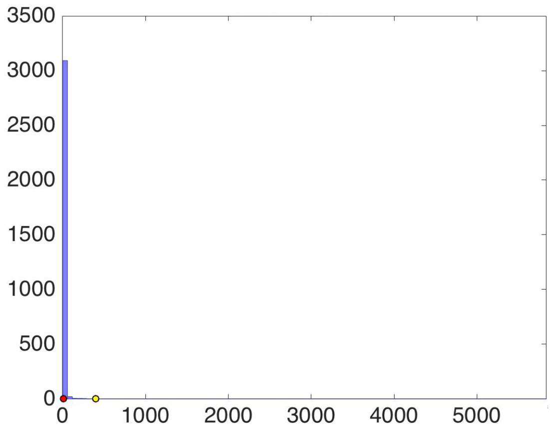


(a) Histogram plot

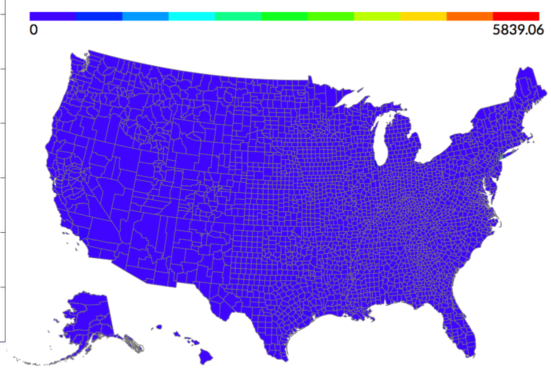


(b) Map plot

**Figure 3.3:** Original data of measure: Number of grocery stores per 100 square miles (Appendix A.1.4.2). Both histogram and map plot show little difference between counties

Some standard transformation techniques for such highly skewed data include the log-transformation[52] and the power-law transformation.[53] In this research we used the Box-Cox transformation, which can be viewed as a combination of the aforementioned two transformations.

#### 3.3.3.2 Box-Cox transformation

The Box-Cox transformation[54,55] of a variable $x$ is defined as:

$$B(x) = \frac{x^{\lambda} - 1}{\lambda} \tag{3.10}$$

where $\lambda$ is determined by maximizing the Log-Likelihood Function (LLF) of the transformed data. As shown in Equation 3.10, the Box-Cox transformation is a power-law transformation. However, when $\lambda$ approaches zero, the Box-Cox transformation reduces to the log-transformation

$$\lim_{\lambda \to 0} \left( \frac{x^\lambda - 1}{\lambda} \right) = \lim_{\lambda \to 0} \left( \frac{x^\lambda \cdot \log_e x}{1} \right) = \log_e x \tag{3.11}$$

where we applied L'Hospital's Rule by taking derivatives of the numerator and denominator of the indefinite form 0/0.

Here we show several examples comparing data after the Box-Cox transformation and log-transformations. Figure 3.4 shows a comparison of the transformed grocery store density data. Both transformations worked well and the transformed data exhibit sufficient variation for use as a measure in our model. Figure 3.5 demonstrates transformations on Percentage of housing units that are not mobile homes (Appendix A.2.2.3), an example of right-skewed data. Log-transformation increased the skewness, while Box-Cox spreads the data entries more evenly.

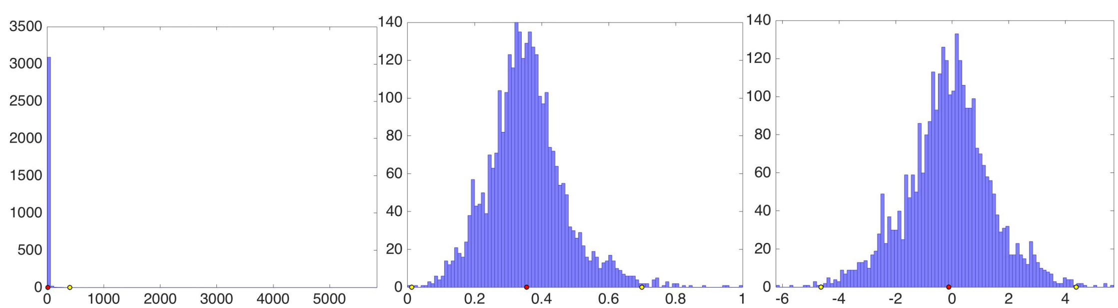


**(a)** Original data **(b)** Log-transformed data **(c)** Box-Cox transformed data

**Figure 3.4:** Comparison of Box-Cox transformation ($\lambda = -0.104$) with log-transformation on left-skewed data. Measure: Number of grocery stores per 100 square miles (Appendix A.1.4.2)

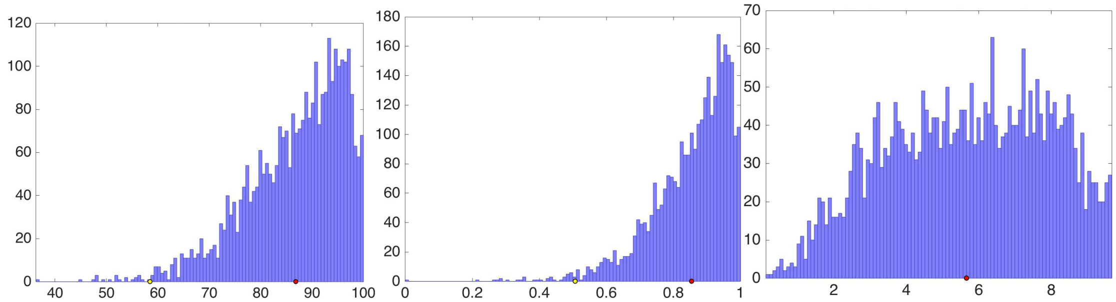

**(a)** Original data **(b)** Log-transformed data **(c)** Box-Cox transformed data

**Figure 3.5:** Comparison of Box-Cox transformation ($\lambda = 4.310$) with log-transformation on right-skewed data. Measure: Percentage of housing units that are not mobile homes (Appendix A.2.2.3)

#### 3.3.3.3 Z-score and truncation

The Z-score is the number of standard deviations by which a data value is above or below the mean. It is defined as

$$z = \frac{x - \mu}{\sigma} \tag{3.12}$$

After a Z-score transformation, all data are centered at 0 and at the same level of variability. In other words, data for different measures are comparable after Z-score transformation, and we can average multiple measures to get aggregated values. To reduce the effect of large outliers on skewing the data (which happens infrequently), we truncate the data at $\pm 3.5$. In this paper we call the result **scaled** data.

The scaled data shown in Figure 3.6 shows far more variation than the original data in Figure 3.3. It is now possible to interpret the data by examining the colors in the figure: grocery stores are more geologically dense in large cities like New York,

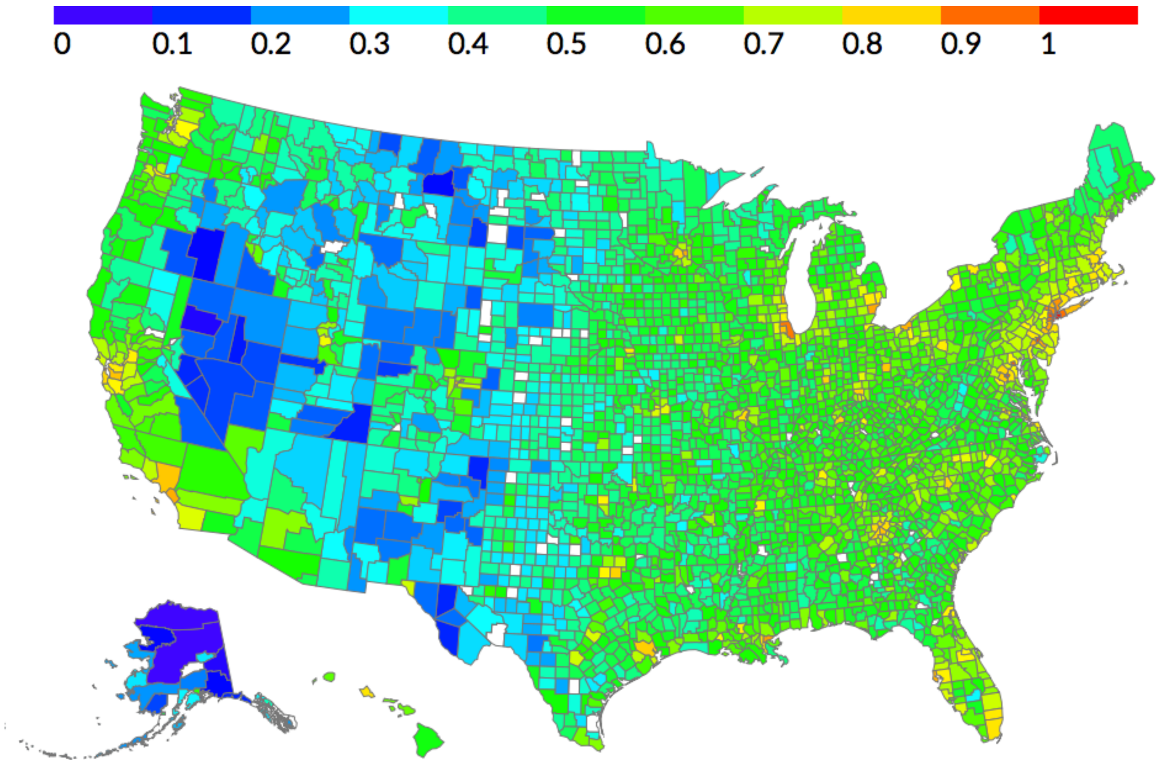


**Figure 3.6:** Map plot of scaled measure: Number of grocery stores per 100 square miles (Appendix A.1.4.2)

Chicago, Seattle and San Francisco, while they are relatively sparse, and hence less accessible in rural counties in states such as Nevada and Utah.

## 3.4 Results and conclusions

### 3.4.1 Aggregated domains

Figure 3.7 shows a color-coded map of the initial value of community functioning computed using an aggregation of transformed measures as explained before. It can be inferred from Figure 3.7 that the Midwest counties have relatively high community functioning, while the counties in the South show relatively low community functioning. The other domains are shown in color-coded maps in Figure 3.8.

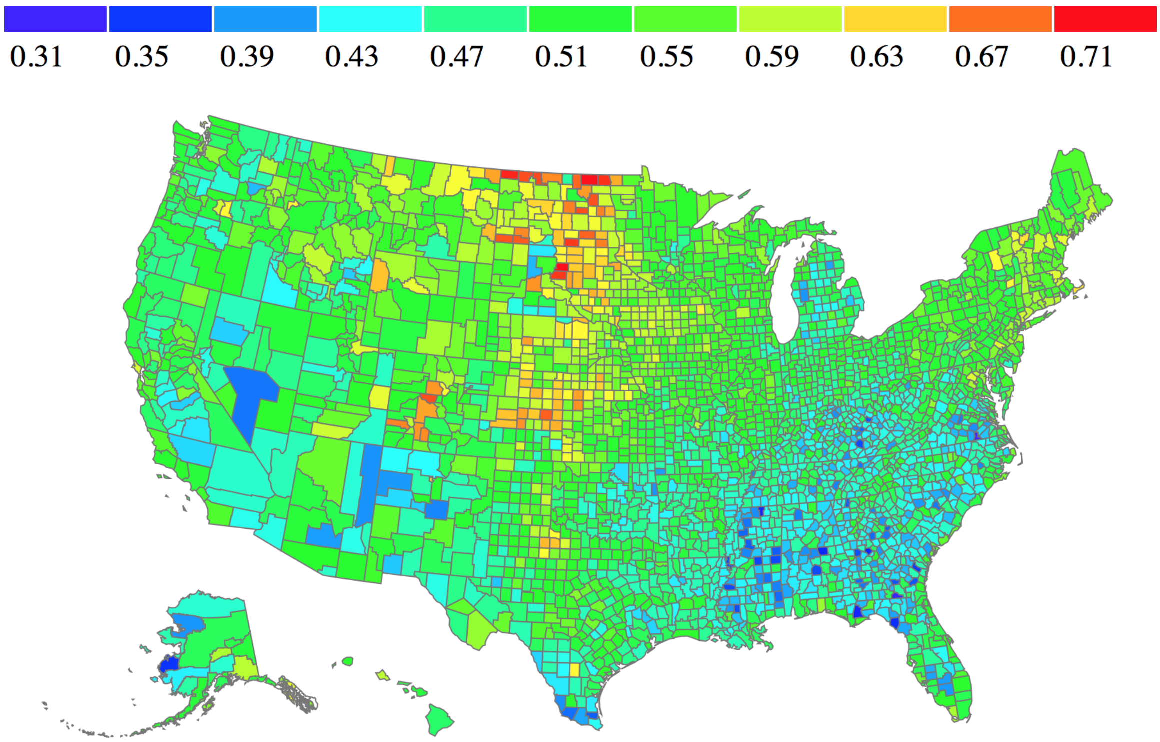


**Figure 3.7:** Map plot of aggregated community functioning

### 3.4.2 Resistance, recovery and resilience

To demonstrate the concepts of resistance, recovery and resilience, we simulate generic natural event to all counties with the same total magnitude and parameters. By solving the ODEs, we obtain a CF trajectory in time as shown in Figure 3.9. $CF_0$ is the initial pre-event community functioning, $CF_{\text{min}}$ is the minimum value of community functioning during the event, and $CF_{\text{middle}}$ is the average of $CF_0$ and $CF_{\text{min}}$.

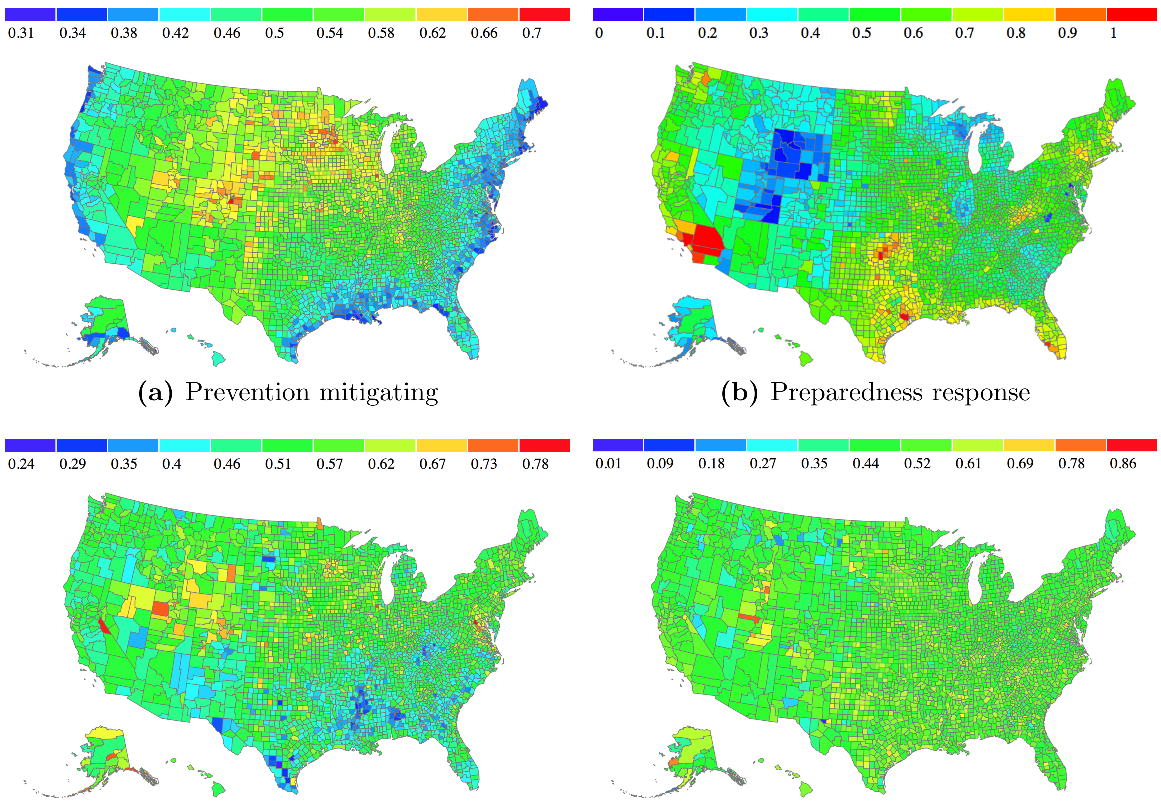


**(a)** Prevention mitigating

**(b)** Preparedness response

**(c)** Population vulnerability, inequality and deprivation

**(d)** Social cohesion

**Figure 3.8:** Map plot of other domains

- **Resistance** is defined as the minimum percentage of remaining CF during an event:

$$\text{Resistance} = \frac{\text{CF}_{\text{min}}}{\text{CF}_0} \tag{3.13}$$

- **Recovery** is defined as the reciprocal of the time it takes for the community to recover half of the CF lost due to the event, as indicated in Figure 3.9. The

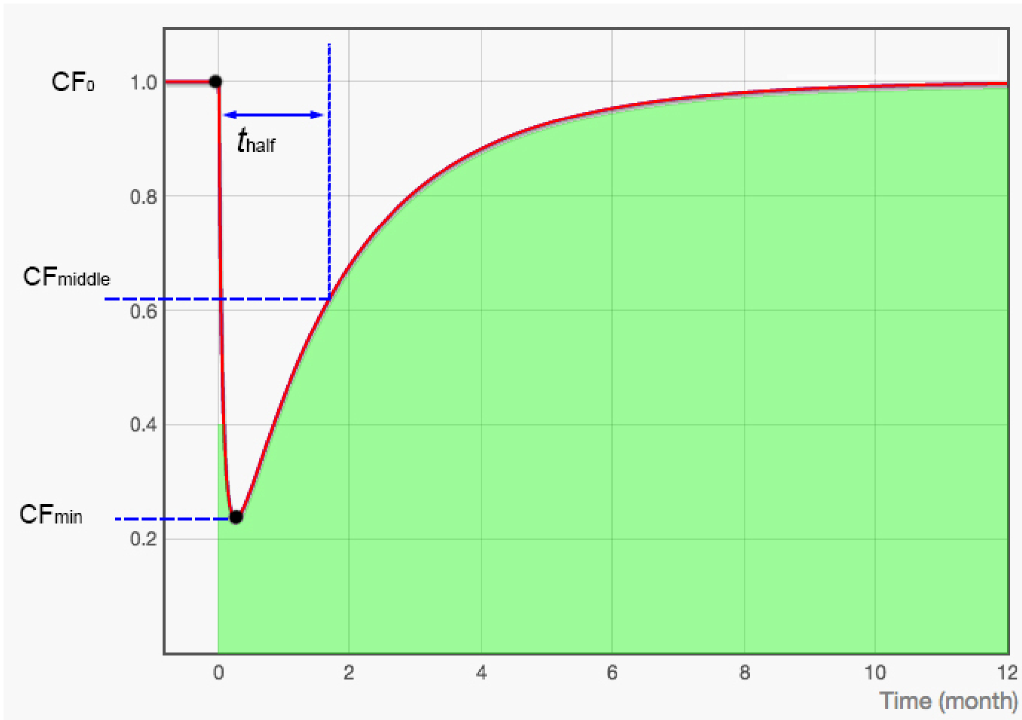


**Figure 3.9:** Graphical definition of resistance and resilience

formulation for resilience is expressed as

$$\text{Recovery} = \frac{1}{t_{\text{half}}} \tag{3.14}$$

where $t_{\text{half}}$ is a time after event at which CF recovers to $\text{CF}_{\text{middle}}$.

- **Resilience** is defined as the average value of CF from beginning of the event to end time of study, as highlighted in Figure 3.9.

$$\text{Resilience} = \int_0^T \text{CF}_t \, \mathrm{d}\, t \Big/ T \tag{3.15}$$

where $T$ is the time period of study, chosen as 12 here.

Figure 3.10 shows the calculated resistance, recovery and resilience. The geographical patterns of resistance and resilience are significantly influenced by PR: counties in the Mountain states with poor preparedness exhibit low resistance, recovery and resilience, while counties in south California exhibit strong recovery due to excellent preparedness. Comparing pre-event CF in Figure 3.7 with resilience and resistance, we also conclude that counties with poor CF could have relatively excellent resistance and resilience, such as the south Texas counties. We can also infer that large cities tend to have better resistance and resilience.

## 3.5 Conclusions

Community resistance and resilience describe the dynamic response of a community to a hazardous event. We realized that these properties cannot be directly derived from the static pre-event community functioning. Therefore, we developed a framework of using system dynamics model to analyze community resistance and resilience. This framework could address needs of policymakers by facilitating the understanding of community stability, assessing current state of resilience and resistance of the United States and evaluating the effectiveness of a proposed intervention policy.

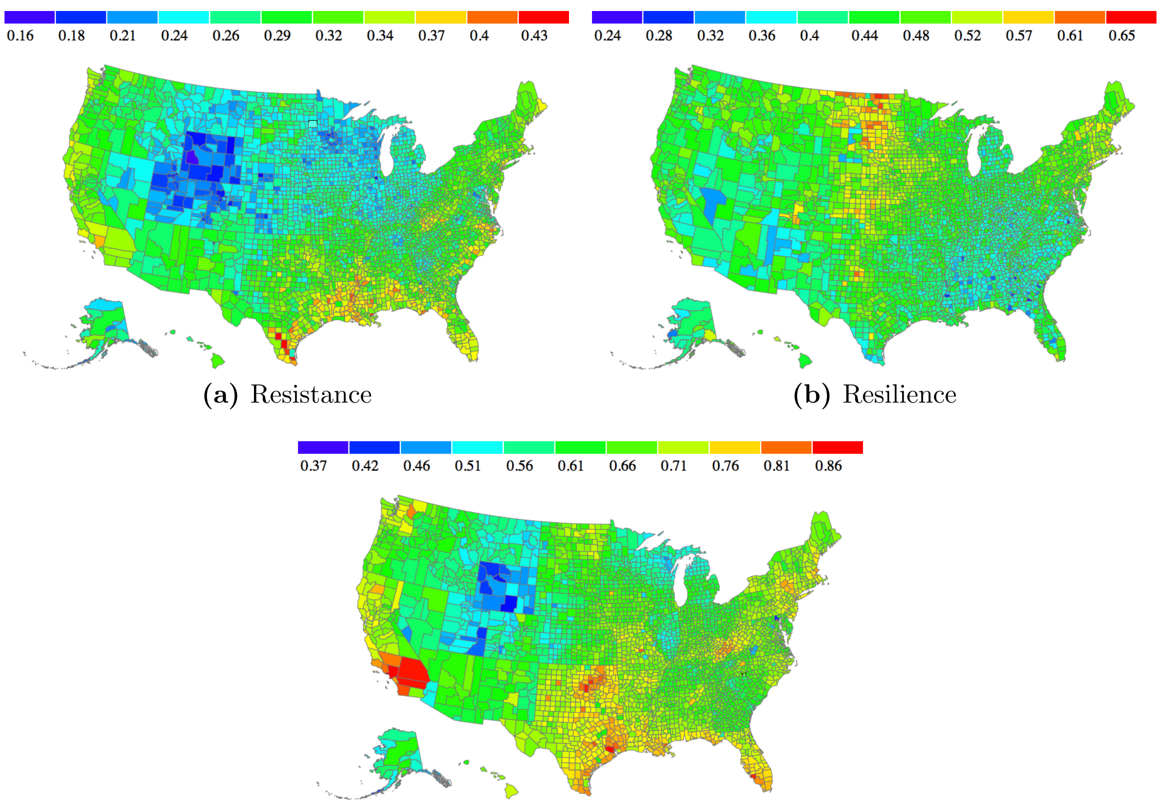


**(a)** Resistance **(b)** Resilience

**(c)** Recovery

**Figure 3.10:** Map plot of model results

# Chapter 4

# System Dynamics Model for Pay-For-Performance Strategy Study in Afghanistan

## Notations

**CLD** Causal Loop Diagram

**DDE** Delayed Differential Equation

**HSS** Health Systems Strengthening

**P4P** Pay for Performance

**NGO** Non-Governmental Organization

**MCH** Maternal and Child Health

**MoPH** Ministry of Public Health

**HF** Health Facility

**SBA** Skilled Birth Attendance

## 4.1 Introduction

Pay for performance (P4P) is an incentive strategy widely used in health systems to strengthen the effectiveness of health care delivery in low- and middle-income counties.[56–59] Charitable organizations pay particular interest to P4P because their traditional approach has been investing in input-based program activities, where the agency problem is inevitable.[56,57] Agency problem arises in organizational design when the "agents" who are placed in control over resources are under obligation to use these resources in the interest of other parties rather than their own interest. "Pay for performance" is a strategy that puts incentives on the performance of the agents with the intent of aligning the agents' interest with the funder's objectives. In the context of public health, the performance is measured as improvement in health services outputs or outcomes.[56,57]

Plenty of practical evidence exist to support that P4P can improve health services delivery in low- and middle-income counties.[57–59] On one hand, some studies in Cambodia, Rwanda, and Haiti showed that P4P led to improved utilization of maternal and child health services.[60–62] On the other hand, some studies suggested that P4P failed to increase health services delivery.[62,63] The importance of P4P implementation is acknowledged in all these studies; however, the interacting effects of involved factors have not been studied.[57–62]

Public provision of health services in Afghanistan was funded significantly during the last decades by Non-Governmental Organizations (NGOs).[64] Utilization and quality of general ambulatory care has been improved by the aforementioned health services delivery contracts; however, utilization of critical Maternal and Child Health (MCH) services was not improved.[64,65] According to Afghanistan Mortality Survey 2010, Skilled Birth Attendance (SBA) at delivery was as low as 19% and the maternal mortality rate of 0.584% was among the highest in the world.

Between September 2010 and December 2012, the Afghanistan Ministry of Public Health (MoPH) tested a P4P intervention at the health facility level in 9 provinces (out of 32) in order to improve the volume and quality of essential MCH services.[66] During the intervention, extra bonuses (on top of regular budgets) were given to health facility managers whose performances were beyond baseline level in aspects like antenatal care for pregnant women, SBA at delivery and immunization services.

A performance bonus program managed by the Afghanistan MoPH did not improve the coverage and general quality of MCH services, as revealed in a study regarding the effectiveness of the P4P intervention.[66] The study attributed the failure of P4P to poor implementation as one of the potential reasons. To capture the dynamic and nonlinear relationships involved, we developed a system dynamic model to provide insights about how various interacting components work together from a holistic viewpoint.

## 4.2 Modeling basic operation of a health facility

The construction of SD models consists of three basic stages:

1. Identify basic components of the system in terms of a set of variables.
2. Develop a Causal Loop Diagram (CLD). A CLD is a visual representation of variables and their causal relationships.
3. Quantify the relationships in the CLD and develop the corresponding Ordinary Differential Equations (ODEs). In some relationships, the affected variables may depend on the affecting variable's value at a previous time rather than its current value. In this case the equations are called Delayed Differential Equations (DDEs).

In this section we explain the process in detail.

### 4.2.1 Variables

The performance of a health facility is measured by its quality and volume of service, as defined below.

#### 4.2.1.1 Volume of service

Volume of service is defined as the number of patients visiting a health facility in a month. This data is based on self-reported information collected through the health information management system of MoPH at the health facility level.

#### 4.2.1.2 Quality of service

Quality of service is a combined measure of infrastructure quality of the health facility (including assessments of health facility equipment, infrastructure functionality and drug availability), equipment presence and functionality, and the perceived quality by clients. These indicators have been previously used to assess quality of health facilities in Afghanistan.[67]

#### 4.2.1.3 Revenue

To build the simplest nontrivial model capturing the basic operations of a health facility, we introduced the variable of revenue, which is defined as the total financial resources (such as wages and salaries) used to maintain the quality of a health facility at a certain level. Revenue covers both capital and operational expenditures, but does not include any performance-based bonus.

### 4.2.2 Causal relationships

As shown in Figure 4.1, we identified all causal relationships. In the CLD, variables are labeled with their names, and relationships are shown as arrows between pairs of variables. All relationships are also marked with a positive or negative sign indicating the direction of influence. The four causal relationships are described in more detail below:

- (A) Revenues are provided to a health facility by government or NGO funds through a health services provision contract. The amount of fund is determined by average cost per patient and the estimated number of patients covered by this health facility.

- (B) The health facility managers use the revenue to maintain infrastructure and purchase supplies and equipment. These management activities convert revenue to quality of services.

- (C) The capability of a health facility of delivering health services is fixed in a short-term period, because it takes time and effort to improve this capability. Therefore, an increment in volume of services would lead to a decrement in quality of services, if the volume is beyond a critical threshold.

- (D) An improvement in service quality attracts other patients to visit the facility, thus increasing the volume of service. This is based on the model assumption that noticeable improvements in quality will have a positive effect on demand and the volume of services. A delay was shown in Figure 4.1 because it takes several weeks for an increased perception of service quality to generate new patients.

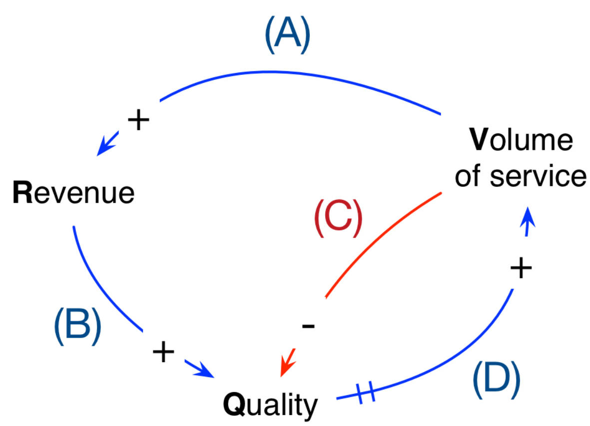


**Figure 4.1:** Causal loop diagram modeling basic operations

Two loops can be found in the CLD. The outer loop ($A \rightarrow B \rightarrow D$) that connects revenue, quality and volume show a positive influence between each variable and the subsequent one. A feedback loop (C) with a negative influence is necessary for the system to achieve an equilibrium, otherwise the outer loop would result in unlimited increases in all variables.

### 4.2.3 DDE model

With the developed CLD, we can move to a stock and flow diagram that is used to graphically represent a set of ordinary differential equations. The three variables in the CLD are modeled as stocks in the stock and flow diagram (shown as boxes in Figure 4.2). Each flow is explained below.

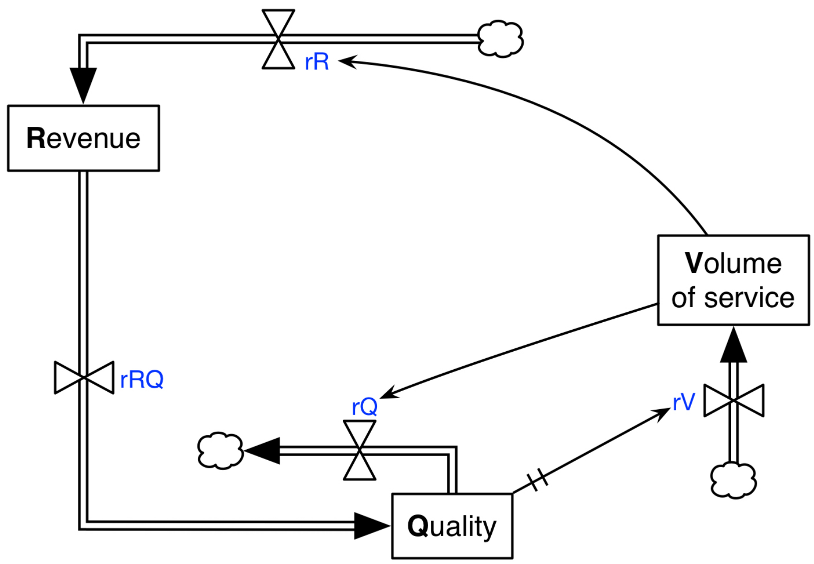


**Figure 4.2:** Flow diagram modeling basic operations

#### 4.2.3.1 Recovery rate of revenue

Recovery rate of revenue $r_R$ is defined as the rate at which revenue is provided to a health facility. The effect of volume on revenue is approximately linear when volume is very small, while revenue cannot increase infinitely even if volume of services enlarges rapidly. As many other relationships, the marginal effect of volume on revenue decreases as volume goes larger and eventually approaches zero. To model this behavior, we introduced a Logistic function

$$\mathcal{L}(x) = \frac{1 - \exp(-kx)}{1 + \exp(-kx)} \tag{4.1}$$

where $k$ is a parameter to control the curvature of the Logistic function. As shown in Figure 4.3, as $k$ increases, the Logistic function becomes steeper. In this research we used $k = 2$.

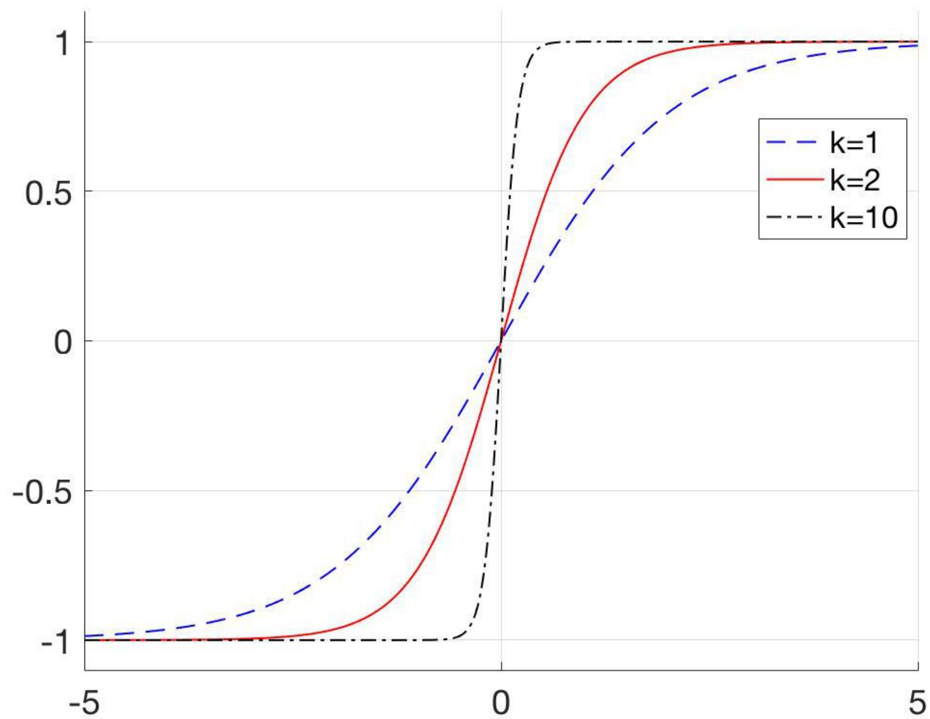


**Figure 4.3:** Demonstration of the Logistic function and the curvature parameter $k$

With the Logistic transformation, we can define $r_R$ to be proportional to transformed volume of services. The coefficient $\alpha$ is determined from survey data, through a model calibration process.

$$r_R = \alpha \cdot \mathcal{L}(V_t) \tag{4.2}$$

#### 4.2.3.2 Conversion rate of revenue

The conversion rate of revenue $r_{RQ}$ to quality is the rate at which a health facility's revenue improves the quality of services. The causal relationship (B) in Figure 4.1 is converted to a flow from revenue to quality, modeling the conversion from financial resources in revenue to a specific amount of quality, with a conversion rate $r_{RQ}$. It is reasonable to assume a fixed portion of revenue will be used to maintain quality. The key feature of this flow is that the source variable essentially sacrifices itself in order to increase the destination variable.

$$r_{RQ} = \alpha \cdot R_t \tag{4.3}$$

#### 4.2.3.3 Depletion rate of quality

The depletion rate of quality $r_Q$ is the rate at which the quality of services declines as the volume of service increases. In accordance with reality, quality in the model exhibits a decaying effect: quality tends to decrease in time unless there are sufficient resources to maintain quality at a constant level. The rate of quality decay is regulated by the value of volume of service. The relationship is different from a flow because no conversion is involved.

$$r_Q = \alpha \cdot \mathcal{L}(V_t) \tag{4.4}$$

#### 4.2.3.4 Recovery rate of volume

The recovery rate of volume $r_V$ is the rate at which the volume of services increases in response to an increase in the quality of service. Volume will increase as HF quality gets better, but it is important to note that this does not involve a conversion. No amount of quality can be converted to volume, although it can boost the increment of volume. In addition, this effect is delayed so that $r_V$ is proportional to quality at an earlier time.

$$r_V = \alpha \cdot \mathcal{L}(Q_{t-\Delta t}) \tag{4.5}$$

#### 4.2.3.5 Summary

Based on the stock and flow diagram, we can build a model of DDEs. The model is not calibrated and only tries to simulate the system qualitatively. The parameters in the DDEs are determined in a way such that the model generates visually meaningful results. The purpose of the model is to provide insights into how key implementation processes could influence outcomes of P4P interventions.

$$\frac{\mathrm{d}\,R}{\mathrm{d}\,t} = 0.3 \cdot \mathcal{L}(V) - 0.2 \cdot R \tag{4.6}$$

$$\frac{\mathrm{d}\,Q}{\mathrm{d}\,t} = 0.2 \cdot R - 0.3 \cdot \mathcal{L}(V) \tag{4.7}$$

$$\frac{\mathrm{d}\,V}{\mathrm{d}\,t} = 0.1 \cdot \mathcal{L}(Q_{t-\Delta t}) \tag{4.8}$$

### 4.2.4 Results and discussion

By solving the DDEs with initial conditions, we can get the results shown in Figure 4.4. To allow straightforward interpretation of the results, we use the Logistic transformed quality and volume, so that $-1, 0, 1$ correspond to far below average, average and far above average, respectively. The baseline model satisfies our model assumption that a health facility, given sufficient funding, should have average quality and volume at equilibrium.

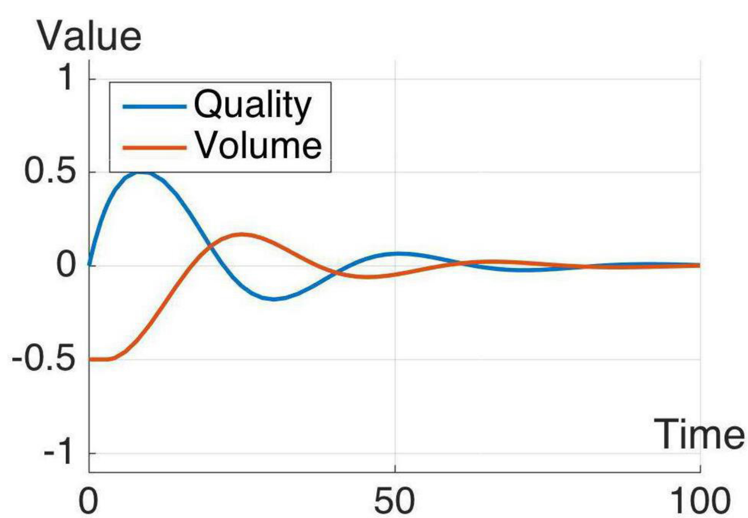


**Figure 4.4:** Results of baseline model

# 4.3 Incorporating P4P, gaming and motivation

## 4.3.1 New variables

In the advanced model we introduce P4P, gaming, motivation and other auxiliary variables.

### 4.3.1.1 P4P bonus

The amount of performance bonus is directly based on the extra volume of service of a health facility. Before the actual allocation of payment, a subset of the volume data chosen at random was verified by independent monitors, who visit patients' home to access their health service satisfaction.[66]

While P4P could be negative or positive from a mathematical point of view, we do not allow P4P to be negative so that a health facility will not be penalized if its volume of service is below average. As studies[68] suggest, the disbursement of P4P was delayed due to technical difficulties. Therefore, the amount of P4P is assumed to be proportional to the volume of service a certain time before. We denote $f_{\mathrm{P4P}}$ to be the parameter that influences the magnitude of P4P.

$$\mathrm{P4P} = \max\left\{0, f_{\mathrm{P4P}} \cdot \mathcal{L}(V_{t-\Delta t})\right\} \tag{4.9}$$

#### 4.3.1.2 Gaming

Gaming is defined as the activities of health workers who aim to get more P4P bonuses than warranted. It is assumed that a bilateral relationship exists between P4P and gaming: the possibility of getting P4P stimulates gaming, which in turn increases P4P. In the model, gaming is defined to be the exponentiation of the sum of baseline gaming $G_0$ and the portion caused by P4P.

$$G = G_0 \cdot \alpha^{\beta^{\mathrm{P4P}}-1} \tag{4.10}$$

#### 4.3.1.3 Extrinsic motivation

The theory of P4P is based on the assumption that monetary incentives could strenthen the extrinsic motivation of health workers. Extrinsic motivation differs from intrinsic motivation in that it is responsive to monetary and/or non-monetary incentives.[69,70] We introduce a variable to assess the extent to which the health workers feel that certain aspects of their job were motivated by P4P. Extrinsic motivation is proportional to the amount of P4P and affects the conversion rate of revenue to quality and the recovery rate of the volume of services. Some baseline motivation $M_0$ is assumed to exist among health workers independent on the P4P bonuses.

$$M = M_0 \cdot \alpha^{\beta \cdot \mathrm{P4P} - \gamma \cdot G} \tag{4.11}$$

### 4.3.2 Causal loops

The theory of P4P is based on the assumption that monetary bonuses provided to health workers can improve their quality and volume of services by stimulating their extrinsic motivation.[68,70] If given sufficient bonuses in the optimal way, health workers are expected to further improve quality of the health facility and thereby attract new clients. The bonuses in themselves are a part of revenue because they help maintain quality at a certain level. Therefore, in Figure 4.5, positive causal relationships are added from P4P to revenue and extrinsic motivation, and from extrinsic motivation to volume and quality of services.

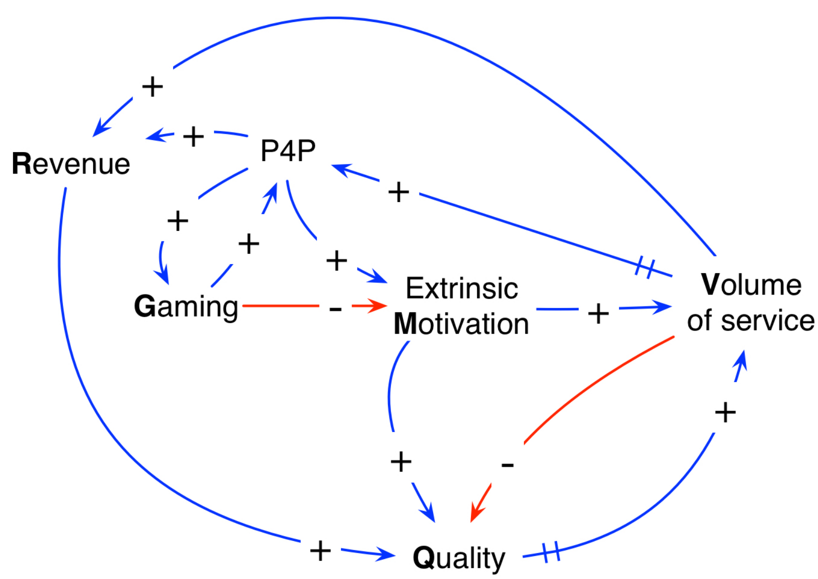


**Figure 4.5:** Causal loop diagram modeling P4P, gaming and motivation

As we argued before, positive relationships exist between P4P and gaming. On the other hand, it is entirely possible that health workers act for the sole purpose of getting more performance-based bonuses. Such behaviors may include cheating with service volume reports and colluding with corrupt monitors who are in charge of approving and verifying P4P.[71,72] Hence, health workers can game the system to get P4P without actually taking actions to improve their performance. The health workers who make real efforts to improve service quality may be discouraged by their colleagues who game the system to get the same or even more bonuses. A negative arrow is added from gaming to extrinsic motivation to reflect this possibility.

### 4.3.3 DDE model

In accordance with the updates in the causal loop diagram (Figure 4.5), we added a few new flows, arrows and stocks in Figure 4.6. P4P is modeled as an extra flow replenishing revenue, with magnitude that primarily depends on the volume of service a certain time earlier. There is a delay because in practice P4P in the current period is determined based on the volume of service of the previous period. P4P bonuses affect extrinsic motivation positively. Extrinsic motivation boosts the conversion rate from revenue to quality of service and the recovery rate of volume of service. Gaming does harm to quality of service and extrinsic motivation, but has a positive effect on P4P bonuses. A mutually strengthening feedback loop exists between P4P and gaming. We call the previous model baseline because if we set P4P, extrinsic motivation and gaming variables to be zero, then the model reduces to the baseline model.

The set of delayed ordinary differential equations are given by Equation (4.12) - (4.14) below. We scaled all stock variables such that zero corresponds to baseline

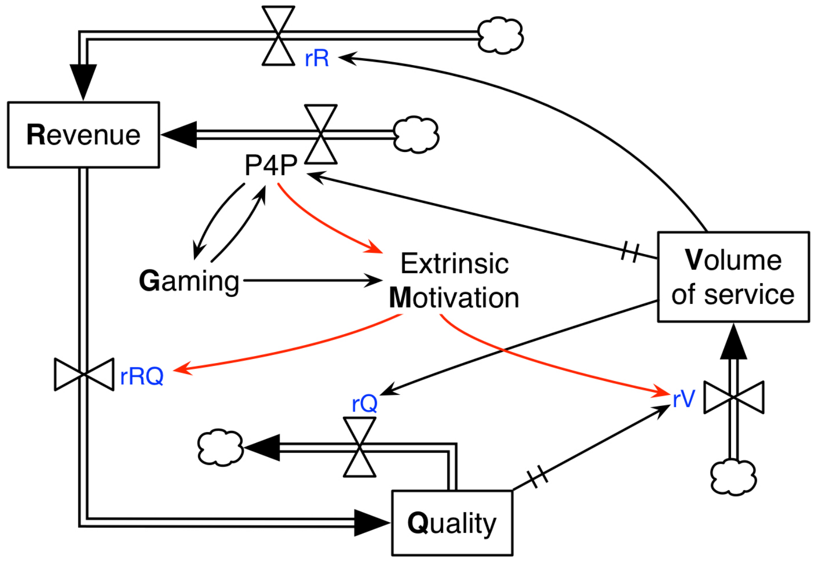


**Figure 4.6:** Flow diagram modeling P4P, gaming and motivation

values. This is convenient in interpreting the model outputs. The modifiers due to extrinsic motivation and gaming are formulated in different ways according to whether volume or quality is positive or negative.

$$\frac{\mathrm{d}\,R}{\mathrm{d}\,t} = 0.3 \cdot \mathcal{L}(V_t) - 0.2 \cdot R \cdot M + \mathrm{P4P} \tag{4.12}$$

$$\frac{\mathrm{d}\,Q}{\mathrm{d}\,t} = 0.2 \cdot R \cdot M - \begin{cases} 0.3 \cdot \mathcal{L}(V_t) \cdot G/M & \text{if } V_t > 0 \\ 0.3 \cdot \mathcal{L}(V_t) \cdot M/G & \text{otherwise} \end{cases} \tag{4.13}$$

$$\frac{\mathrm{d}\,V}{\mathrm{d}\,t} = \begin{cases} 0.1 \cdot \mathcal{L}(Q_{t-\Delta t}) \cdot M & \text{if } Q_{t-\Delta t} > 0 \\ 0.1 \cdot \mathcal{L}(Q_{t-\Delta t})/M & \text{otherwise} \end{cases} \tag{4.14}$$

## 4.4 Scenarios analysis and discussions

In this section, we use our model to simulate the effect of P4P in different allocation scenarios. There is not a standard approach to allocate the P4P bonuses within a health facility among health workers. Studies show that HF managers tend to distribute these bonuses in one of the three ways:[68]

1. Bonuses allocated to all staff members equally. This is the easiest to implement.
2. Bonuses allocated proportional to health worker salaries.
3. Bonuses allocated based on the direct contributions of the individual health workers to services that triggered the P4P payments.

In all simulations, we let a health facility start with average quality ($\mathcal{L}Q_0 = 0$) and below-average volume ($\mathcal{L}V_0 = -0.5$). The volume deficit was introduced so that we could examine whether the various scenarios could converge to an equilibrium with higher quality and volume. We first conduct the baseline experiment with P4P only (no extrinsic motivation, gaming or P4P delay), and in each scenario we answer the question: how much extra P4P bonus is required to yield the same level of performance as in the baseline? The average of volume and quality of service was used as the performance indicator.

### 4.4.1 P4P only

"P4P only" is chosen as the baseline scenario. In this case, the time delay of P4P disbursement, $\Delta t$, is set to zero to model timely disbursement. It is worth mentioning that other delays remain positive, such as the delay between improved quality and increased volume. Figure 4.7 shows the result. The system takes 59 units of time to reach the final state: both volume and quality of the health facility are above average.

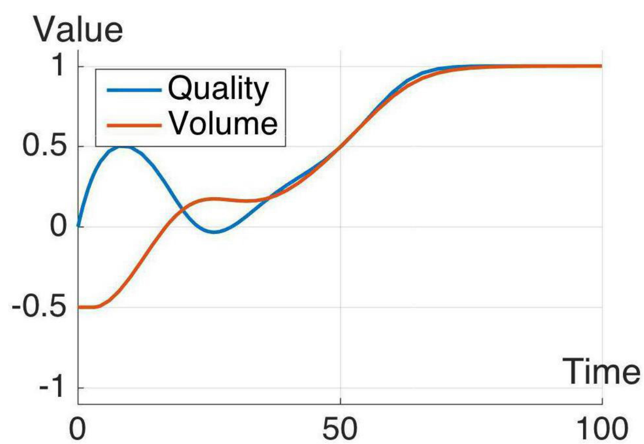


**Figure 4.7:** P4P only. $f_{P4P} = 0.2$, no time delay of P4P. Time to equilibrium = 59

### 4.4.2 Equal allocation to all staff

Studies show that the extent to which health workers are motivated is determined by the relative size of their bonuses compared to their regular earnings.[73] In the case of equal allocation, the bonuses may be comparable only for low-level workers due to their relatively low wages. Then we can assume that extrinsic motivation and gaming will be at a moderate level. If we let $M_0 = 0.1$ and $G_0 = 0.3$, keeping $f_{P4P} = 0.2$ and introducing a 3-month delay of P4P disbursement to simulate the actual situation, then we get results shown in Figure 4.8. If we want to achieve the same performance as in the baseline scenario (Section 4.4.1), we need $f_{P4P} = 0.823$ which is 411% of the baseline bonus.

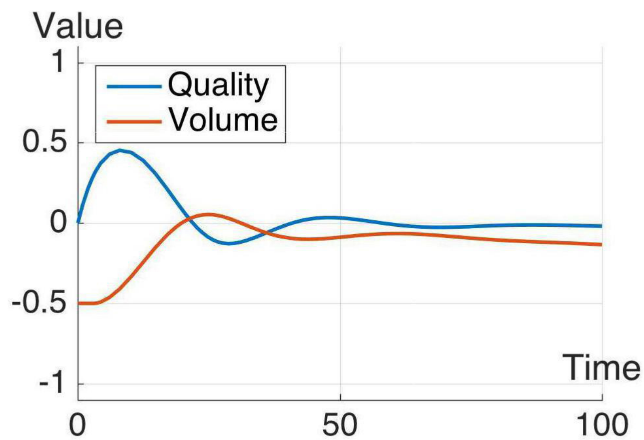


**Figure 4.8:** Equal bonus allocation strategy

### 4.4.3 Proportionate to salaries

It is reasonable to assume that the leadership of a health facility receive more salaries than health workers. If bonuses are allocated based on salaries, then the leadership gets relatively high bonuses. Since most of the effects to improve quality and volume need to be carried out by the lower-level health workers and since these workers will receive relatively low performance-based bonuses, they will not be motivated to act. On the other hand, it is the leadership's responsibility to compile and finalize the data reported by each health workers or middle-level managers, and thus they are better positioned to game the system for more bonuses. Therefore, the strategy would be harmful to performance. We let $M_0 = 0.05$ and $G_0 = 0.8$ for this scenario and we get results shown in Figure 4.9. In this case, increasing P4P would not have a beneficial effect.

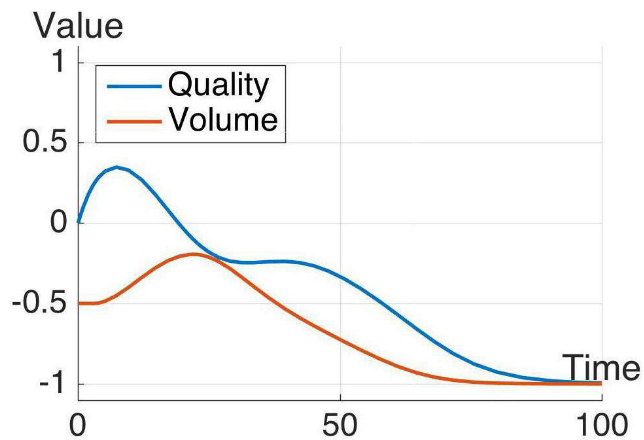


**Figure 4.9:** Bonuses proportional to salary

### 4.4.4 Proportionate to contribution

If we can recognize each health worker's efforts in improving the health facility's performance, then each individual health worker would be strongly motivated to do so. Leadership would be less prone to game because they will need to demonstrably contribute to improvement of performance in order to get performance-based bonuses. For this scenario, we let $M_0 = 0.3$ and $G_0 = 0.05$ to get the results shown in Figure 4.10. If we want to achieve the same performance as in the baseline scenario (Section 4.4.1), we need $f_{P4P} = 0.22$ which is 110% of that in the baseline scenario.

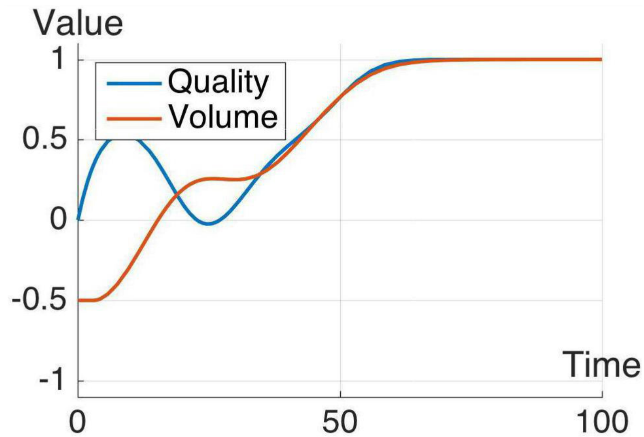


**Figure 4.10:** Bonuses proportional to contribution

# 4.5 Conclusions

An effective P4P intervention should deliver the bonus incentives to key health workers at the health facility level. Specific strategies that could increase the probability of a successful P4P intervention include prompt disbursement of performance-based bonus, adequate levels of bonus according to health worker's contribution, and frequent monitoring on the reported volume of services. A P4P intervention, if designed poorly, could be harmful to the public health service delivery system by encouraging gaming and damaging extrinsic motivation.

# Chapter 5

# Future Work

## 5.1 Limitations and future work on the obesity ABM

While we demonstrate that our ABM can simulate children growth and obesity within an inner-city food environment, there are several limitations of the model. We have previously described several of these limitations, and we briefly summarize the key issues here.

1. The model only considered children walking to school, while in reality some children take school buses or public transportation to school. The model also did not distinguish between schools of different levels.

2. The model does not account for social interactions which can influence eating

behaviors.[74] For instance, peer pressure can be positive or negative. People may eat healthier food or exercise more if they are in the right environment. On the other hand, people in an obesogenic environment may not even realize that their weight is unhealthy. Our next step is to employ graphical models to capture the dependency of children's preferences on local environment.

3. In the current model, children purchase their food based on store information, food availability and promotions. Children's purchasing preferences and storeowner's stocking strategies are assumed to be static in the model, but they should be dynamic and interact with each other as they do in the real world. Store owners will adjust their inventory according to children's purchasing preferences, which implies a feedback loop will need to be included to account for this interaction between children and store owners. Future versions of the ABM would benefit from incorporating system dynamic sub-models for the food sources, such that storeowners can adjust their stocking, pricing, and promotional policies based on children's purchasing behaviors.

## 5.2 Limitations and future work on the community resilience system dynamics model

It has been demonstrated that the model can be used as a decision support tool for public policy makers. This tool would be improved through the following research tasks.

### 5.2.1 Calibration and validation

In the current model, the time scale was arbitrarily set to create CF trajectories with approximately a one-year time span before nearly fully recovery. We set the other model parameters based on expert opinion. In future work, we would calibrate the model parameters based on observed patterns of CF after natural or pandemic disasters.

Another important work is validation. The model yields a predicted curve of community functioning, which resembles the often cited functioning curve of a Christchurch hospital[75] after the 2011 Christchurch Earthquake. We have initiated the validation process by choosing six events and associated counties as shown in Table 5.1. Upon obtaining CF curves during and after these events at a relatively fine time resolution, we will be able to validate the model output with the observed CF curves.

**Table 5.1:** Counties and events chosen for future validation

| **State** | **County (FIPS)** | **Event** | **Year** |
|---|---|---|---|
| Missouri | Jasper County (29097) | Joplin Tornadoes | 2011 |
| California | Shasta County (6089) | California Wildfires | 2013 |
| Oklahoma | Cleveland County (40027) | Moore, OK Tornadoes | 2013 |
| New York | Bronx County (36005)<br>Kings County (36047)<br>New York County (36061)<br>Queens County (36081)<br>Richmond County (36085) | Super storm Sandy | 2012 |
| Texas | McLennan County (48309) | Non-Purposive Explosion | 2013 |
| Colorado | Boulder County (8013) | Colorado Flash Floods | 2013 |

### 5.2.2 Expansion of the model

The model captures the most essential components related with community functioning, but it may be too simplistic to serve as a predictive tool. We would expand the model in the following aspects.

- Incorporating the notion of "leadership/political system effectiveness" (perhaps as a modifier on the valves for social cohesion, preparedness, and external resources).

- Explicitly including supply chain and critical infrastructure, because they are frequently identified as of prime importance, and are currently only implicitly included (and thus buried) in Engineered Systems.

- Adding details to Engineered Systems according to the specific type of event. The damage on engineered systems by an event largely depend on the nature of the event and type of engineered systems. For example, the Fukushima

Nuclear Power Plants are designed to withstand a severe earthquake, as proven by the fact that its engineered systems successfully resisted direct damage from the Great East Japan Earthquake (2011). However, its engineered systems are not capable of mitigating damage due to the strong tsunami caused by this earthquake. This weakness led to the worst nuclear disaster in history.[76]

- In the current model all counties are treated individually. A county would experience the same effect from a national event as from a localized event. However, in reality both social cohesion and preparedness / response may be influenced by other neighboring counties. In the future version of this model, we will incorporate the potentially beneficial interactions from adjacent counties.

## 5.3 Future work on the P4P system dynamics model

The system dynamics model for the Pay-For-Performance intervention in Afghanistan can be improved if additional, possibly latent, variables were added to the existing data set. Specifically, we need variables that quantify the extent of gaming in each health facility and degree of motivation among the health facilities' workers. Latent variable techniques, such as SEM (Structural Equation Modeling), may lead to estimates for gaming and motivation. Once these estimates are obtained, then they can be appended to the existing data and subsequently used to calibrate and validate our system dynamics model.

The approach would be essentially nonlinear maximum likelihood estimation (MLE), in which the unknown parameters are the coefficients and other parameters listed in Section 4.3 and the output variables are the two main stocks, quality and volume. Uncertainties in these parameters can be estimated using statistical bootstrapping,[77] in which the health facilities used in the MLE analysis are randomly sampled with replacement.

In the future, when other similar bonus-based interventions are planned in low- and middle-income countries, we would recommend survey instruments that can quantify measures related to health worker motivation. Obviously, it would be difficult if not impossible to measure gaming at the health facility level; hence indirect measures of gaming that could be of use in SEM would be of interest.

# Appendix A

# Measure Data and Source in Community Stability Research

## Notations

**ACS** American Community Survey of Census

**AHRF** Area Health Resources Files

**BRFSS** Behavioral Risk Factor Surveillance System of CDC

**CBP** County Business Patterns of Census

**CDC** Centers for Disease Control and Prevention

**CMS** Centers for Medicare & Medicaid Services

## APPENDIX A. MEASURE DATA AND SOURCE IN COMMUNITY STABILITY RESEARCH

**CHAS** Comprehensive Housing Affordability Strategy

**EPA** Environmental Protection Agency

**FCC** Federal Communications Commission

**FEMA** Federal Emergency Management Agency

**NCES** National Center for Education Statistics

**NOAA** National Oceanic and Atmospheric Administration

**NAICS** North American Industry Classification System

**HRSA** Health Resources and Services Administration

**HUD** Housing and Urban Development Office

**SAIPE** Small Area Income and Poverty Estimates of Census

**SAHIE** Small Area Health Insurance Estimates of Census

**USDA** United States Department of Agriculture

**WONDER** Wide-ranging Online Data for Epidemiologic Research of CDC

# A.1 Community Functioning (CF)

## A.1.1 Communication

### A.1.1.1 Percentage of households with Internet service over 200 kbps

The data is obtained from Form 477 (Local Telephone Competition and Broadband Reporting) collected by Federal Communications Commission (FCC). Each data entry is as of 12/30 of the corresponding year. The data is categorical, with 0: zero; 1: zero to 20%; 2: 20% to 40%; 3: 40% to 60%; 4: 60% to 80%; 3: 80% to 100%.

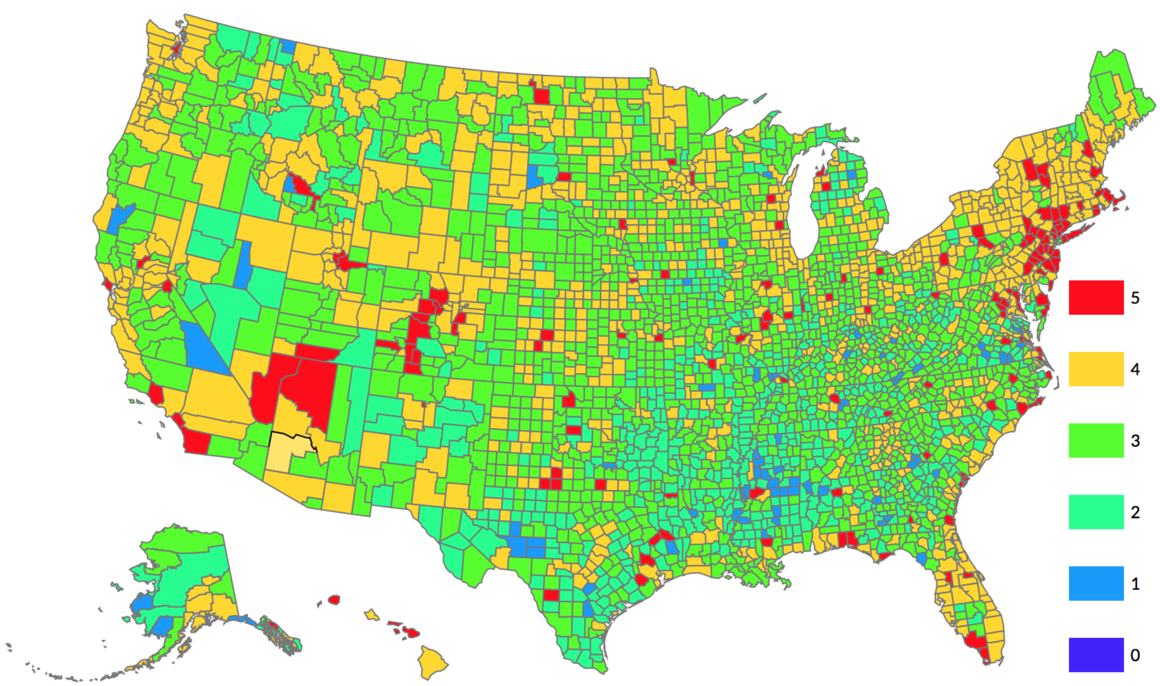


**Figure A.1:** Percentage of households with Internet service over 200 kbps (2010)

### A.1.2 Economy

#### A.1.2.1 Number of finance and insurance companies per 10k population

The data is obtained from County Business Patterns (CBP) of Census Bureau. CBP collects number of establishments, number of employees and payroll information of each county every year. The data is additionally grouped by industry, specified using NAICS code (North American Industry Classification System). For this measure we used the industry code "52" representing the industry of "Finance and Insurance".

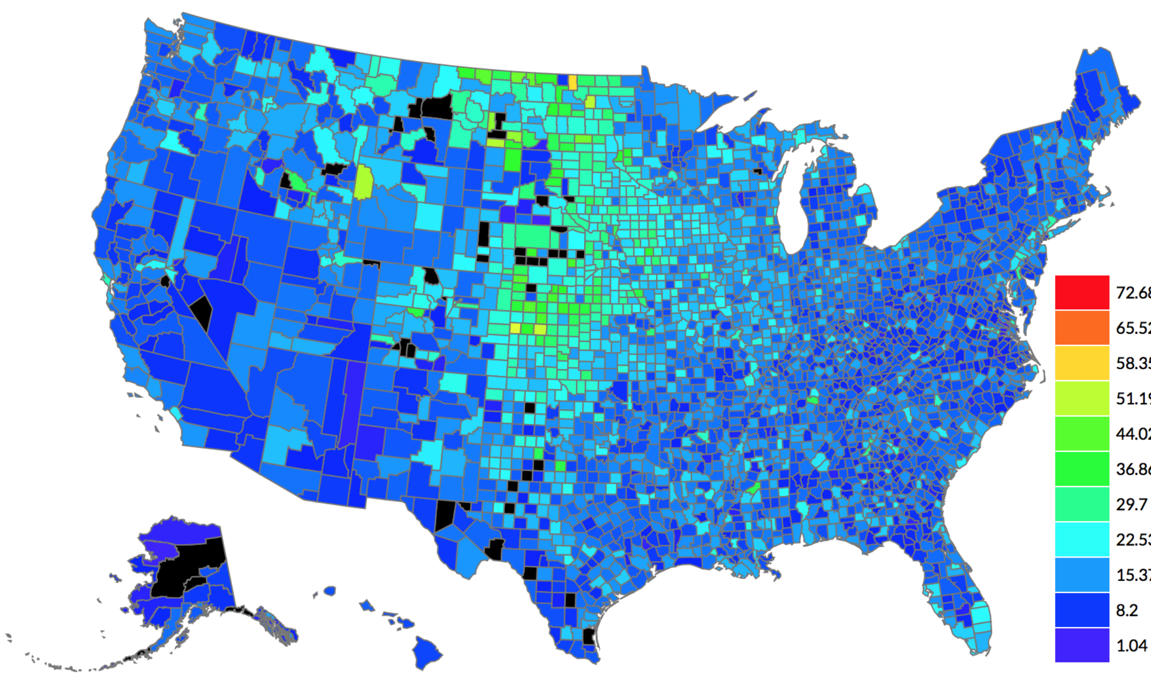


**Figure A.2:** Number of finance and insurance companies per 10k population (2010)

### A.1.2.2 Median household income

The data is directly available from Small Area Income and Poverty Estimates (SAIPE) of Census Bureau.

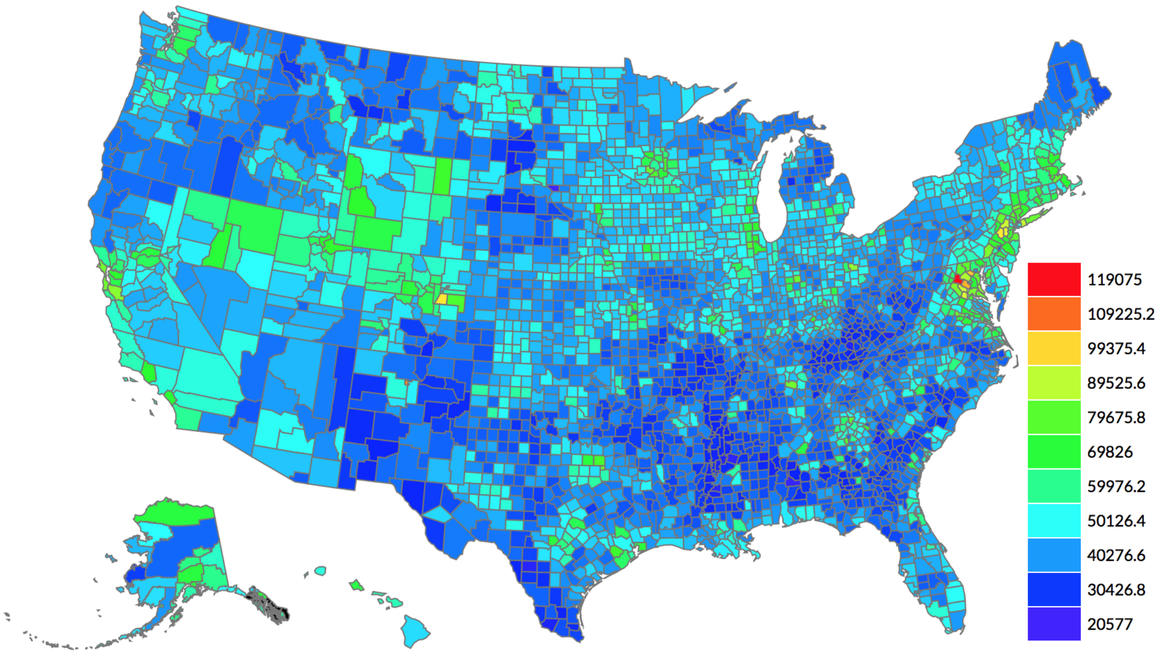


**Figure A.3:** Median household income in dollars (2010)

### A.1.2.3 Number of employers per 10k population

The data is obtained from County Business Patterns (CBP) of Census Bureau. For this measure we used all industries. It is worth to mention that all employers are counted the same way regardless of their size.

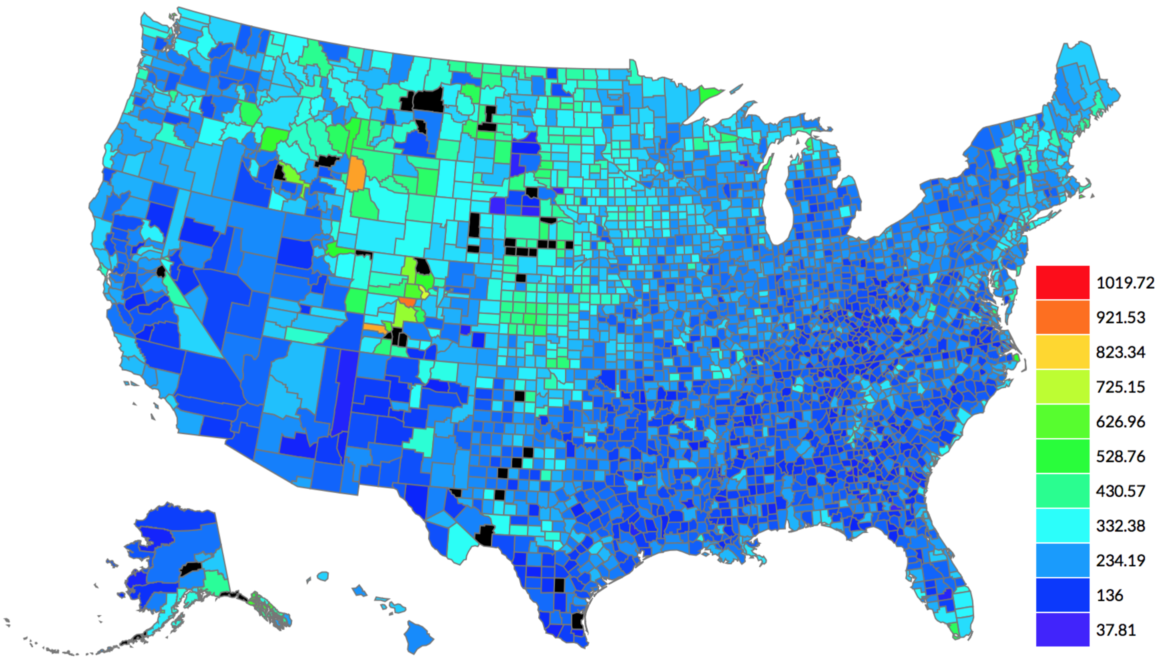


**Figure A.4:** Number of employers per 10k population (2010)

## A.1.3 Education

### A.1.3.1 Pupil/teacher ratio (public school)

The data is obtained from National Center for Education Statistics (NCES). The data year means the ending year of a school year; for example, data in 2015 means the school year 2014 - 2015. It is worth to mention that a lot counties have missing data.

### A.1.3.2 High school graduation rate

High school graduation rate is measured by the percentage of ninth graders who graduated in four years. The data is obtained from EDfacts Initiative, U.S. Depart-

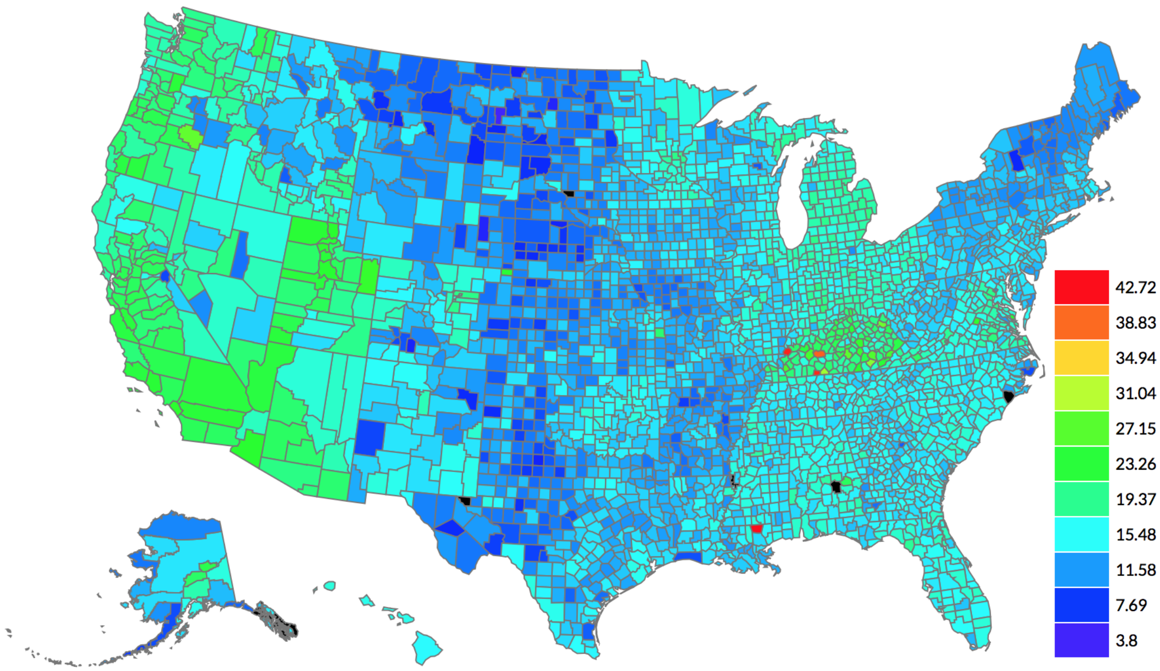


**Figure A.5:** Pupil/teacher ratio (public school) (2010)

ment of Education. A significant correlation was observed between pupil/teacher ratio and high school graduation rate.

### A.1.4 Food and water

#### A.1.4.1 Number of grocery stores per 10k population

Number of grocery stores and supermarkets is obtained from County Business Patterns (CBP) of Census Bureau. The NAICS code for this category is "445110", including establishments of supermarkets and general line of food retailing stores (such as canned and frozen foods, fresh fruits and vegetables, and fresh or prepared meats, fish, and poultry). Convenience stores and warehouse club stores are excluded.

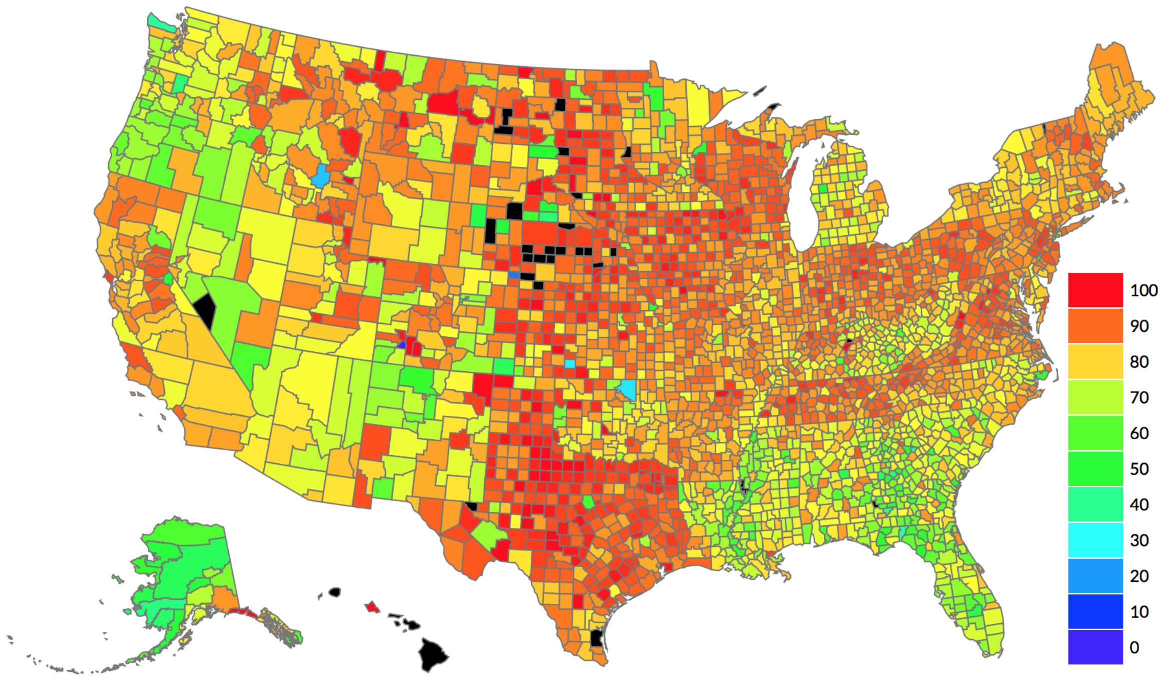


**Figure A.6:** High school graduation rate (2010)

The number of stores are then divided by population of the corresponding year.

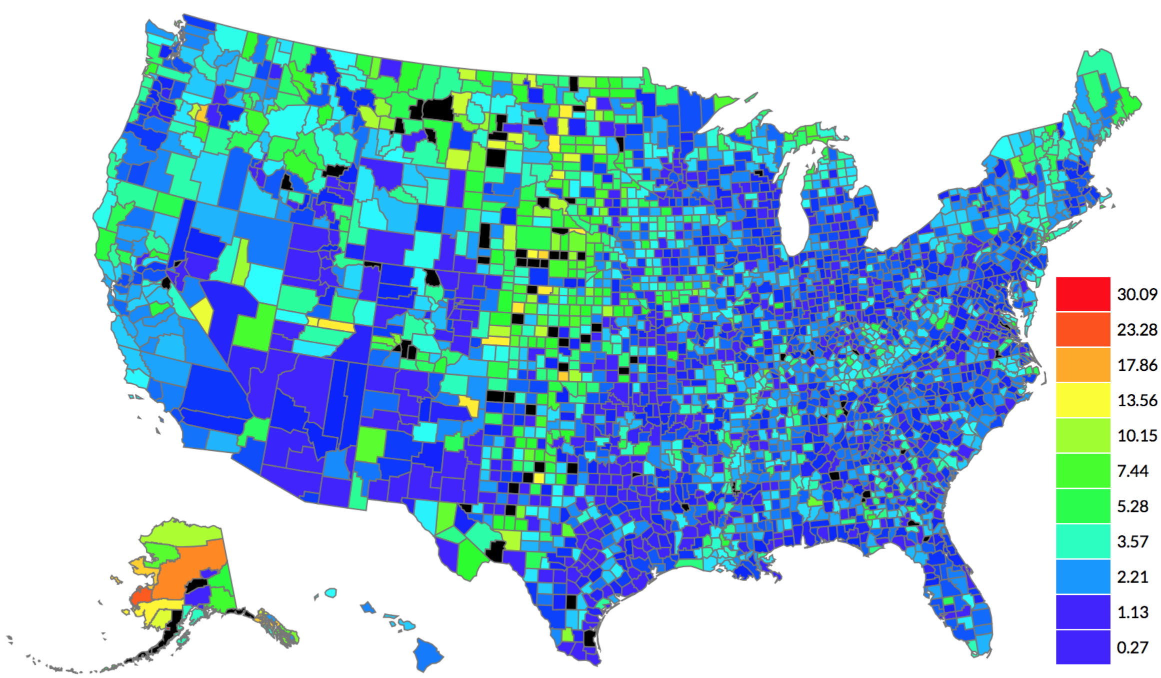


**Figure A.7:** Number of grocery stores per 10k population (2010; colored in log scale)

#### A.1.4.2 Number of grocery stores per 100 square miles

Number of grocery stores and supermarkets is obtained from (CBP) and processed in the same way as the above one. The number of stores are then divided by population of the corresponding year. The data shows that the per capita number of grocery stores is roughly the same across United States, with the exception that areas with sparse populations have relatively more and most likely smaller grocery stores.

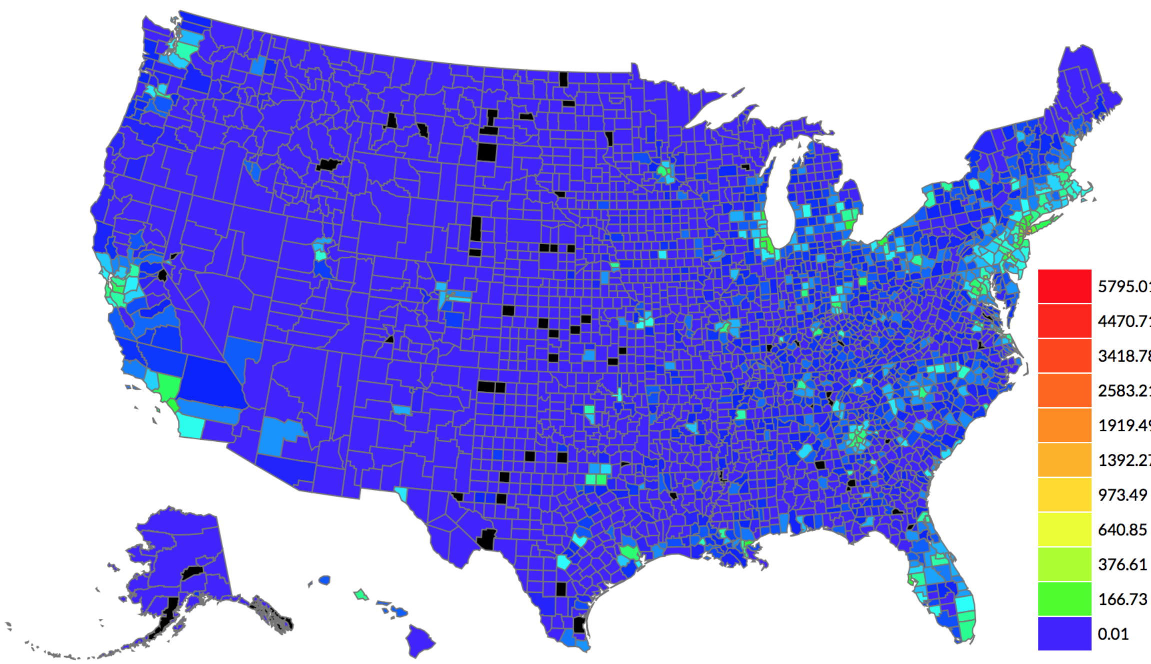


**Figure A.8:** Number of grocery stores per 100 square miles (2010; colored in log scale)

#### A.1.4.3 Percentage of population on public water

The data is obtained from Water Use Report, United States Geological Survey. The data shows strong state patterns, suggesting that this policy is usually made at the state level.

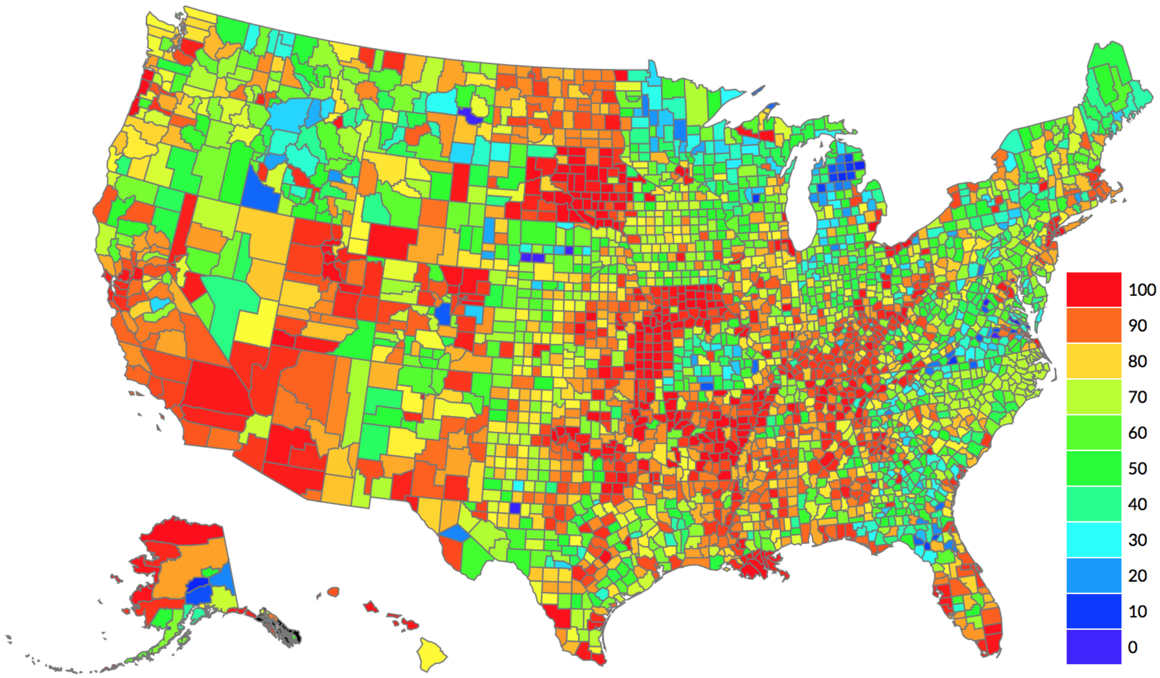


**Figure A.9:** Percentage of population on public water (2010)

#### A.1.4.4 Low access to grocery store

Percentage of Households in the county that have no car and are further than 1 mile away from a grocery store. The data is directly available in Food Environment Atlas, Economic Research Service of USDA. Alaska is shown to have exceptionally low access to grocery stores.

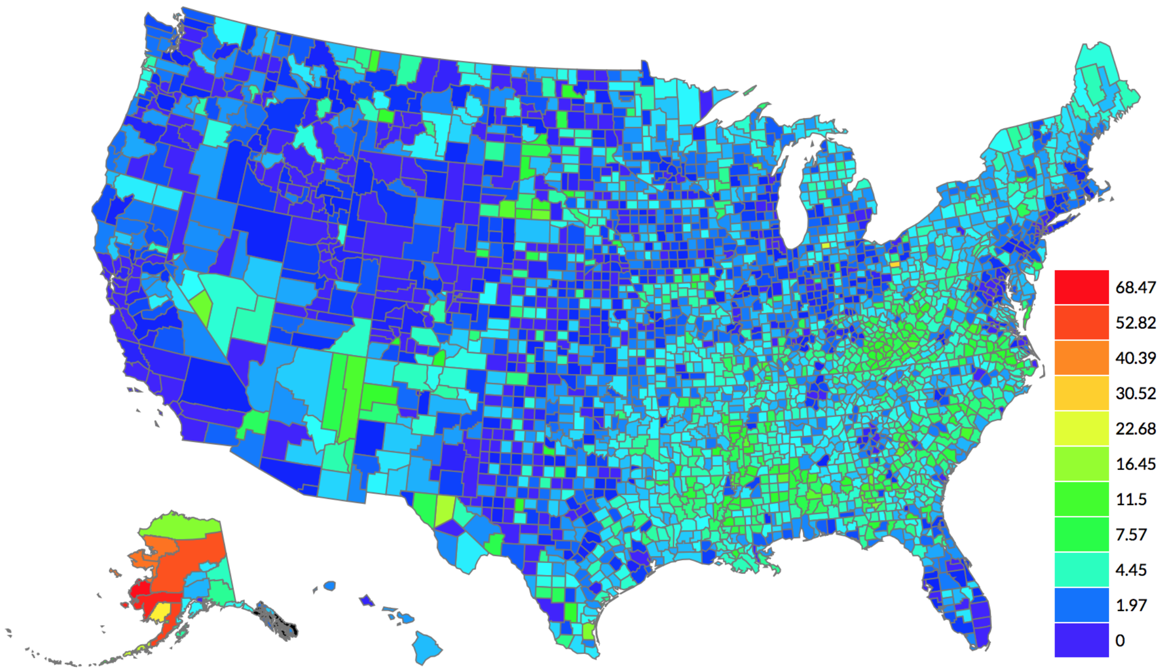


**Figure A.10:** Low access to grocery store (2010; colored in log scale)

### A.1.5 Government

#### A.1.5.1 Per capita federal government spending

The amount of government spending in thousand dollars is obtained from Federal Funds Statistics, Economic Research Service of USDA, and then divided by population of the corresponding year.

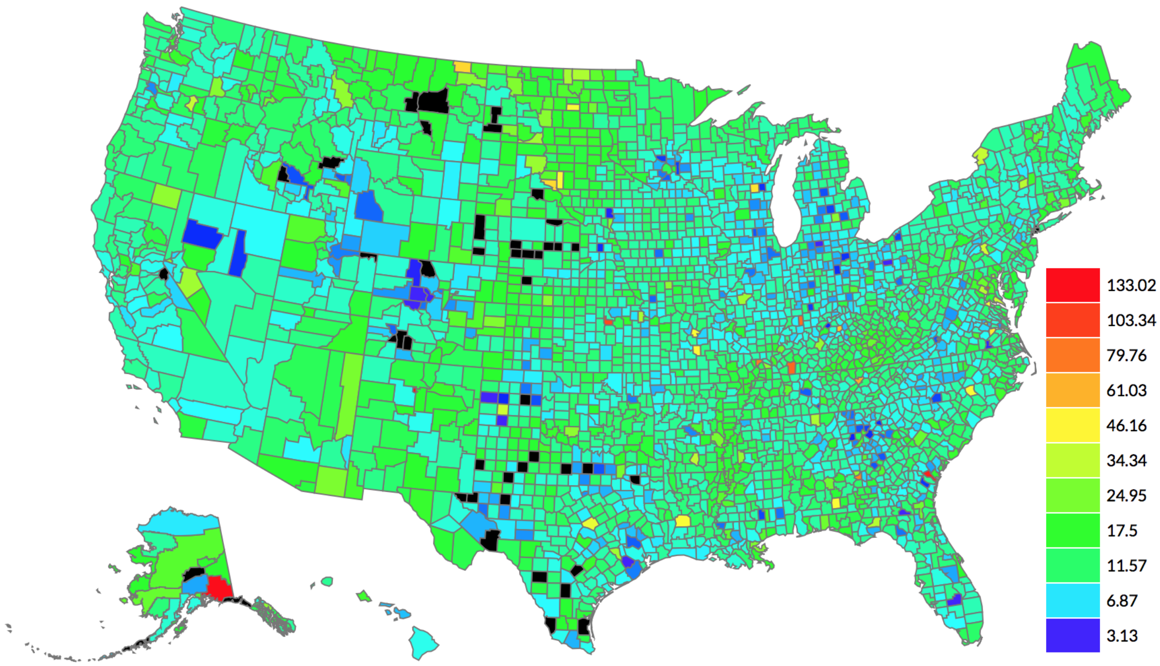


**Figure A.11:** Per capita federal government spending in 1000 dollars (2010; colored in log scale)

## A.1.6 Housing

### A.1.6.1 Percentage of household with severe problems

Household means all people, related as a family or unrelated, living in a housing unit. The data is obtained from Comprehensive Housing Affordability Strategy (CHAS) Data, Housing and Urban Development Office (HUD). A household is considered as "with severe problems" if it experiences any one or more of the following four problems:

1. is missing complete kitchen facilities

2. lacks complete plumbing facilities

3. overcrowding; there are 1 or more people living in one room on average.

4. cost burdened; a household is cost burdened if the monthly housing utility-included cost is more than 30% of monthly income (adjusted for inflation) of the household.

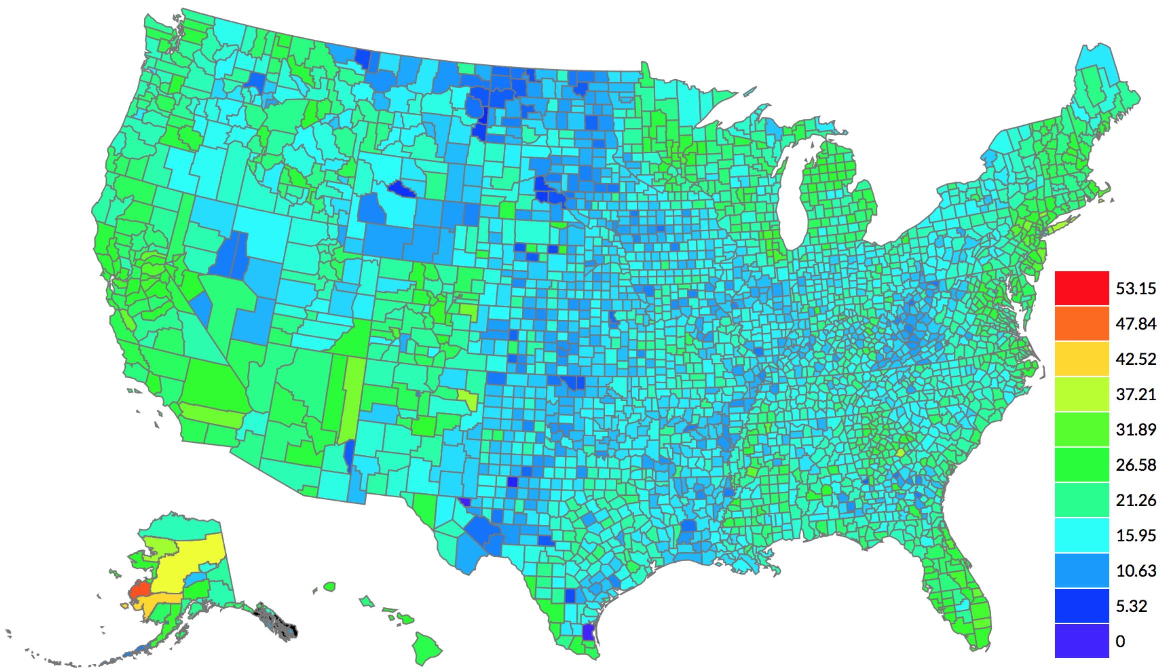


**Figure A.12:** Percentage of household with severe problems (2010)

### A.1.6.2 Number of house units per capita

The data is obtained from Census Bureau. According to Census, a housing unit is a house, an apartment, a group of rooms, or a single room occupied or intended for occupancy as separate living quarters. An outlier in the data is Hamilton County, New York, with FIPS code 36041. The county lies entirely within the Adirondack

Park and is the least populous county in New York State.

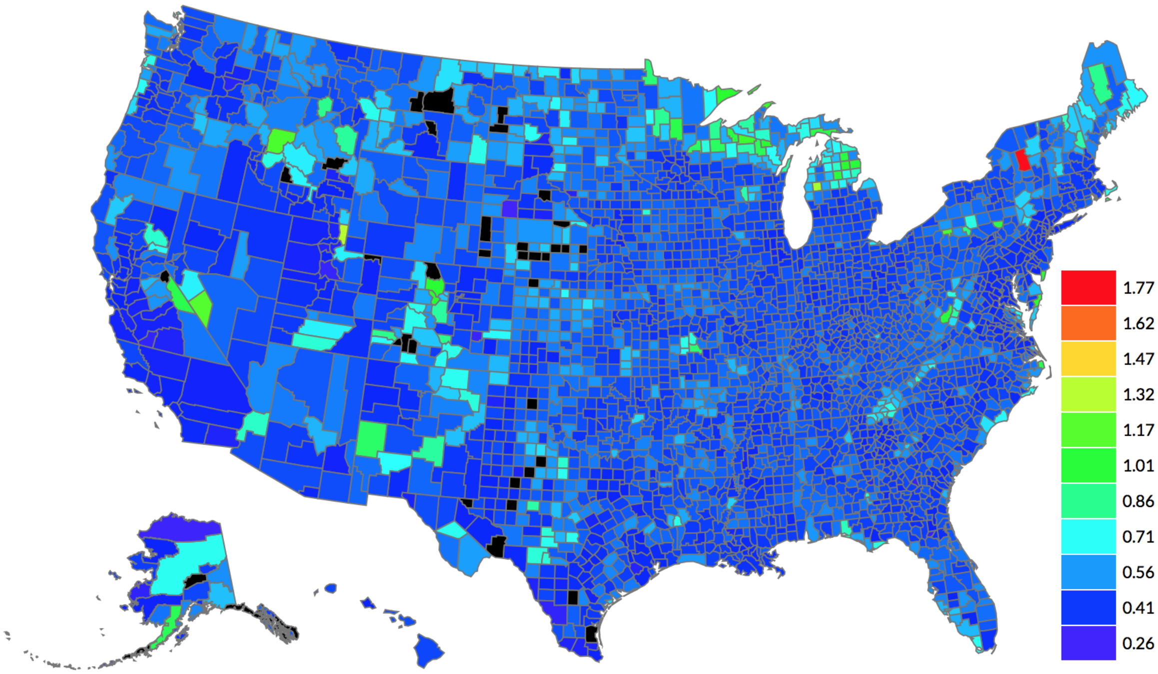


**Figure A.13:** Number of house units per capita (2010)

### A.1.7 Healthcare delivery and public health services

#### A.1.7.1 Number of mental health care providers per 10k population

The data is obtained from Centers for Medicare & Medicaid Services (CMS)

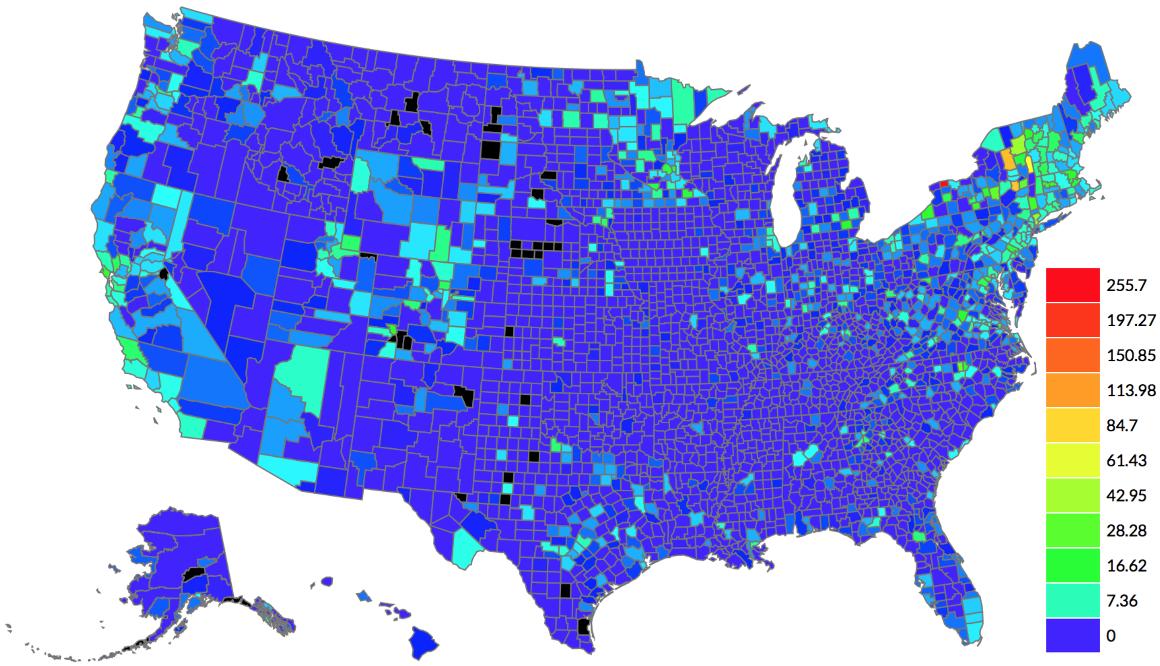


**Figure A.14:** Number of of mental health care providers per 10k population (2008; colored in log scale)

#### A.1.7.2 Number of primary care physicians per 10k population

The data is obtained from Area Health Resources Files (AHRF), Health Resources and Services Administration (HRSA)

#### A.1.7.3 Number of hospital beds per 10k population

The data is obtained from Area Health Resources Files (AHRF), Health Resources and Services Administration (HRSA)

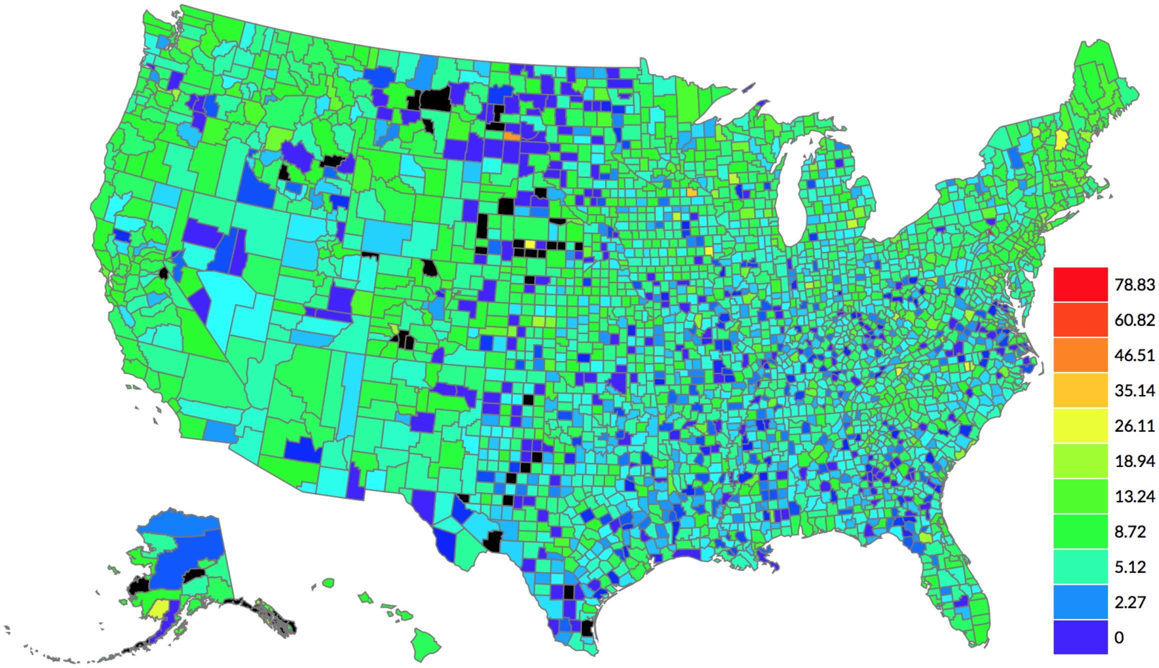


**Figure A.15:** Number of primary care physicians per 10k population (2010; colored in log scale)

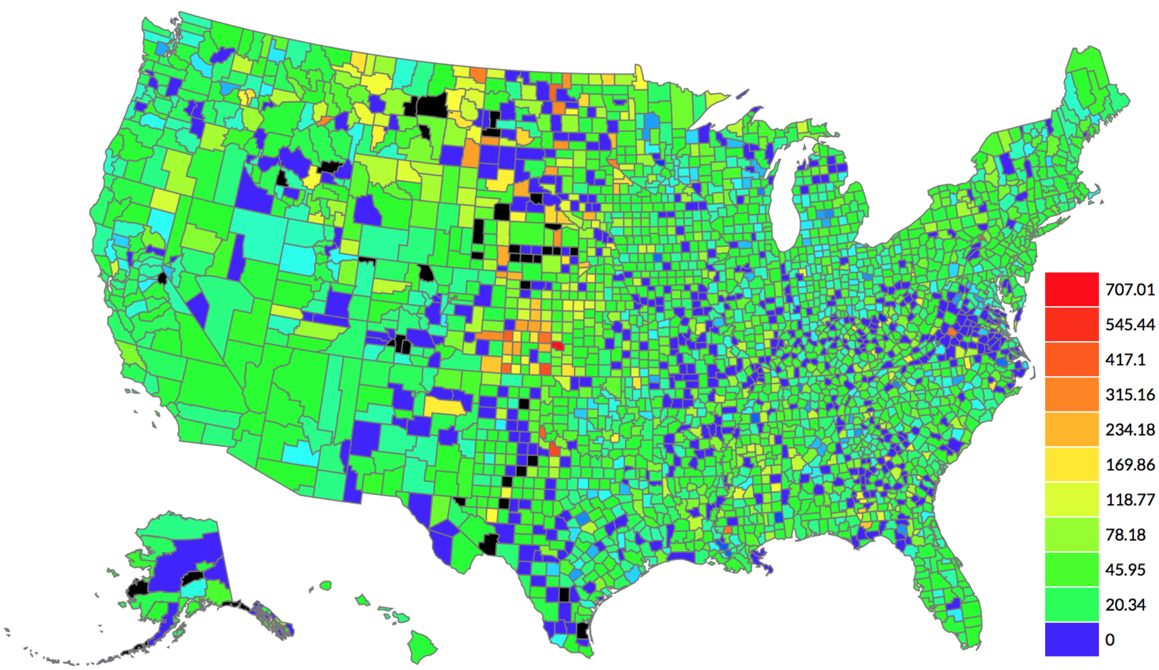


**Figure A.16:** Number of hospital beds per 10k population (2010; colored in log scale)

#### A.1.7.4 Percentage of female Medicare enrollees aged 67 to 69 that receive mammography screening

The data is obtained from Dartmouth Atlas of Health Care.

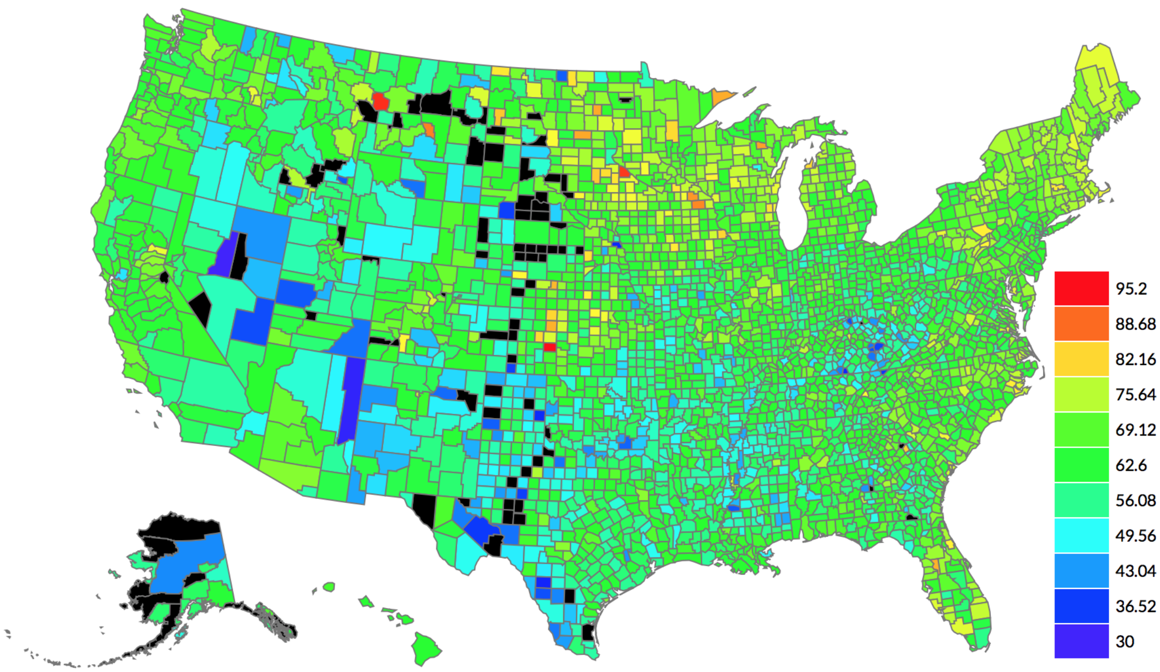


**Figure A.17:** Percentage of female Medicare enrollees aged 67 to 69 that receive mammography screening (2010)

#### A.1.7.5 Percentage of diabetic Medicare enrollees ages 65 to 75 that receive HbA1c monitoring

The data is obtained from Dartmouth Atlas of Health Care.

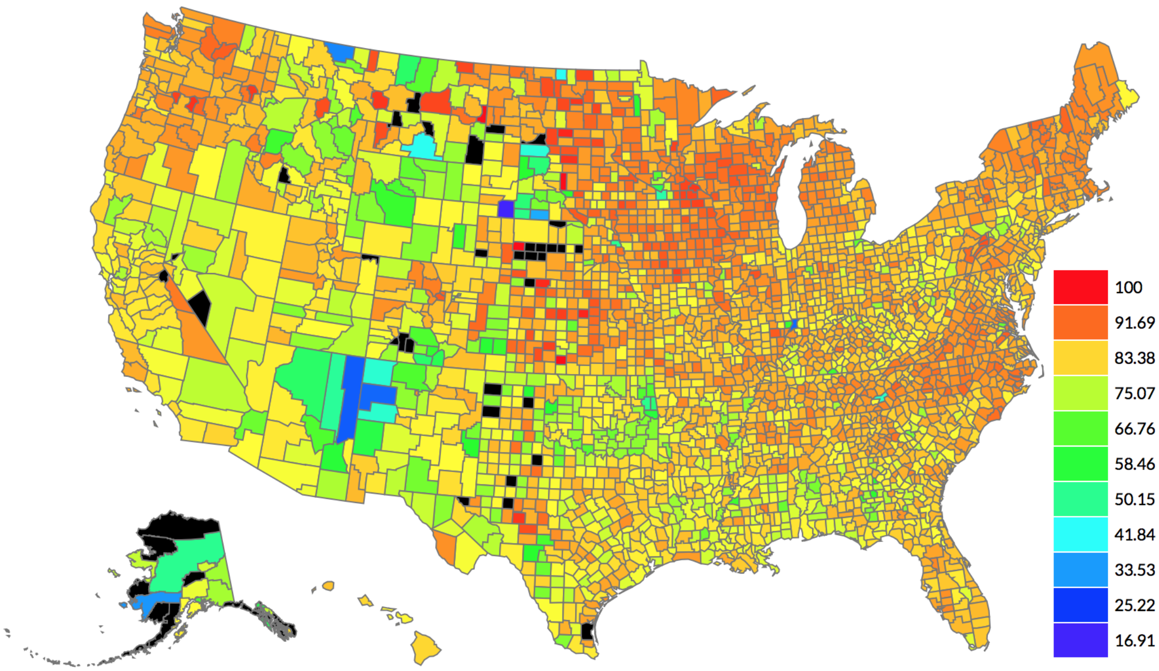


**Figure A.18:** Percentage of diabetic Medicare enrollees ages 65 to 75 that receive HbA1c monitoring (2010)

#### A.1.7.6 Percentage of uninsured adults in age group 16 to 64

The data is obtained from Model-based Small Area Health Insurance Estimates (SAHIE) for Counties, Census Bureau.

#### A.1.7.7 Percentage of adults who are current smokers

The data is obtained from Behavioral Risk Factor Surveillance System (BRFSS) of CDC. Smokers are those adults (over 18 years old) who reported have smoked more than 100 cigarettes during their lifetime and who now smoke every day or some days. An interesting fact to note is that smokers in Utah are relatively rare due to the religion of Mormonism.

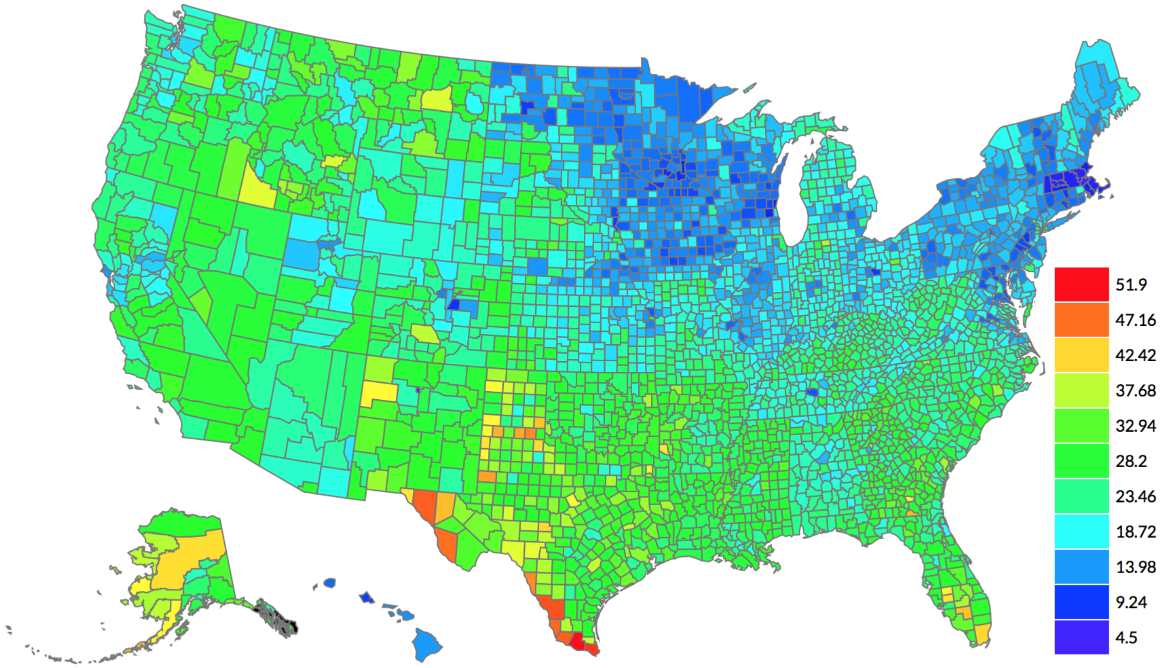


**Figure A.19:** Percentage of uninsured adults in age group 16 to 64 (2010)

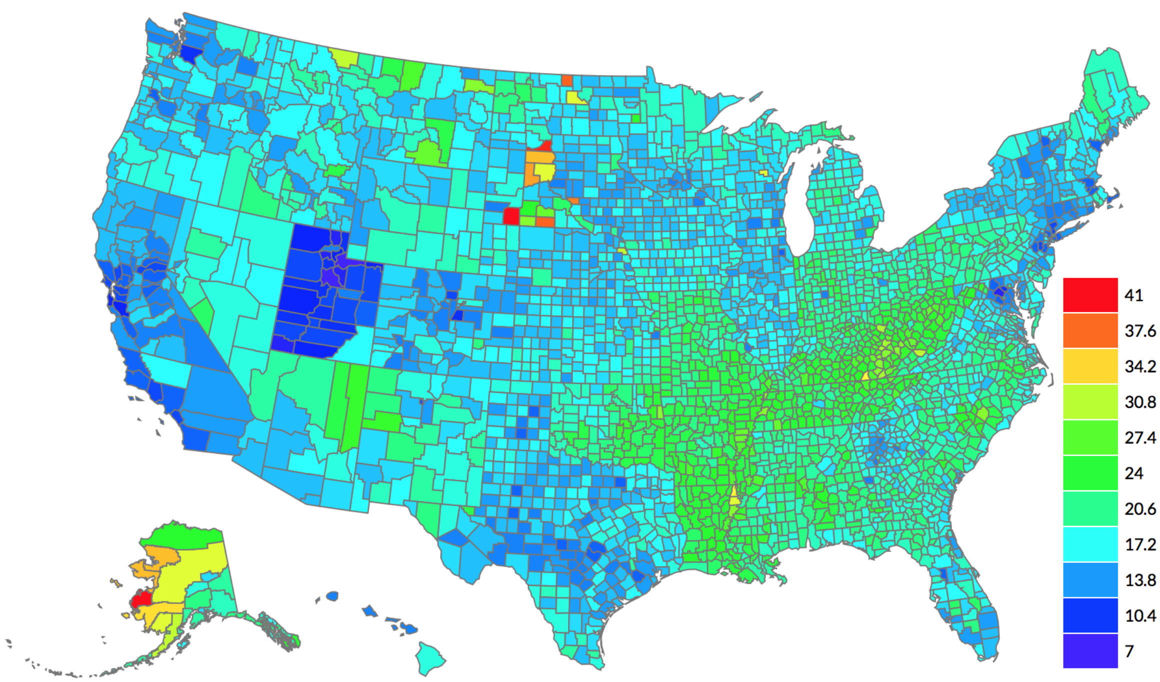


**Figure A.20:** Percentage of adults who are current smokers (2014)

#### A.1.7.8 Percentage of leisure-time physical inactivity prevalence

The data is obtained from CDC Diabetes Statistics. It has been widely acknowledged that physical inactivity is closely correlated with obesity and other chronic diseases. The definition of physical inactivity can be found in Physical activity guidelines advisory committee report.[78]

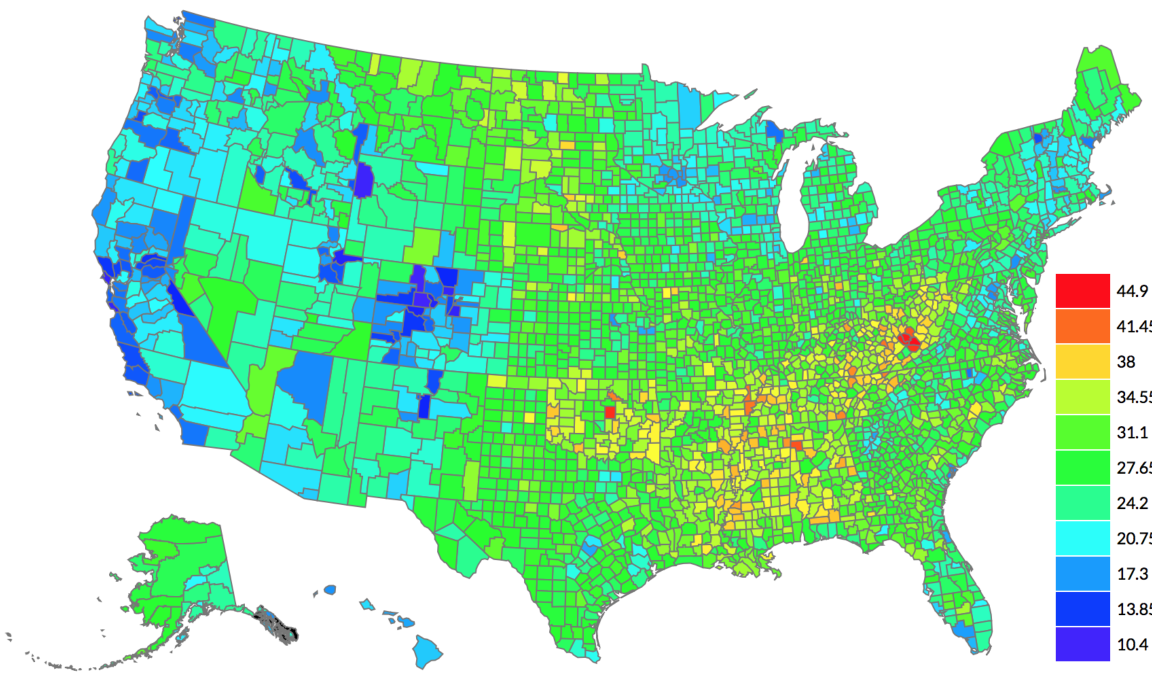


**Figure A.21:** Percentage of leisure-time physical inactivity prevalence (2010)

## A.1.8 Nurturing and care

### A.1.8.1 Number of nursing care facilities per 10k population

The data is obtained from County Business Patterns (CBP) of Census Bureau. The measured used NAICS code "623110" which represents "Nursing Care Facilities (Skilled Nursing Facilities)".

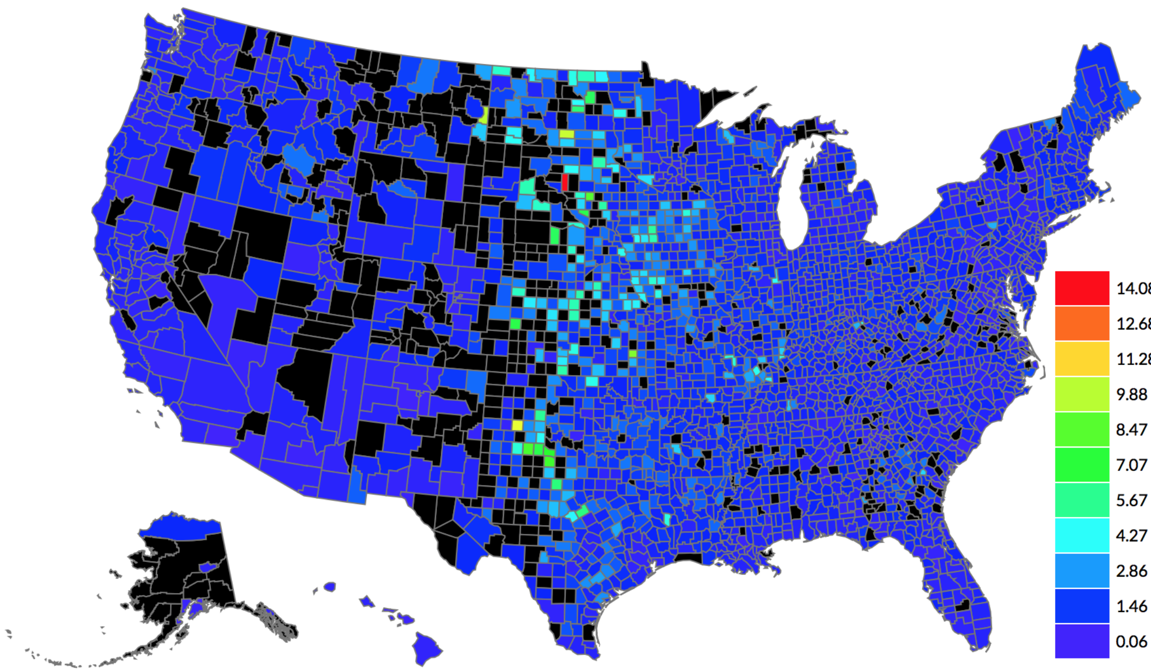


**Figure A.22:** Number of nursing care facilities per 10k population (2010)

## A.1.9 Transportation

### A.1.9.1 Percentage of population walk or cycle to work

The data is obtained from American Community Survey (ACS), Census Bureau.

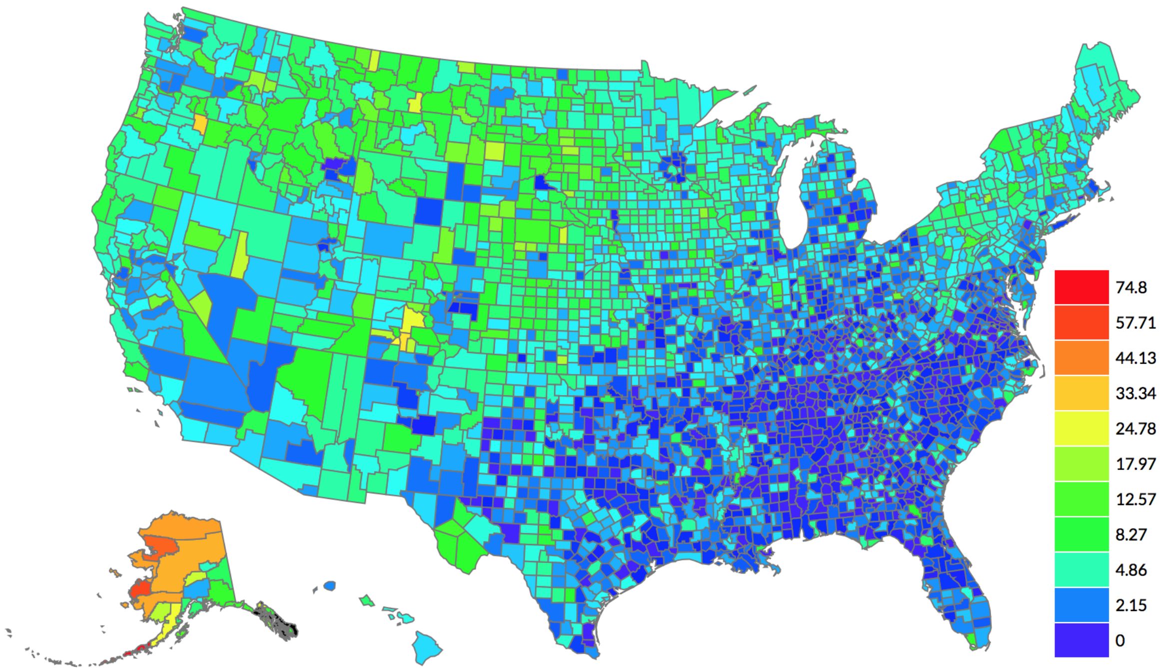


**Figure A.23:** Percentage of population walk or cycle to work (2010; colored in log scale)

## A.1.10 Population well being

### A.1.10.1 Average life expectancy

The data is obtained from Global Health Data Exchange.

### A.1.10.2 All cause mortality per 100k population

The data is obtained from Wide-ranging Online Data for Epidemiologic Research (WONDER), CDC.

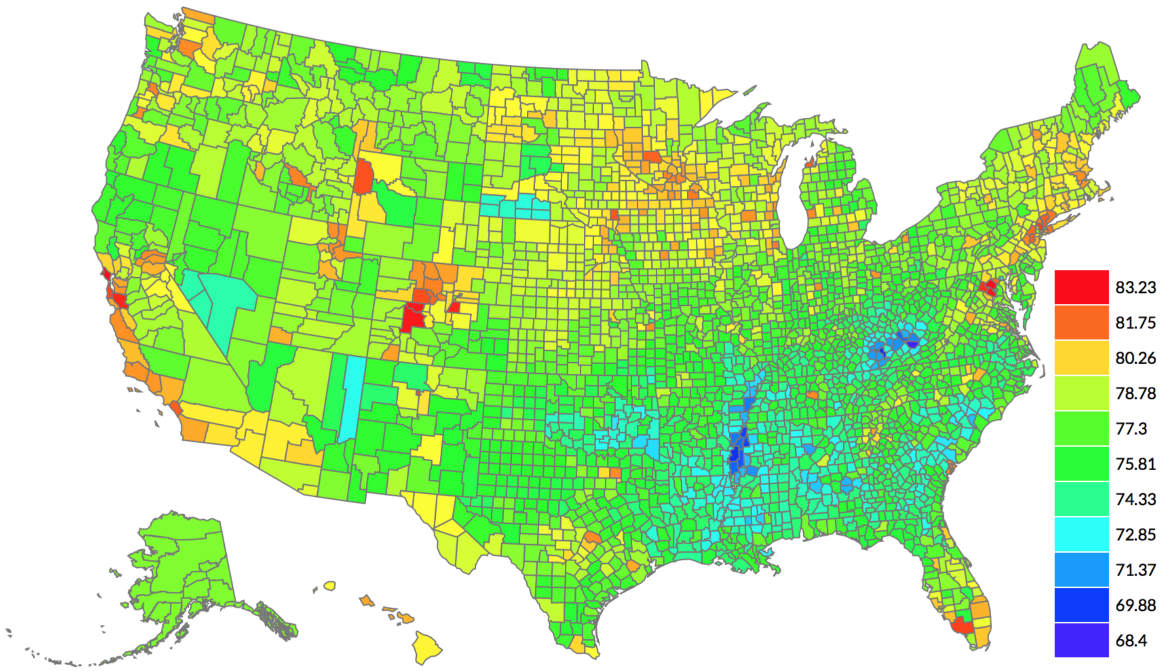


**Figure A.24:** Average life expectancy (2010)

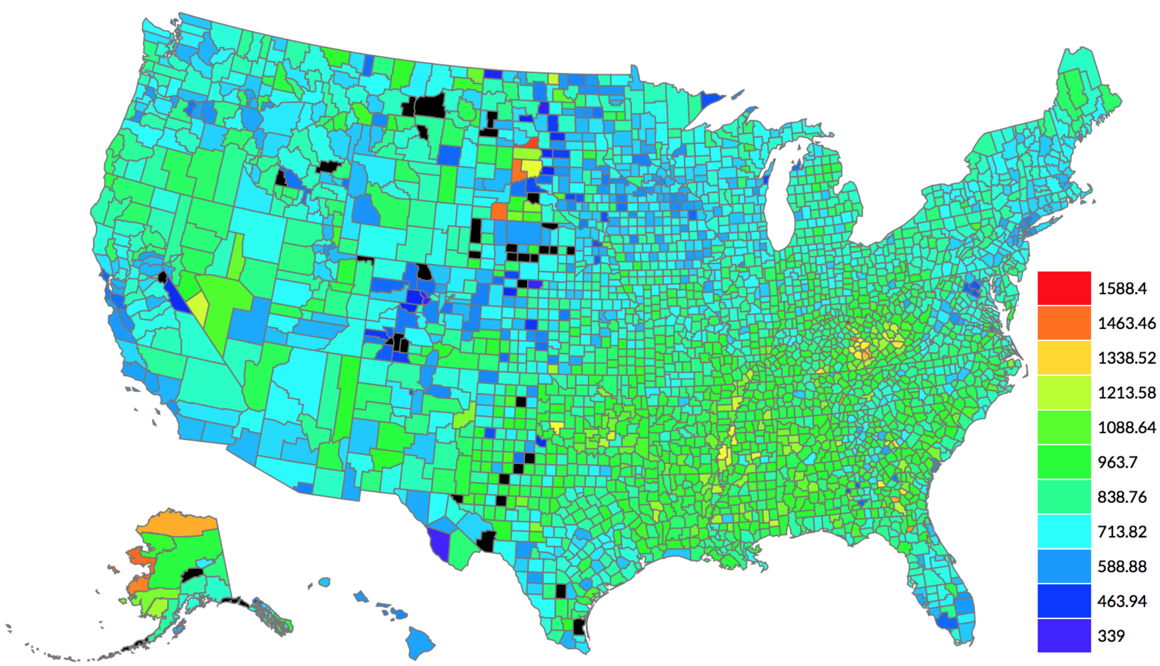


**Figure A.25:** All cause mortality per 100k population (2010)

#### A.1.10.3 Percentage of self-reported excellent or very good health

The data is obtained from Behavioral Risk Factor Surveillance System (BRFSS) of CDC.

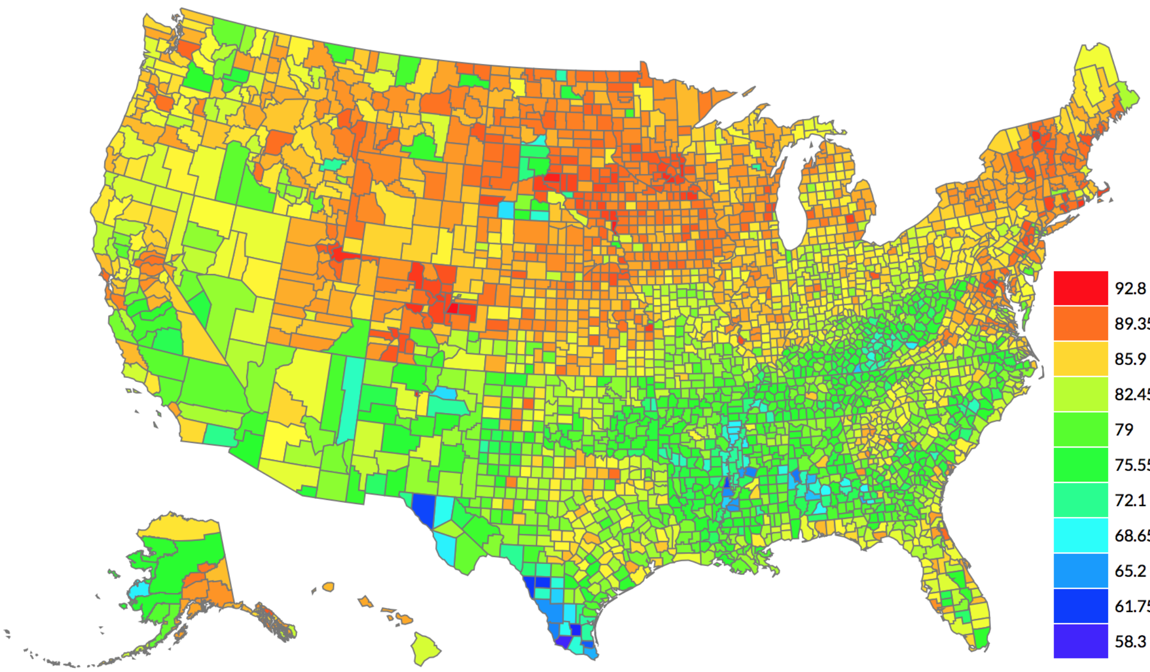


**Figure A.26:** Percentage of self-reported excellent or very good health (2014)

#### A.1.10.4 Percentage of adults with frequent mental distress

The data is obtained from Behavioral Risk Factor Surveillance System (BRFSS) of CDC.

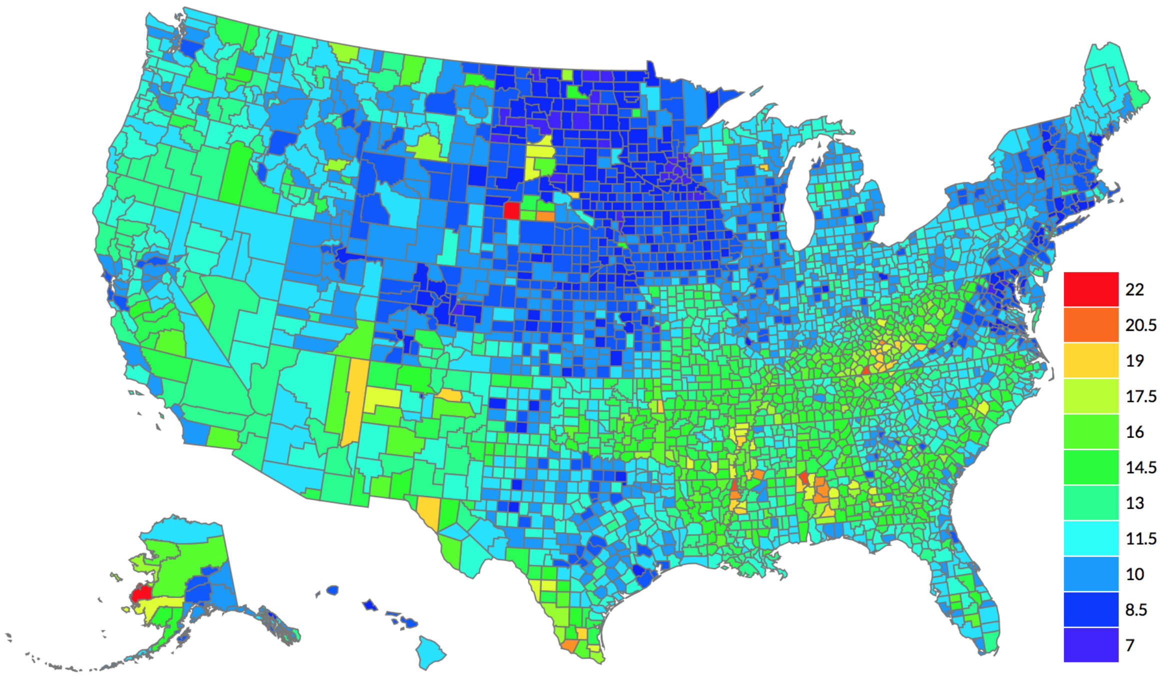


**Figure A.27:** Percentage of adults with frequent mental distress (2014)

# A.2 Prevention Mitigation (PM)

## A.2.1 Natural systems

### A.2.1.1 Distance to the nearest coast

The data is obtained from National Oceanic and Atmospheric Administration. We assume this data does not change during the years of the study.

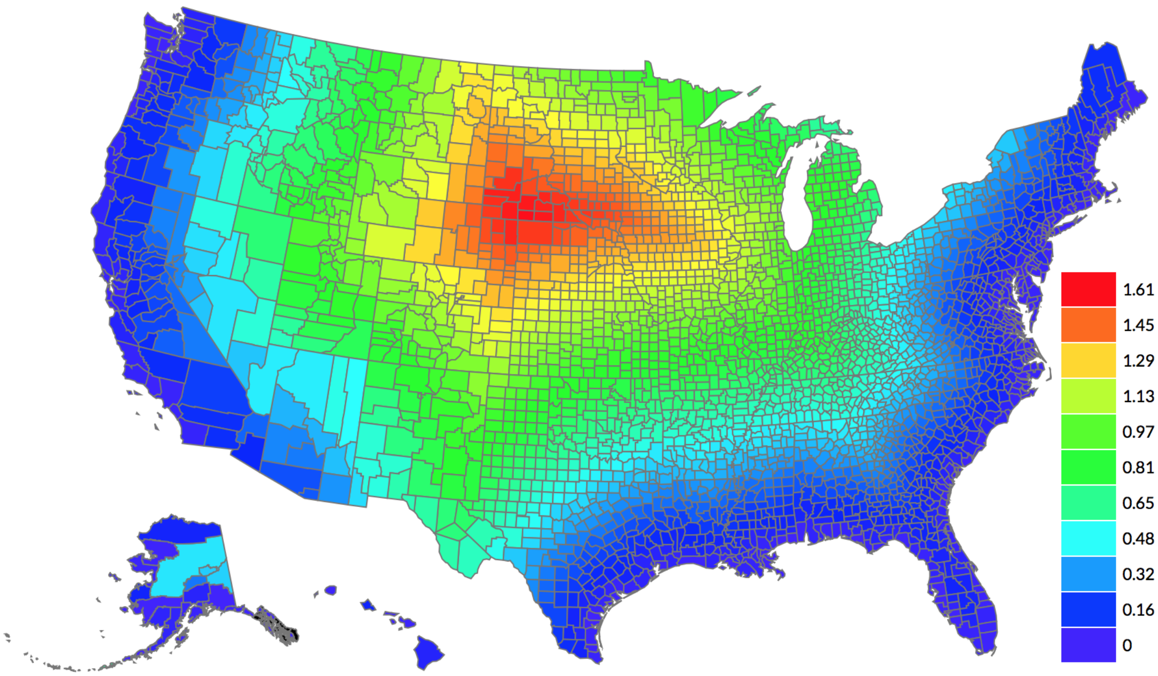


**Figure A.28:** Distance to the nearest coast in 1000 miles

## A.2.2 Engineered systems

### A.2.2.1 Percentage of bridges with structural deficiencies

The data is obtained from Federal Highway Administration. The data shows strong state patterns, suggesting that this policy is usually made at the state level.

### A.2.2.2 Average age of housing stock

The data is obtained from American Community Survey (ACS), Census Bureau.

### A.2.2.3 Percentage of housing units that are not mobile homes

The data is obtained from American Community Survey (ACS), Census Bureau

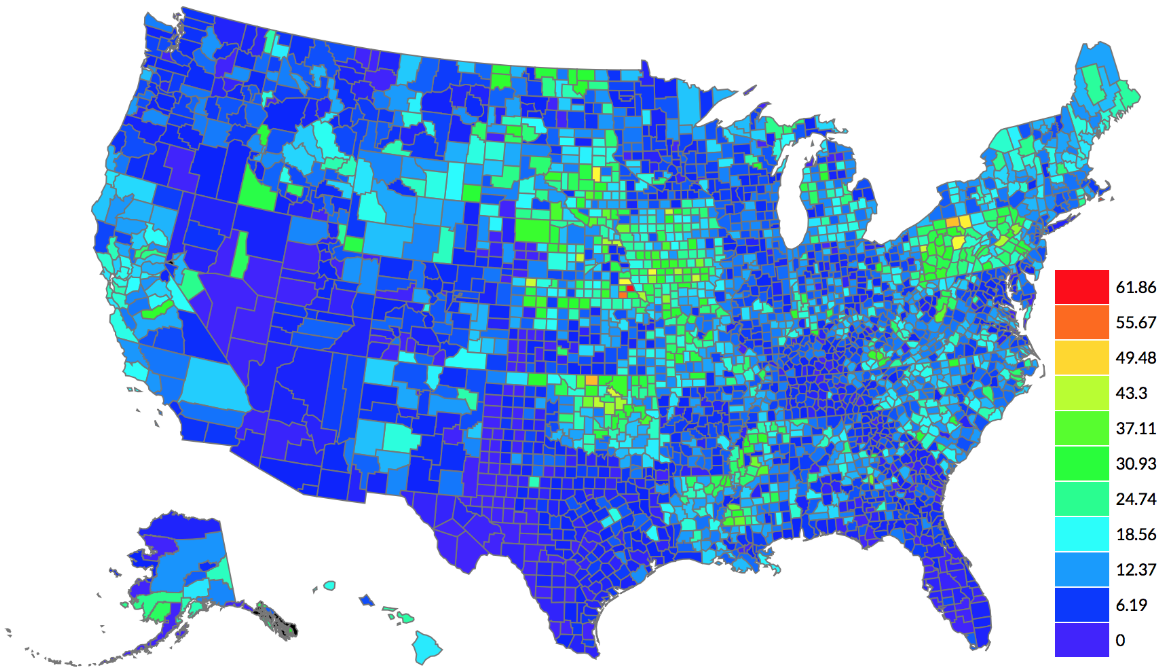


**Figure A.29:** Percentage of bridges with structural deficiencies (2010)

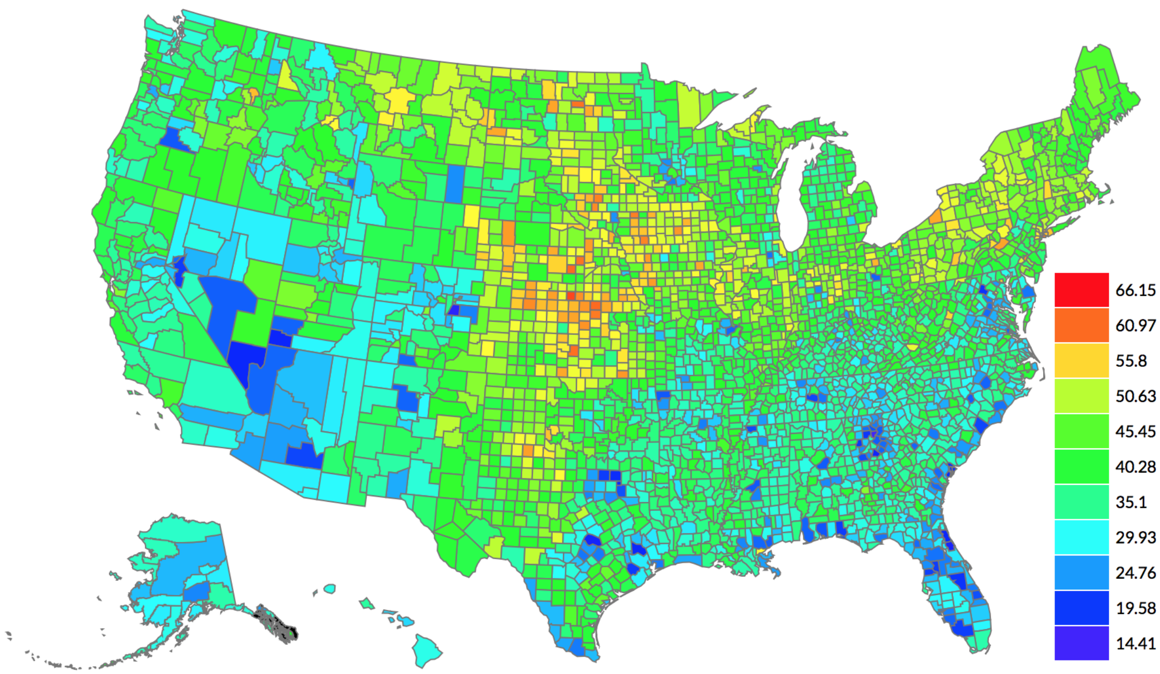


**Figure A.30:** Average age of housing stock (2010)

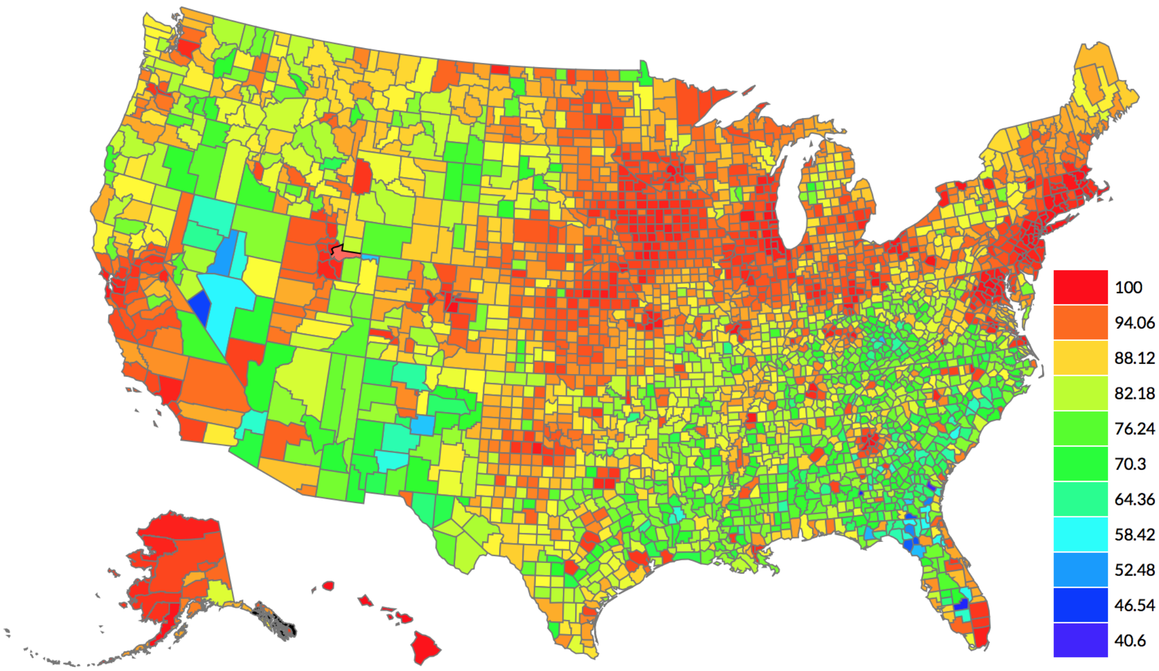


**Figure A.31:** Percentage of housing units that are not mobile homes (2010)

#### A.2.2.4 Percentage of population affected by water violation of those served by public water system

The data is obtained from United States Environmental Protection Agency (EPA)

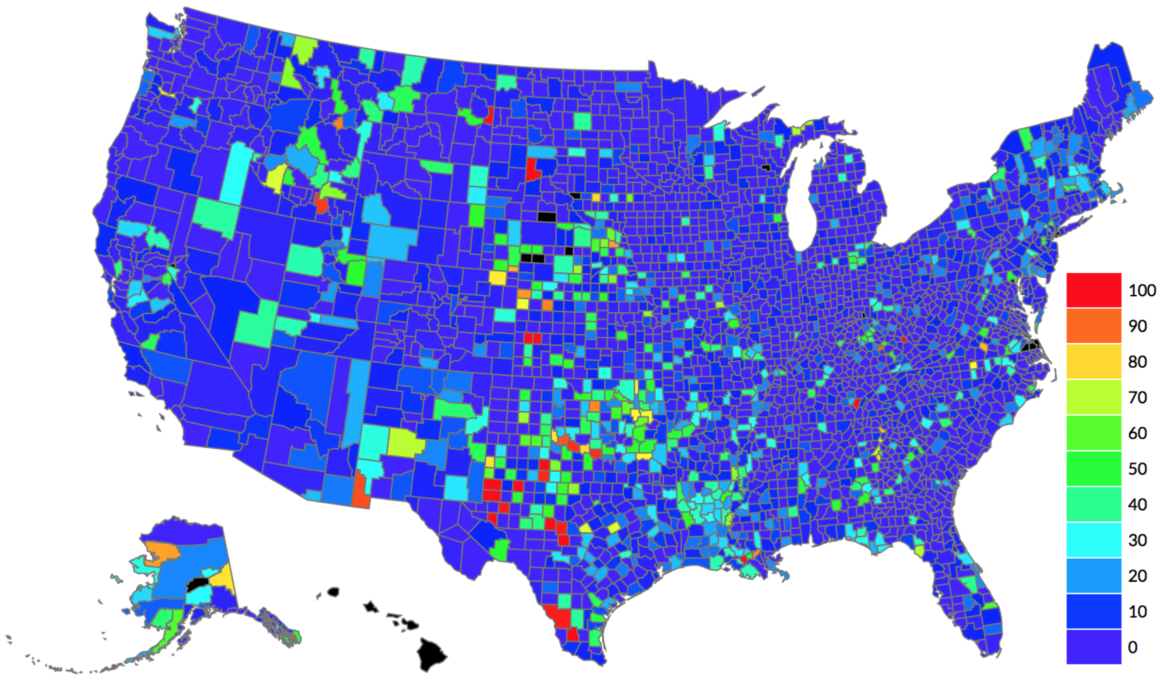


**Figure A.32:** Percentage of population affected by water violation of those served by public water system (2014)

# A.3 Population Vulnerability Inequality Deprivation (PVID)

## A.3.1 Vulnerability

### A.3.1.1 Percentage of children in population (below 18)

The data is obtained from American Community Survey (ACS), Census Bureau

### A.3.1.2 Percentage of elderlies in population (65 and older)

The data is obtained from American Community Survey (ACS), Census Bureau.

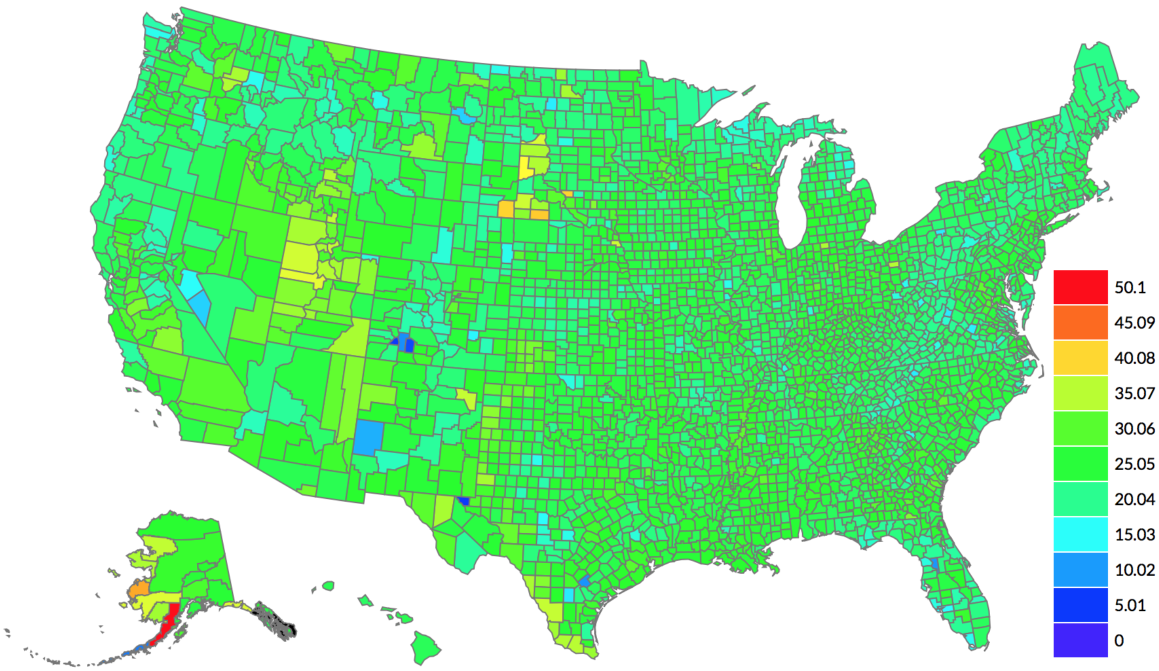


**Figure A.33:** Percentage of children in population (below 18) (2010)

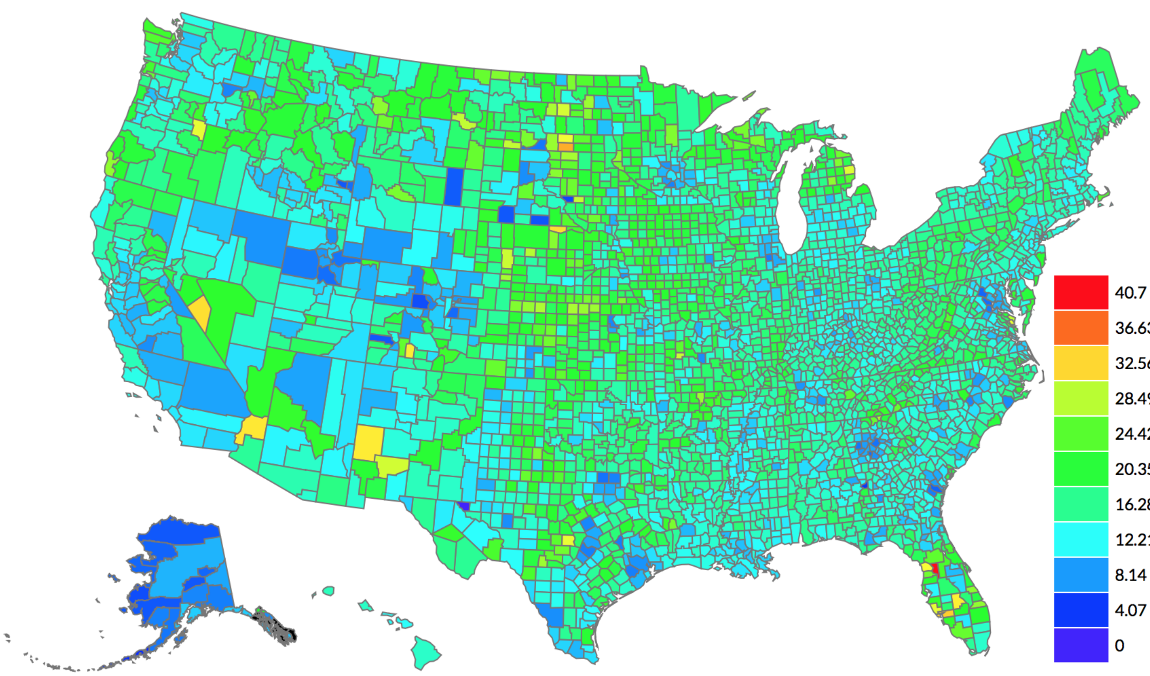


**Figure A.34:** Percentage of elderlies in population (65 and older) (2010)

### A.3.1.3 Percentage of population in institutions

The data is obtained from Summary File of Census Bureau. According to Census, "the institutionalized population is persons residing in institutional group quarters such as adult correctional facilities, juvenile facilities, skilled-nursing facilities, and other institutional facilities such as mental (psychiatric) hospitals and in-patient hospice facilities." People in institution are unlikely or unable to participate in labor force.

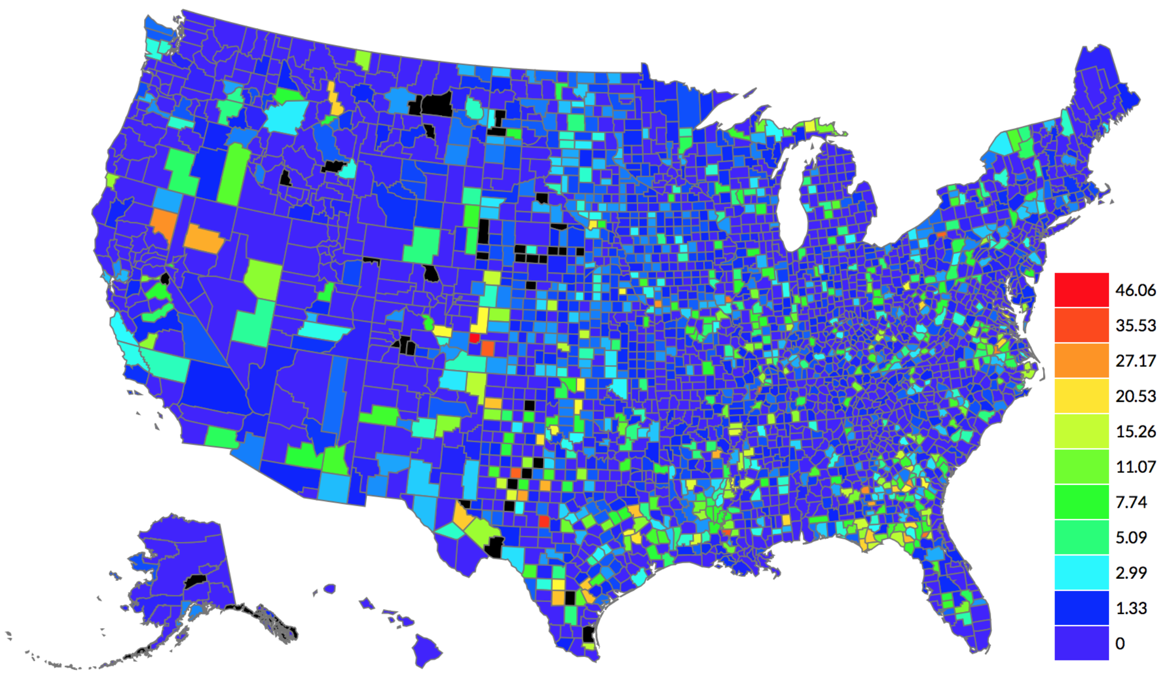


**Figure A.35:** Percentage of population in institutions (2010; colored in log scale)

#### A.3.1.4 Percentage of with a disability in civilian noninstitutionalized population

The data is obtained from American Community Survey (ACS), Census Bureau

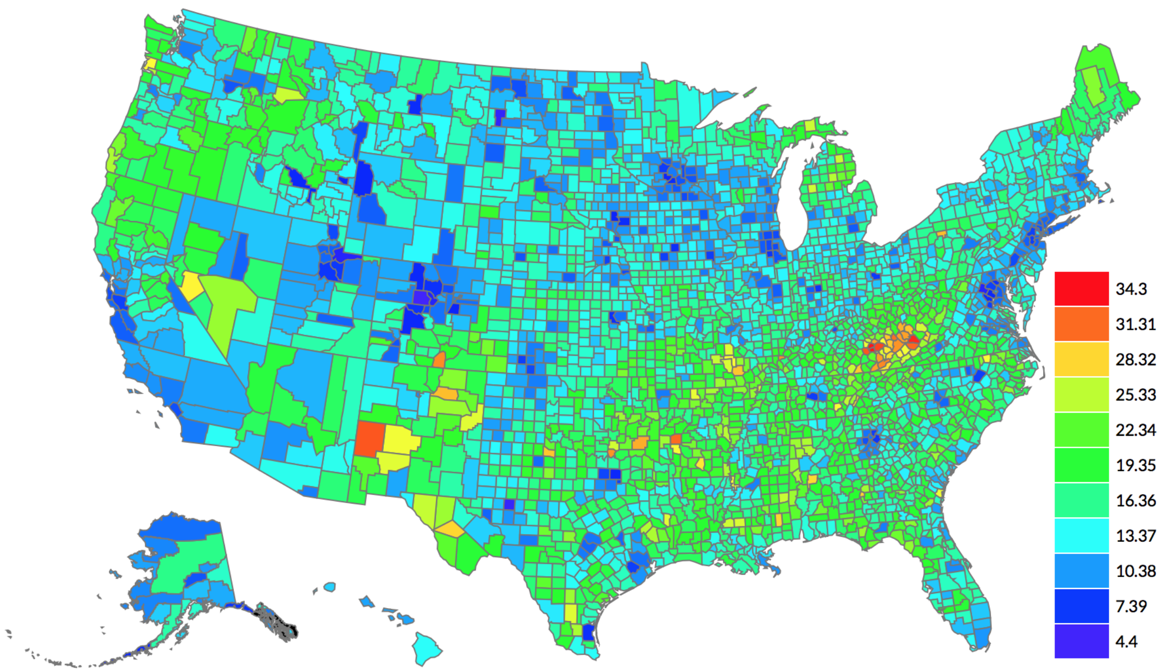


**Figure A.36:** Percentage of with a disability in civilian noninstitutionalized population (2014)

### A.3.2 Inequality

#### A.3.2.1 Gini index of income inequality

The data is directly available in Table B19083, “Gini Index of Income Inequality” of ACS. Gini index is a normalized number ranged between 0 and 1 indicating the statistical dispersion of the household incomes, and it is commonly used as a measure of income inequality.[79]

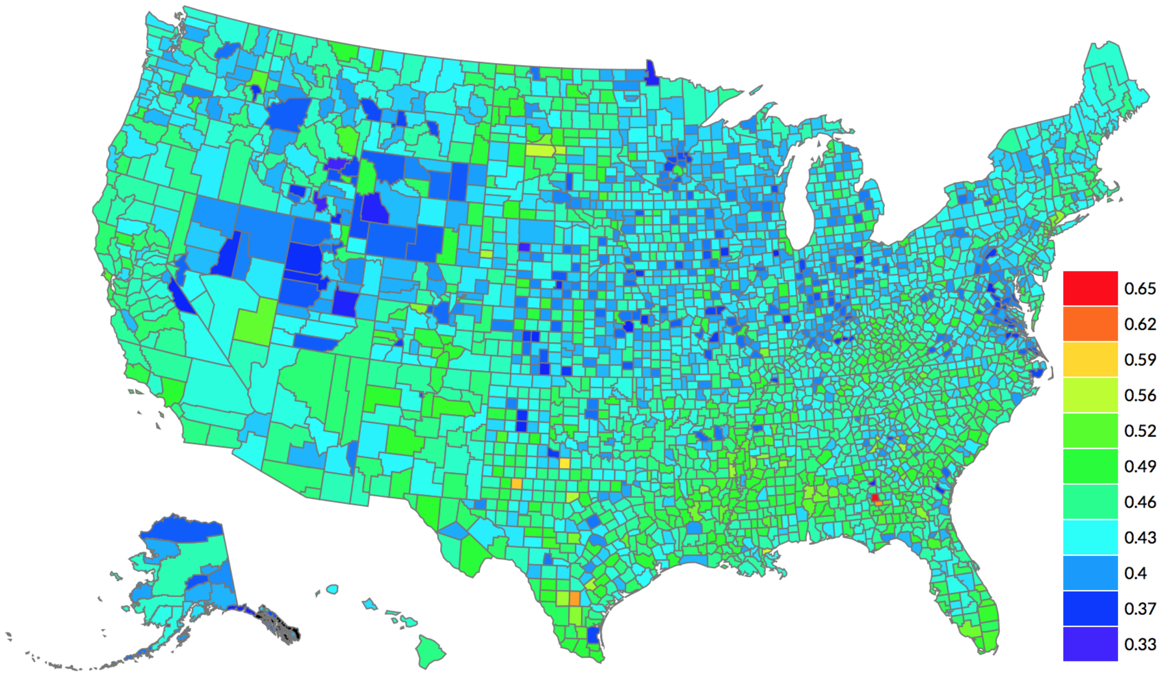


**Figure A.37:** Gini index of income inequality (2014)

### A.3.3 Deprivation

#### A.3.3.1 Percentage of population (18 to 24 years) with less than high school education

The data is obtained from American Community Survey (ACS), Census Bureau

#### A.3.3.2 Percentage of population (16 years and over) not in the labor force

The data is obtained from American Community Survey (ACS), Census Bureau

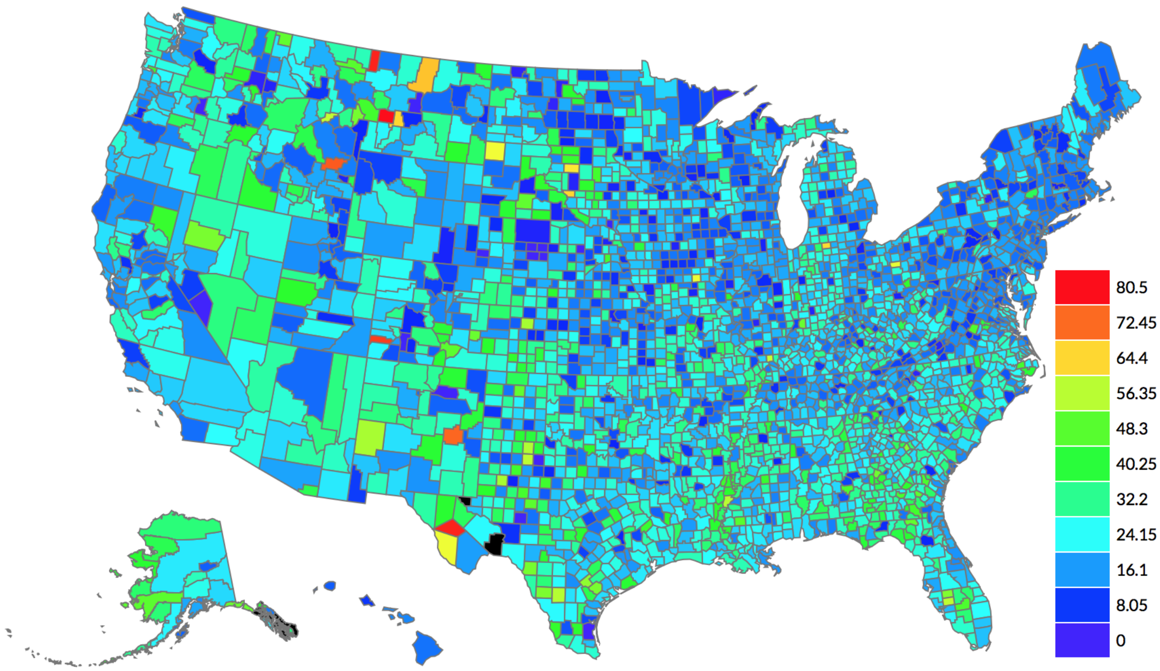


**Figure A.38:** Percentage of population (18 to 24 years) with less than high school education (2010)

### A.3.3.3 Percentage of children in poverty

The data is obtained from American Community Survey (ACS), Census Bureau

### A.3.3.4 Percentage of civilian in labor force but unemployed

The data is obtained from American Community Survey (ACS), Census Bureau

### A.3.3.5 Percentage of household on public assistance and food stamps

The data is obtained from Table B19058, "Public Assistance Income or Food Stamps/Snap in the Past 12 Months For Households" of ACS. The data column

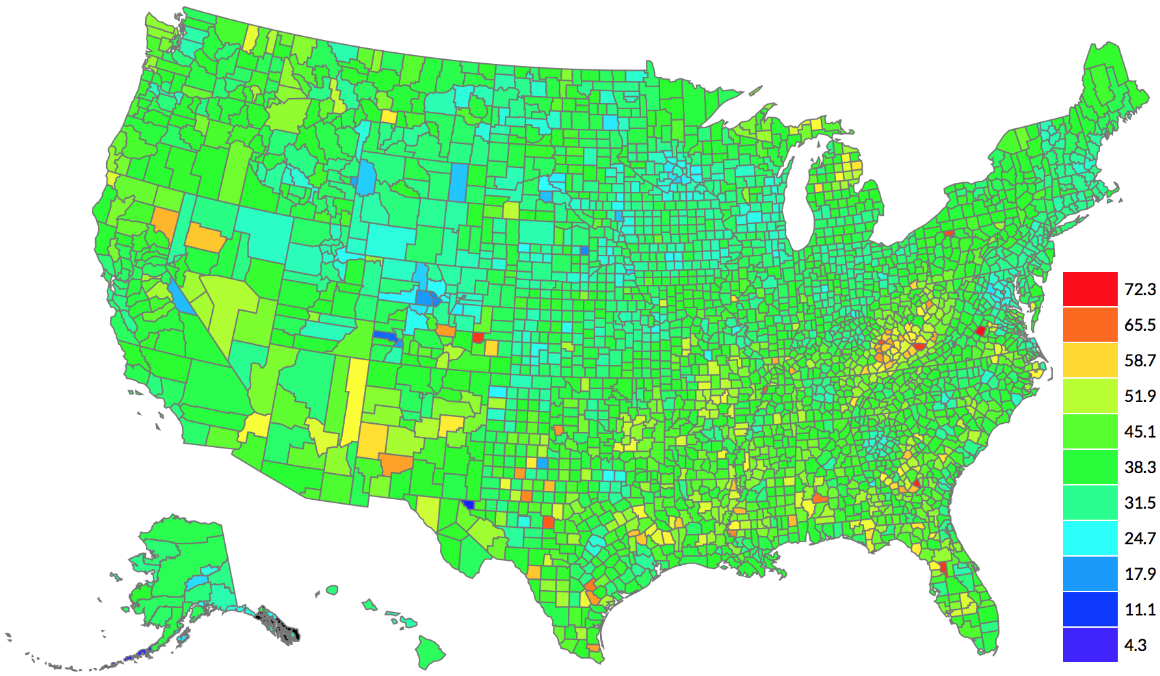


**Figure A.39:** Percentage of population (16 years and over) not in the labor force (2010)

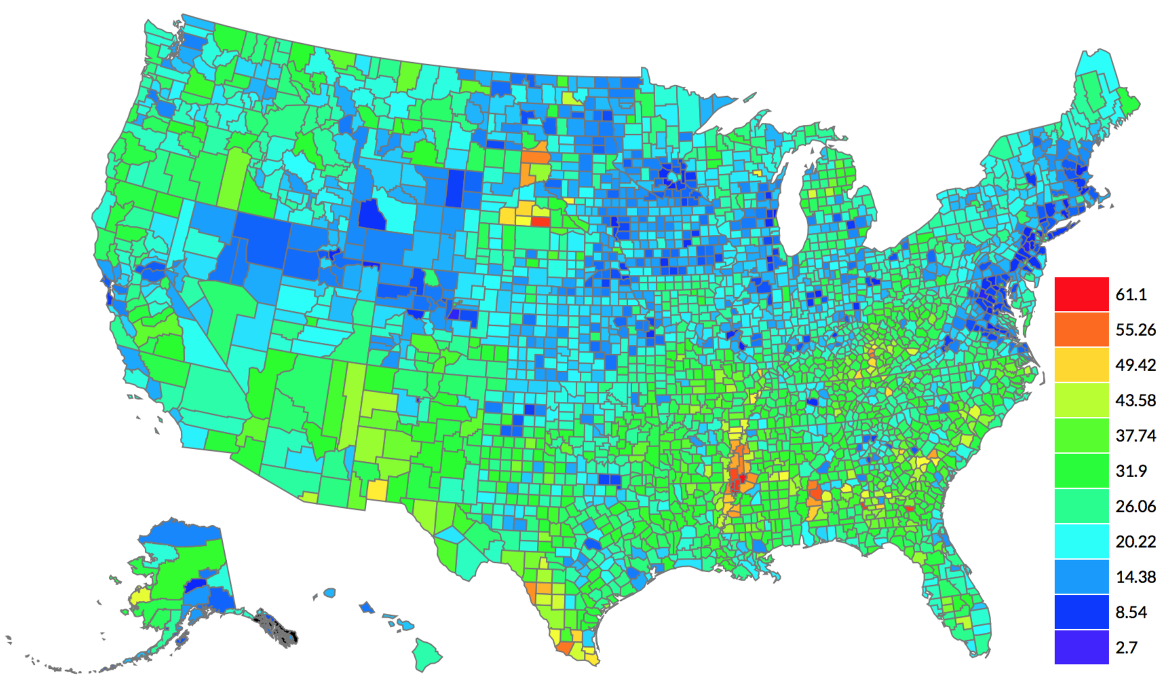


**Figure A.40:** Percentage of children in poverty (2010)

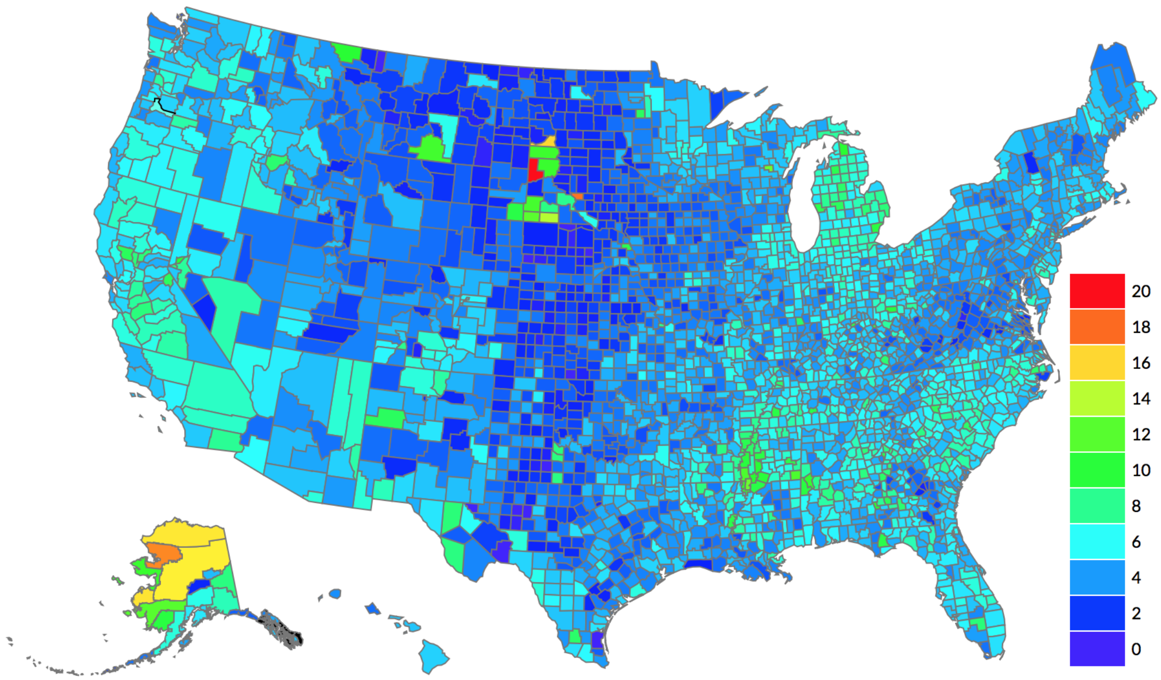


**Figure A.41:** Percentage of civilian in labor force but unemployed (2010)

labeled "With cash public assistance or Food Stamps/SNAP" is used.

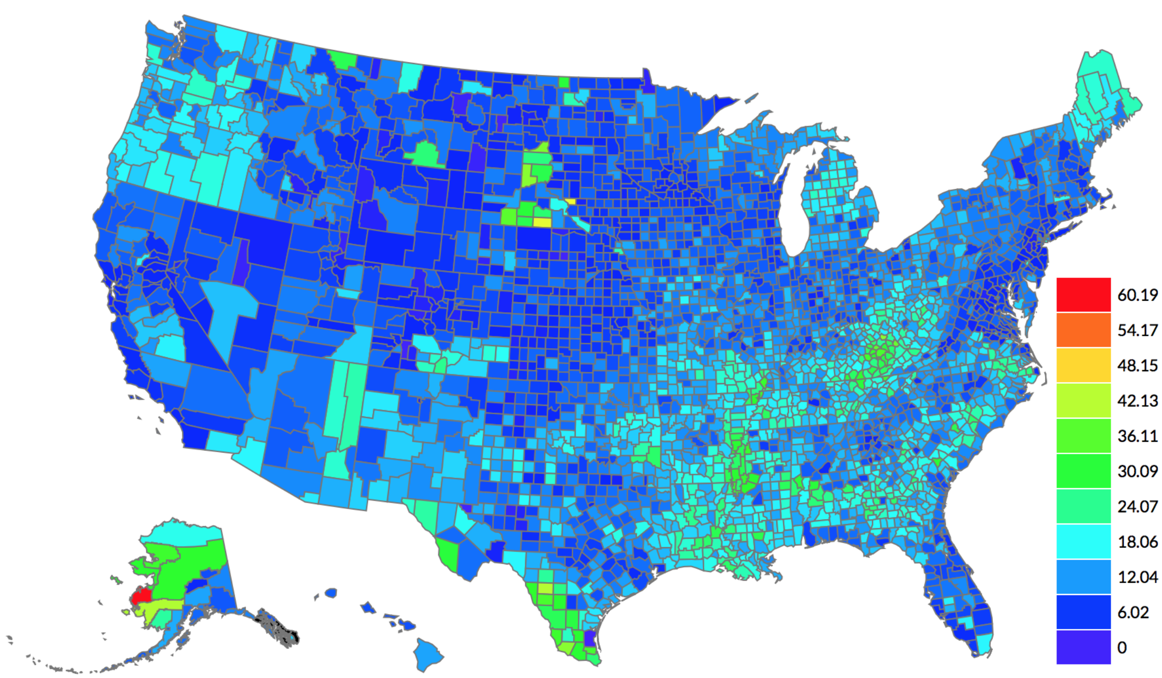


**Figure A.42:** Percentage of household on public assistance and food stamps (2010)

# A.4 Social Cohesion (SC)

## A.4.1 Social capital and cohesion

### A.4.1.1 Percentage of population who use carpool to work

The data is obtained from American Community Survey (ACS), Census Bureau. All the surveyed means of going to work are listed as below:

- Car, truck, or van: drove alone or carpooled
- Public transportation: bus or trolley bus, streetcar or trolley car, subway or elevated railroad, ferryboat,
- Bicycle
- Walked
- Taxicab, motorcycle, or other means
- Worked at home

### A.4.1.2 Percentage of population affiliated with religious group

The data is obtained from U.S. Religion Census. NAICS code for religious organizations is “813110”.

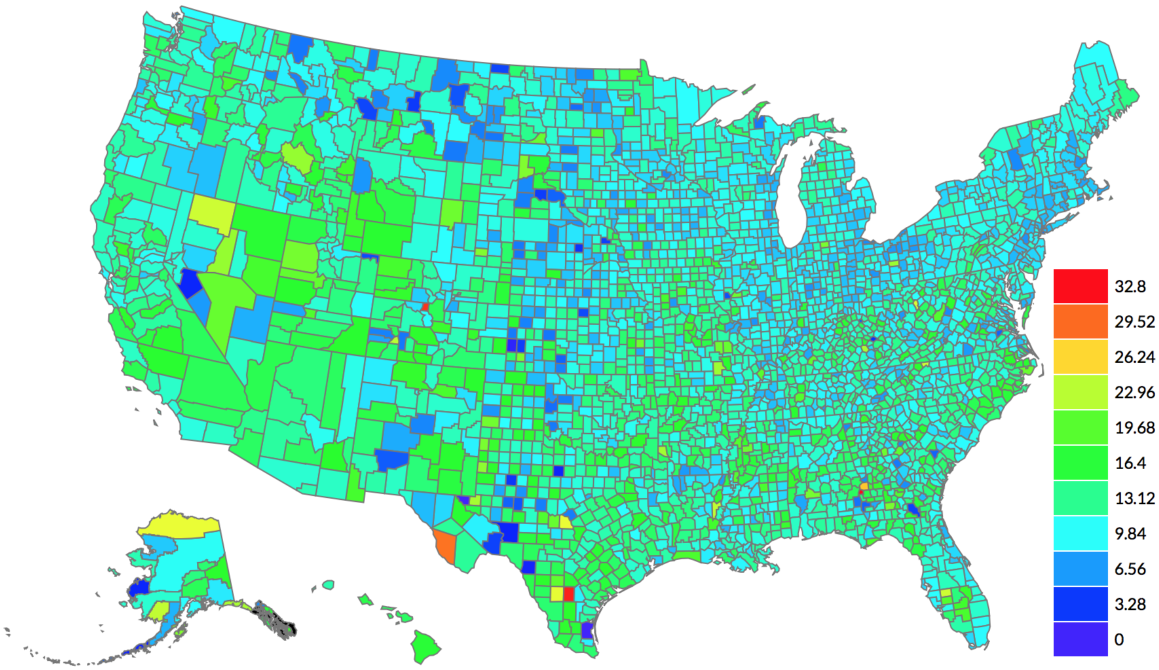


**Figure A.43:** Percentage of population who use carpool to work (2010)

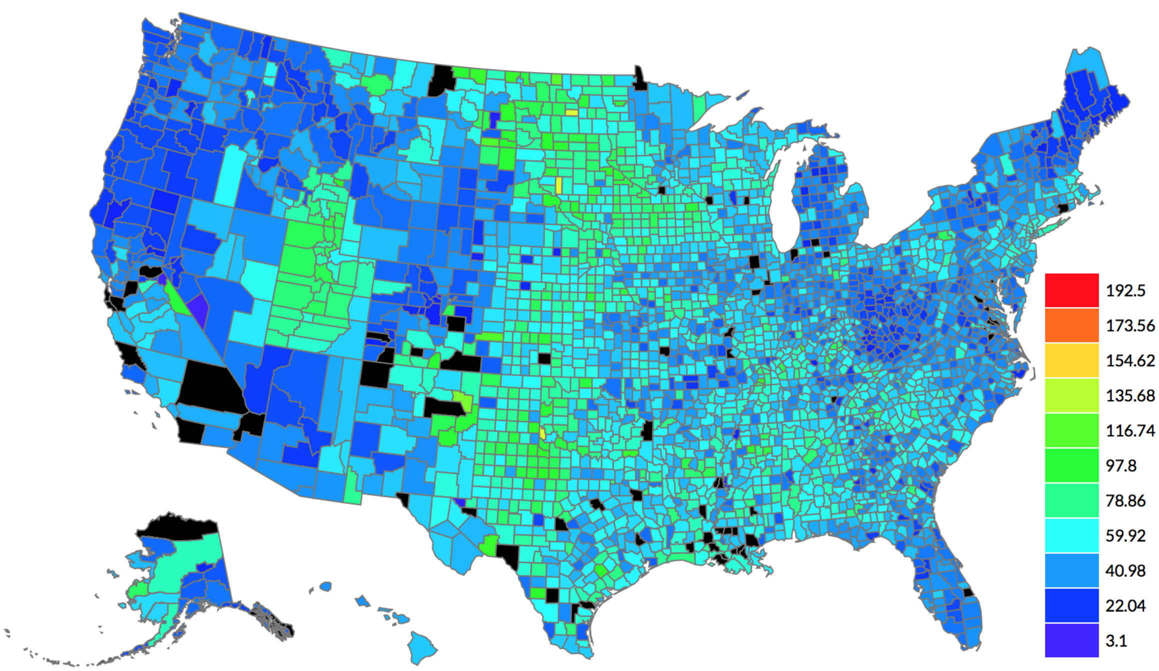


**Figure A.44:** Percentage of population affiliated with religious group (2010)

#### A.4.1.3 Number of religious organizations per 100 square mile

The data is obtained from County Business Patterns (CBP) of Census Bureau. NAICS code for religious organizations is “813110”.

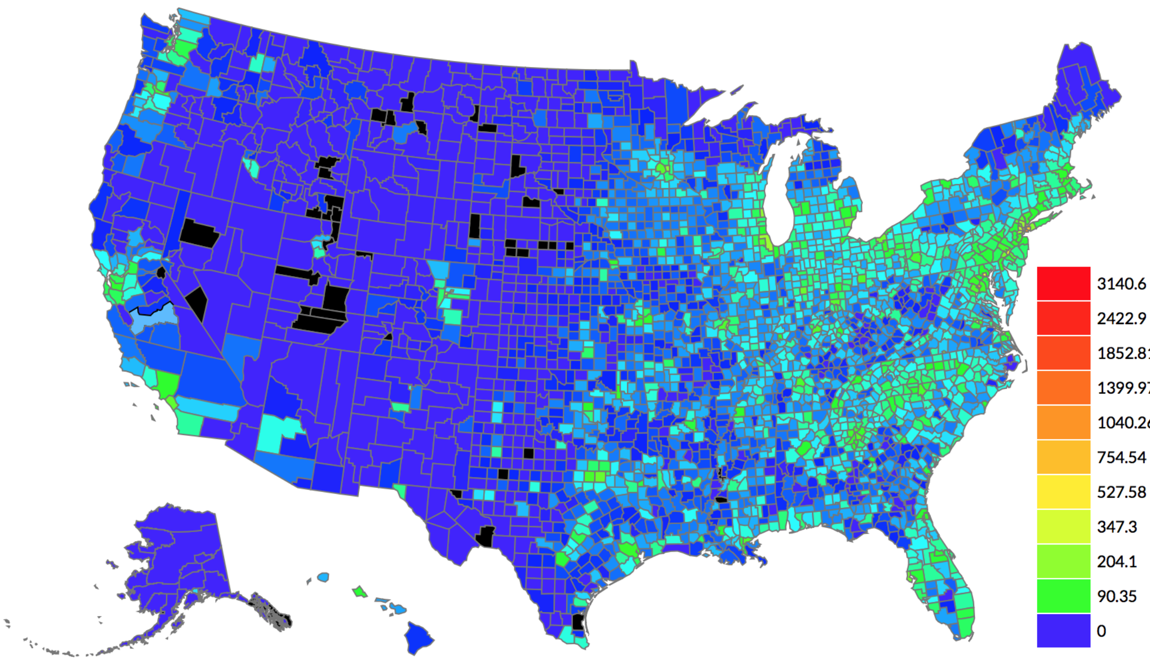


**Figure A.45:** Number of religious organizations per 100 square mile (2010; colored in log scale)

#### A.4.1.4 Number of social advocacy organizations per 10k population

The data is obtained from County Business Patterns (CBP) of Census Bureau, with the category “Social Advocacy Organizations” and NAICS code “8133”.

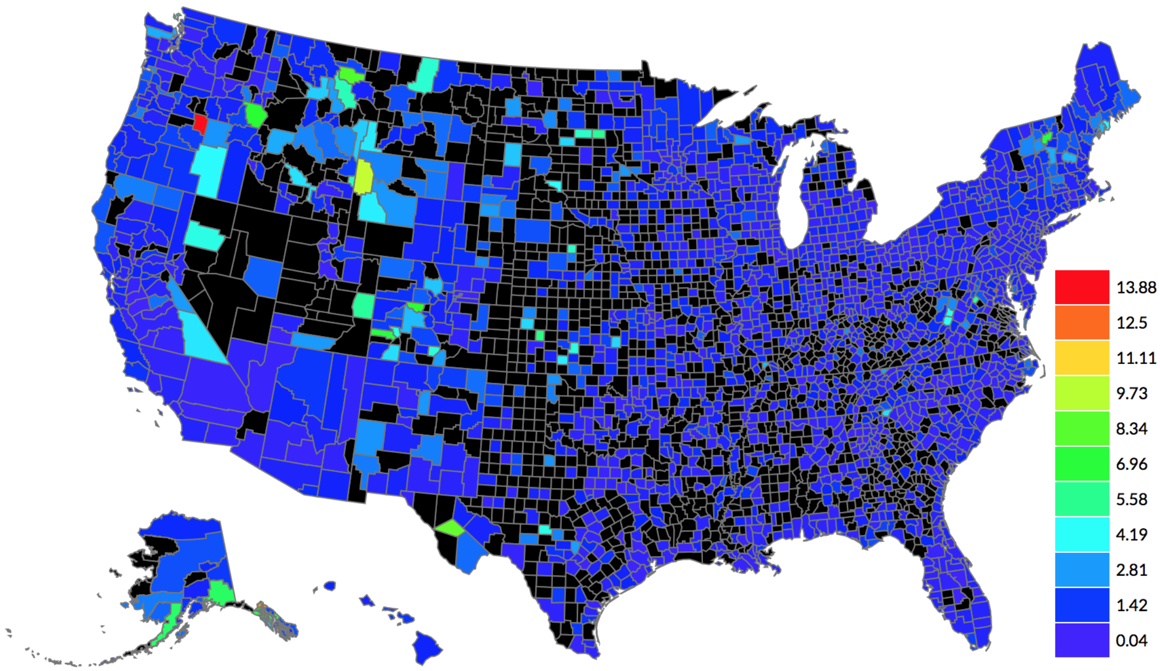


**Figure A.46:** Number of social advocacy organizations per 10k population (2010)

# A.5 Preparedness Response (PR)

## A.5.1 Preparedness

### A.5.1.1 Total number of FEMA events from 1986 to 2015

The data is obtained from Federal Emergency Management Agency.

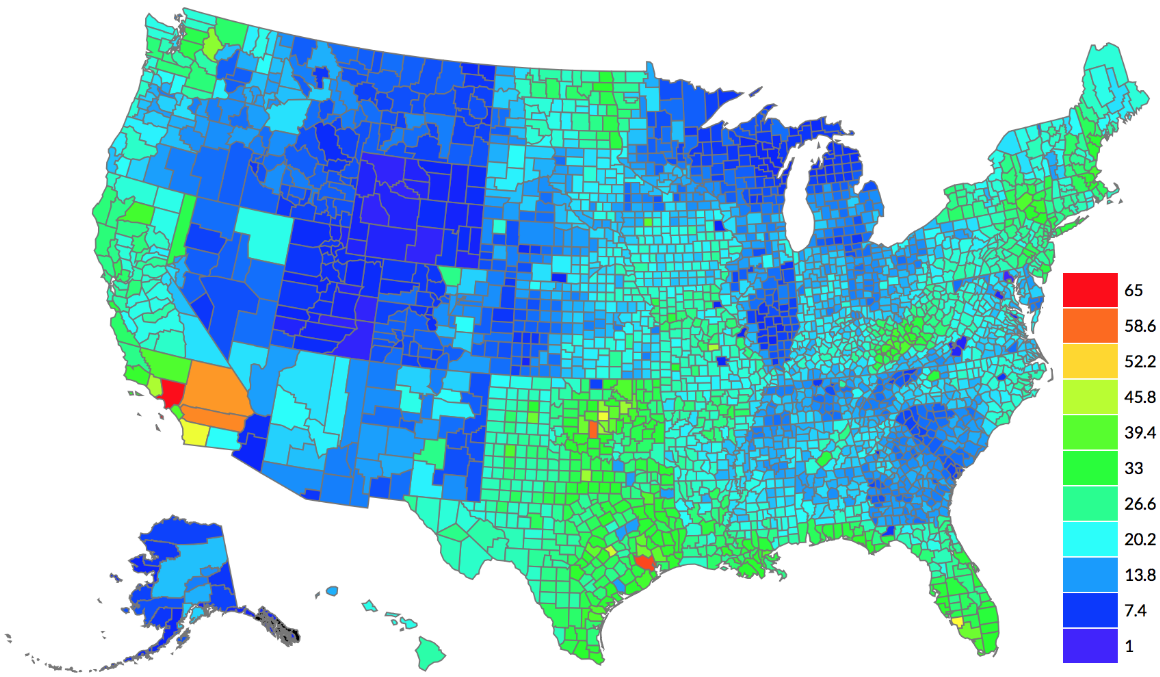


**Figure A.47:** Total number of FEMA events from 1986 to 2015

# Appendix B

# Implementation of Community Stability Research

## B.1 Data transformation and aggregation

### B.1.1 Data files

We provide all the raw data files:

1. "county_48ALHI.csv" contains all the counties in this study. FIPS code is a 5-digit number that unique identifies a county.

2. "list.csv" gives the list of measures along with their domain, subdomain and directions.

3. The folder of "OriginalMeasure" contains raw data files for all measures. Each data file is named after its identifier (id) as in "list.csv", and it is composed of two columns: FIPS code and value.

### B.1.2 Data aggregation framework

Here we provide the data aggregation framework developed in Python. The framework take inputs of the following:

1. Individual measure data
2. Domain and subdomain of each measure
3. The set of counties to be processed

The framework then transforms each measure and aggregate them to get subdomain and domain values. Currently we did not develop the graphical user interface and only provide the source code with documentations. To use the code, one needs to configure his or her computer as follows:

1. Install Python 3.5 and pip (python package manager)
2. Make sure the dependent packages have been already installed. A requirements file is provided, and to install all packages one simply needs to execute `pip install -r requirements.txt`

3. Execute the source code “prepare_data.py” with Python3.5. It will create a database file name “data.db” and a table containing all domain level data in “domain.csv”. In the database file, table “scaled” contains all transformed and scaled measure data, “subdomain” contains the aggregated data at subdomain level, and “domain” save an extra copy of domain data.

The source code is in the file named “prepare_data.py” and also attached below.

```
from scipy import stats
import pandas
import sqlite3
import numpy
import os

# Load in the list of measures
LS = pandas.DataFrame.from_csv('list.csv')


def init_df():
    return pandas.DataFrame.from_csv('county_48ALHI.csv')[[]]


def load_and_scale():
    """
    Load measure data from files salved in OriginalMeasure and scale them.
    :return: The scaled measures
    """
    measures = init_df()
    for id, row in LS.iterrows():
        # Load data from file
        df = pandas.DataFrame.from_csv('OriginalMeasure/{}.csv'.format(id))

        # Remove possibly duplicate rows
        df = df[~df.index.duplicated()]

        # Remove negative entries
        df.query('value >= 0', inplace=True)
```

```

        # Shift up a little to avoid zero in Box-Cox transformation.
        tiny = 0.000001 * (df['value'].max() - df['value'].min())
        df['value'] += - df['value'].min() + tiny

        # Box cox transformation
        df['value'], lam = (stats.boxcox(df['value']))

        # Take Z-score
        df['value'] = stats.zscore(df['value'])

        # Truncation with +- 3.5
        df['value'][df['value'] > 3.5] = 3.5
        df['value'][df['value'] < -3.5] = -3.5

        # Adjust for direction
        if row['direction'] == '-':
            df['value'] *= -1

        # Scale from [-3.5, 3.5] to [0, 1]
        df['value'] = (df['value'] + 3.5) / 7

        # Save to data frame
        measures[id] = df['value']
    return measures


def aggregate(measures):
    """
    Aggregate individual measures to domains
    :param measures: data frame of measures
    :return: data frame of domains
    """
    # Aggregate to subdomain level
    SD = init_df()
    for subdomain in set(LS['subdomain']):
        df = init_df()
        df['value'] = 0
        df['cnt'] = 0
        for id in LS.query('subdomain == "{}"'.format(subdomain)).index:
            df['value'] += numpy.nan_to_num(measures[id])
            df['cnt'] += 1 - numpy.isnan(measures[id])
```

```

        SD[subdomain] = df['value'] / df['cnt']

    # Aggregate to domain level
    D = init_df()
    for domain in set(LS['domain']):
        df = init_df()
        df['value'] = 0
        df['cnt'] = 0
        for subdomain in set(LS.query('domain == "{}"'.format(domain))['subdomain']):
            df['value'] += numpy.nan_to_num(SD[subdomain])
            df['cnt'] += 1 - numpy.isnan(SD[subdomain])
        D[domain] = df['value'] / df['cnt']

    # Save to database
    con = sqlite3.connect('data.db')
    measures.to_sql('scaled', con, if_exists='replace')
    SD.to_sql('subdomain', con, if_exists='replace')
    D.to_sql('domain', con, if_exists='replace')

    # Fill missing value with state average
    for domain in set(LS['domain']):
        con.cursor().execute("""
            UPDATE domain SET `{0}` = (
              SELECT AVG(`{0}`)
              FROM domain AS domain2
              WHERE domain2.fips/1000 == domain.fips/1000
            ) WHERE `{0}` IS NULL""".format(domain))
    D = pandas.read_sql('SELECT * FROM domain', con).set_index('fips')
    con.close()
    return D


measures = load_and_scale()
domains = aggregate(measures)
domains.to_csv('domain.csv')
```

## B.2 The ODE model

### B.2.1 Solving ODEs

We also provide a Matlab file that loads in data from “domain.csv”, solve ODEs, calculate resilience and resistance, and then save the results back to file “domain.csv”.

```matlab
clear, clc
filename = 'domain.csv';
T = readtable(filename, 'ReadRowNames',true);
T.Resilience = zeros(size(T, 1), 1);
T.Resistance = zeros(size(T, 1), 1);
T.Recovery = zeros(size(T, 1), 1);
T.CFend = zeros(size(T, 1), 1);
tspan = linspace(0, 12, 121); % unit: month

global var_list;
var_list = {'ER', 'CF', 'SC', 'PR', 'PreCF', 'PVID', 'PM'};
N_counties = size(T,1);

%% Solving
for i_county = 1 : N_counties
    fprintf('>>> Calculating county %d\n', i_county);

    % Assemble the initial state vector
    W0 = zeros(length(var_list), 1);
    for i_var = 1:length(var_list)
        switch var_list{i_var}
            case {'PreCF'}
                W0(i_var) = T{i_county, 'CF'};
            case {'ER'}
                W0(i_var) = 0.5;
            otherwise
                W0(i_var) = T{i_county, var_list{i_var}};
        end
    end

    % solving
```

```
    [~, W ] = ode45( @fdW, tspan, W0);

    % Solve for resilience and resistance
    [T{i_county, 'Resistance'}, T{i_county, 'Recovery'}, T{i_county, 'Resilience'}] = res(W(:,2)
    T{i_county, 'CFend'} = W(end,2);
end
writetable(T, filename, 'WriteRowNames', true);
```

## B.2.2 Definition of ODEs

```
function dW = fdW(t, W)
%% Parameters
isPandemic = false;
Event0 = 1;
global var_list;

for i = 1:length(var_list)
    eval(sprintf('%s = max(W(%d), 0);', var_list{i}, i));
end

%% constant variables
Event_damage_rate_constant = 4;
ER_flow_rate_constant = 1;
PR_flow_rate_constant = 1;
SC_flow_rate_constant = 1;
CF_depletion_rate_constant = 5;

%% CF replenish
CF_drop = max( PreCF - CF, 0 );
SC_flow_rate = SC_flow_rate_constant * CF * SC * CF_drop;
PR_flow_rate = PR_flow_rate_constant * PR * CF_drop;
ER_flow_rate = ER_flow_rate_constant * ER * CF_drop;
CF_replenish_rate = SC_flow_rate + PR_flow_rate + ER_flow_rate;

%% CF depletion rate
if isPandemic
    tau = 2; % event peak (mean)
    sigma = 1; % event spead (std)
    coef = 1 / sqrt(2*pi*sigma^2);
```

```
    Event_t = Event0 * coef * exp(-(t-tau)^2 / (2*sigma^2));
else
    k = Event_damage_rate_constant;
    Event_t = Event0 * k * exp(-k * t);
end

Event_damage_rate =  Event_t * (PM + PVID)/2;
CF_depletion_rate = CF_depletion_rate_constant * CF * Event_damage_rate;

%% Derivatives
dSC = - SC_flow_rate;
dPR = - PR_flow_rate;
dER = - ER_flow_rate;
dCF = - CF_depletion_rate + CF_replenish_rate ;

dW = zeros(length(var_list), 1);
for i = 1:length(var_list)
    fieldname = var_list{i};
    switch fieldname
        case {'PreCF', 'PVID', 'PM'} % for constant values.
            dW(i) = 0;
        otherwise
            eval(sprintf('dW(%d) = d%s;', i, fieldname));
    end
end
```

### B.2.3 Definition of resistance and resilience

```
function [resistance, recovery, resilience] = res(CF, tspan)
resilience = mean(CF);
CF0 = CF(1);
[CF_min, idx_min] = min(CF);

% Resistance is the percentage of CF that remained during event.
resistance = CF_min / CF0;

CFrecovery = (CF(idx_min : end) - CF_min) / (CF0 - CF_min);
if max(CFrecovery) > 0.5
    tHalf = interp1(CFrecovery, tspan(idx_min : end), 0.5);
```

```
else
    tHalf = 12;
end
% Resilience is the speed of half recovery.
recovery = 1 / tHalf;
```

## B.3 Map visualization tool

A map visualizer was developed to facilitate the examination and studying of data and model results in folder “maps”. The tool is developed mainly in JavaScript and works as a standalone web application. The first column of “data.csv” should always be FIPS code and be named exactly as “fips”. Table B.1 gives an example of such table.

**Table B.1:** Example format of data table to be visualized

| fips | Variable name 1 | Variable name 2 |
|---|---|---|
| 1001 | 4.3 | 0.1 |
| 1003 | 9.2 | 0.3 |
| 1005 | 1.4 | 0.8 |

Each of the other columns is one variable to be visualized on the map. The tool draws each column as one map titled with the column name. To use the tool:

1. Place you data into “data.csv” as specified before.

2. If you use “Safari”, simply open “index.html”.

   If you use other web browser: make sure Python is installed, go the source code folder, and start a mini server: `python -m SimpleHTTPServer 8000` . Then you can visit the web application in your browser: `http://localhost:8000`

## B.4 CF simulation tool

A community function simulation tool was developed to perform sensitivity analysis in a straightforward way: `http://slinjhu.github.io/CFSimulator` . Figure B.1 gives a preview. Source code is also available.

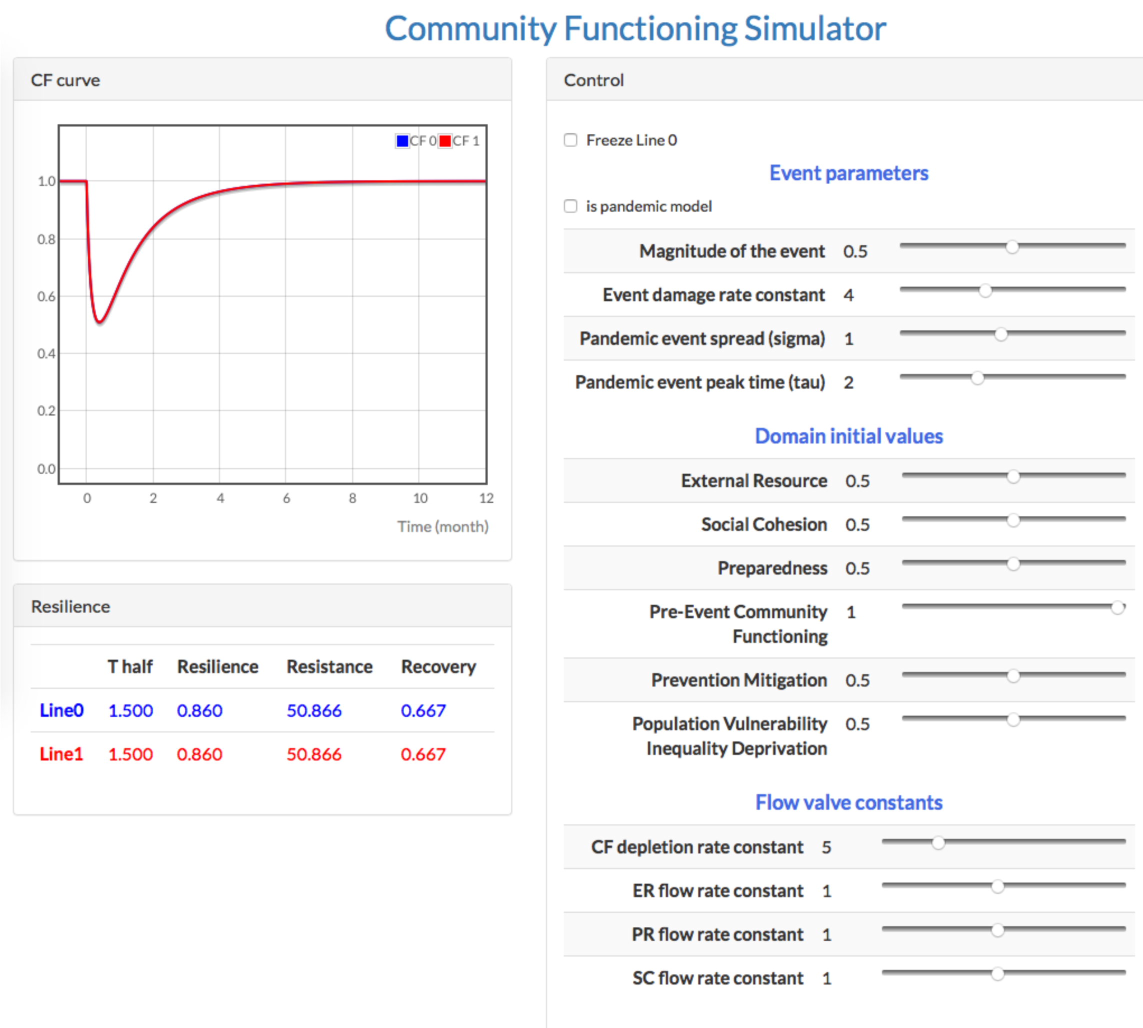


**Figure B.1:** Preview of the CF simulation tool

# Bibliography

[1] T. H. Tulchinsky and E. A. Varavikova, *The new public health.* Academic Press, 2014.

[2] D. A. Luke and K. A. Stamatakis, "Systems science methods in public health: dynamics, networks, and agents," *Annual review of public health*, vol. 33, p. 357, 2012.

[3] J. M. Epstein, *Agent_Zero: Toward neurocognitive foundations for generative social science.* Princeton University Press, 2014.

[4] G. An, Q. Mi, J. Dutta-Moscato, and Y. Vodovotz, "Agent-based models in translational systems biology," *Wiley Interdisciplinary Reviews: Systems Biology and Medicine*, vol. 1, no. 2, pp. 159–171, 2009.

[5] Y. Wang and M. A. Beydoun, "The obesity epidemic in the united statesgender, age, socioeconomic, racial/ethnic, and geographic characteristics: a systematic review and meta-regression analysis," *Epidemiologic reviews*, vol. 29, no. 1, pp. 6–28, 2007.

[6] K. M. Flegal, M. D. Carroll, B. K. Kit, and C. L. Ogden, "Prevalence of obesity and trends in the distribution of body mass index among us adults, 1999-2010," *Jama*, vol. 307, no. 5, pp. 491–497, 2012.

[7] S. J. Olshansky, D. J. Passaro, R. C. Hershow, J. Layden, B. A. Carnes, J. Brody, L. Hayflick, R. N. Butler, D. B. Allison, and D. S. Ludwig, "A potential decline in life expectancy in the united states in the 21st century," *New England Journal of Medicine*, vol. 352, no. 11, pp. 1138–1145, 2005.

[8] C. L. Ogden, M. D. Carroll, B. K. Kit, and K. M. Flegal, "Prevalence of obesity and trends in body mass index among us children and adolescents, 1999-2010," *Jama*, vol. 307, no. 5, pp. 483–490, 2012.

[9] J. J. Reilly and J. Kelly, "Long-term impact of overweight and obesity in childhood and adolescence on morbidity and premature mortality in adulthood: systematic review," *International journal of obesity*, vol. 35, no. 7, pp. 891–898, 2011.

[10] D. S. Freedman, L. K. Khan, M. K. Serdula, C. L. Ogden, and W. H. Dietz, "Racial and ethnic differences in secular trends for childhood bmi, weight, and height," *Obesity*, vol. 14, no. 2, pp. 301–308, 2006.

[11] R. C. Whitaker, J. A. Wright, M. S. Pepe, K. D. Seidel, and W. H. Dietz, "Predicting obesity in young adulthood from childhood and parental obesity," *New England Journal of Medicine*, vol. 337, no. 13, pp. 869–873, 1997.

[12] L. M. Rossen and K. C. Schoendorf, "Measuring health disparities: trends in racial- ethnic and socioeconomic disparities in obesity among 2-to 18-year old youth in the united states, 2001–2010," *Annals of epidemiology*, vol. 22, no. 10, pp. 698–704, 2012.

[13] A. H. Auchincloss, R. L. Riolo, D. G. Brown, J. Cook, and A. V. D. Roux, "An agent-based model of income inequalities in diet in the context of residential segregation," *American journal of preventive medicine*, vol. 40, no. 3, pp. 303–311, 2011.

[14] K. Van Der Horst, A. Oenema, I. Ferreira, W. Wendel-Vos, K. Giskes, F. van Lenthe, and J. Brug, "A systematic review of environmental correlates of obesity-related dietary behaviors in youth," *Health education research*, vol. 22, no. 2, pp. 203–226, 2007.

[15] M. Y. Kubik, L. A. Lytle, P. J. Hannan, C. L. Perry, and M. Story, "The association of the school food environment with dietary behaviors of young adolescents," *American journal of public health*, vol. 93, no. 7, pp. 1168–1173, 2003.

[16] M. D. Hearn, T. Baranowski, J. Baranowski, C. Doyle, M. Smith, L. S. Lin, and K. Resnicow, "Environmental influences on dietary behavior among children: availability and accessibility of fruits and vegetables enable consumption," *Journal of Health Education*, vol. 29, no. 1, pp. 26–32, 1998.

[17] R. R. Briefel, M. K. Crepinsek, C. Cabili, A. Wilson, and P. M. Gleason, "School

food environments and practices affect dietary behaviors of us public school children," *Journal of the American Dietetic Association*, vol. 109, no. 2, pp. S91–S107, 2009.

[18] N. I. Larson, M. T. Story, and M. C. Nelson, "Neighborhood environments: disparities in access to healthy foods in the us," *American journal of preventive medicine*, vol. 36, no. 1, pp. 74–81, 2009.

[19] A. Timperio, K. Ball, R. Roberts, K. Campbell, N. Andrianopoulos, and D. Crawford, "Children's fruit and vegetable intake: associations with the neighbourhood food environment," *Preventive medicine*, vol. 46, no. 4, pp. 331–335, 2008.

[20] S. A. Bowman, S. L. Gortmaker, C. B. Ebbeling, M. A. Pereira, and D. S. Ludwig, "Effects of fast-food consumption on energy intake and diet quality among children in a national household survey," *Pediatrics*, vol. 113, no. 1, pp. 112–118, 2004.

[21] J. Wardle, M. Jarvis, N. Steggles, S. Sutton, S. Williamson, H. Farrimond, M. Cartwright, and A. Simon, "Socioeconomic disparities in cancer-risk behaviors in adolescence: baseline results from the health and behaviour in teenagers study (habits)," *Preventive medicine*, vol. 36, no. 6, pp. 721–730, 2003.

[22] R. E. Mazur, G. S. Marquis, and H. H. Jensen, "Diet and food insufficiency among hispanic youths: acculturation and socioeconomic factors in the third

national health and nutrition examination survey," *The American journal of clinical nutrition*, vol. 78, no. 6, pp. 1120–1127, 2003.

[23] D. T. Levy, P. L. Mabry, Y. C. Wang, S. Gortmaker, T.-K. Huang, T. Marsh, M. Moodie, and B. Swinburn, "Simulation models of obesity: a review of the literature and implications for research and policy," *Obesity reviews*, vol. 12, no. 5, pp. 378–394, 2011.

[24] S. Fallah-Fini, H. Rahmandad, T. T.-K. Huang, R. M. Bures, and T. A. Glass, "Modeling us adult obesity trends: a system dynamics model for estimating energy imbalance gap," *American journal of public health*, vol. 104, no. 7, pp. 1230–1239, 2014.

[25] D. T. Finegood, T. D. Merth, and H. Rutter, "Implications of the foresight obesity system map for solutions to childhood obesity," *Obesity*, vol. 18, no. S1, pp. S13–S16, 2010.

[26] P. J. Salsberry and P. B. Reagan, "Dynamics of early childhood overweight," *Pediatrics*, vol. 116, no. 6, pp. 1329–1338, 2005.

[27] L. Jódar, F. J. Santonja, and G. González-Parra, "Modeling dynamics of infant obesity in the region of valencia, spain," *Computers & Mathematics with Applications*, vol. 56, no. 3, pp. 679–689, 2008.

[28] R. M. Axelrod, *The complexity of cooperation: Agent-based models of competition and collaboration.* Princeton University Press, 1997.

[29] E. Bonabeau, "Agent-based modeling: Methods and techniques for simulating human systems," *Proceedings of the National Academy of Sciences*, vol. 99, no. suppl 3, pp. 7280–7287, 2002.

[30] M. W. Macy and R. Willer, "From factors to actors: Computational sociology and agent-based modeling," *Annual review of sociology*, pp. 143–166, 2002.

[31] J. M. Epstein and R. Axtell, *Growing artificial societies: social science from the bottom up.* Brookings Institution Press, 1996.

[32] J. M. Epstein, *Generative social science: Studies in agent-based computational modeling.* Princeton University Press, 2006.

[33] L. Tesfatsion, "Agent-based computational economics: A constructive approach to economic theory," *Handbook of computational economics*, vol. 2, pp. 831–880, 2006.

[34] D. G. Brown and D. T. Robinson, "Effects of heterogeneity in residential preferences on an agent-based model of urban sprawl," *Ecology and society*, vol. 11, no. 1, p. 46, 2006.

[35] P. M. Torrens, "Simulating sprawl," *Annals of the Association of American Geographers*, vol. 96, no. 2, pp. 248–275, 2006.

[36] A. H. Auchincloss and A. V. D. Roux, "A new tool for epidemiology: the usefulness of dynamic-agent models in understanding place effects on health," *American journal of epidemiology*, vol. 168, no. 1, pp. 1–8, 2008.

[37] K. L. Edwards and G. P. Clarke, "The design and validation of a spatial microsimulation model of obesogenic environments for children in leeds, uk: Simobesity," *Social science & medicine*, vol. 69, no. 7, pp. 1127–1134, 2009.

[38] M. J. Widener, S. S. Metcalf, and Y. Bar-Yam, "Agent-based modeling of policies to improve urban food access for low-income populations," *Applied Geography*, vol. 40, pp. 1–10, 2013.

[39] U. Wilensky, "{NetLogo}," 1999.

[40] R. J. Kuczmarski, C. L. Ogden, S. S. Guo, L. M. Grummer-Strawn, K. M. Flegal, Z. Mei, R. Wei, L. R. Curtin, A. F. Roche, and C. L. Johnson, "2000 cdc growth charts for the united states: methods and development." *Vital and health statistics. Series 11, Data from the national health survey*, no. 246, pp. 1–190, 2002.

[41] J. Gittelsohn, E. A. Steeves, Y. Mui, A. Y. Kharmats, L. C. Hopkins, and D. Dennis, "Bmore healthy communities for kids: design of a multi-level intervention for obesity prevention for low-income african american children," *BMC Public Health*, vol. 14, no. 1, p. 1, 2014.

[42] K. M. Christiansen, F. Qureshi, A. Schaible, S. Park, and J. Gittelsohn, "Environmental factors that impact the eating behaviors of low-income african american adolescents in baltimore city," *Journal of nutrition education and behavior*, vol. 45, no. 6, pp. 652–660, 2013.

[43] S. H. Lee-Kwan, S. Goedkoop, R. Yong, B. Batorsky, V. Hoffman, J. Jeffries, M. Hamouda, and J. Gittelsohn, "Development and implementation of the baltimore healthy carry-outs feasibility trial: process evaluation results," *BMC Public Health*, vol. 13, no. 1, p. 1, 2013.

[44] N. Budd, A. Cuccia, J. K. Jeffries, D. Prasad, K. D. Frick, L. Powell, F. A. Katz, and J. Gittelsohn, "Bmore healthy: retail rewards-design of a multi-level communications and pricing intervention to improve the food environment in baltimore city," *BMC public health*, vol. 15, no. 1, p. 1, 2015.

[45] M. Franco, A. V. D. Roux, T. A. Glass, B. Caballero, and F. L. Brancati, "Neighborhood characteristics and availability of healthy foods in baltimore," *American journal of preventive medicine*, vol. 35, no. 6, pp. 561–567, 2008.

[46] N. F. Butte, E. Christiansen, and T. I. Sørensen, "Energy imbalance underlying the development of childhood obesity," *Obesity*, vol. 15, no. 12, pp. 3056–3066, 2007.

[47] J. Rose, J. G. Gamble, J. Lee, R. Lee, and W. L. Haskell, "The energy expenditure index: a method to quantitate and compare walking energy expenditure

for children and adolescents." *Journal of Pediatric Orthopaedics*, vol. 11, no. 5, pp. 571–hyhen, 1991.

[48] S. Dai, D. R. Labarthe, J. A. Grunbaum, R. B. Harrist, and W. H. Mueller, "Longitudinal analysis of changes in indices of obesity from age 8 years to age 18 years project heartbeat!" *American journal of epidemiology*, vol. 156, no. 8, pp. 720–729, 2002.

[49] A. Borshchev and A. Filippov, "From system dynamics and discrete event to practical agent based modeling: reasons, techniques, tools," in *Proceedings of the 22nd international conference of the system dynamics society*, vol. 22. Citeseer, 2004.

[50] J. C. Butcher, *The numerical analysis of ordinary differential equations: Runge-Kutta and general linear methods.* Wiley-Interscience, 1987.

[51] J. Aitchison and J. A. C. Brown, *The lognormal distribution.* CUP Archive, 1976, vol. 5.

[52] O. N. Keene, "The log transformation is special," *Statistics in medicine*, vol. 14, no. 8, pp. 811–819, 1995.

[53] D. Hinkley, "On quick choice of power transformation," *Applied Statistics*, pp. 67–69, 1977.

[54] G. Box and D. Cox, "An analysis of transformations revisited, rebutted." DTIC Document, Tech. Rep., 1981.

[55] R. Sakia, "The box-cox transformation technique: a review," *The statistician*, pp. 169–178, 1992.

[56] B. Meessen, A. Soucat, and C. Sekabaraga, "Performance-based financing: just a donor fad or a catalyst towards comprehensive health-care reform?" *Bulletin of the World Health Organization*, vol. 89, no. 2, pp. 153–156, 2011.

[57] A. D. Oxman and A. Fretheim, "Can paying for results help to achieve the millennium development goals? overview of the effectiveness of results-based financing," *Journal of Evidence-Based Medicine*, vol. 2, no. 2, pp. 70–83, 2009.

[58] L. A. Petersen, L. D. Woodard, T. Urech, C. Daw, and S. Sookanan, "Does pay-for-performance improve the quality of health care?" *Annals of internal medicine*, vol. 145, no. 4, pp. 265–272, 2006.

[59] F. Eijkenaar, "Pay for performance in health care: an international overview of initiatives," *Medical Care Research and Review*, p. 1077558711432891, 2012.

[60] J. Brad Schwartz and I. Bhushan, "Improving immunization equity through a public-private partnership in cambodia," *Bulletin of the World Health Organization*, vol. 82, no. 9, pp. 661–667, 2004.

[61] P. Basinga, P. J. Gertler, A. Binagwaho, A. L. Soucat, J. Sturdy, and C. M.

Vermeersch, “Effect on maternal and child health services in rwanda of payment to primary health-care providers for performance: an impact evaluation,” *The Lancet*, vol. 377, no. 9775, pp. 1421–1428, 2011.

[62] R. Eichler and R. Levine, *Performance incentives for global health: potential and pitfalls.* CGD Books, 2009.

[63] F. Ssengooba, B. McPake, and N. Palmer, “Why performance-based contracting failed in uganda–an open-box evaluation of a complex health system intervention,” *Social science & medicine*, vol. 75, no. 2, pp. 377–383, 2012.

[64] O. Alonge, S. Gupta, C. Engineer, A. S. Salehi, and D. H. Peters, “Assessing the pro-poor effect of different contracting schemes for health services on health facilities in rural afghanistan,” *Health policy and planning*, p. czu127, 2014.

[65] T. A. Belay *et al.*, “Building on early gains in afghanistan’s health, nutrition, and population sector: challenges and options,” *World Bank Publications*, 2010.

[66] C. Y. Engineer, E. Dale, A. Agarwal, A. Agarwal, O. Alonge, A. Edward, S. Gupta, H. B. Schuh, G. Burnham, and D. H. Peters, “Effectiveness of a pay-for-performance intervention to improve maternal and child health services in afghanistan: a cluster-randomized trial,” *International journal of epidemiology*, p. dyv362, 2016.

[67] D. H. Peters, A. A. Noor, L. P. Singh, F. K. Kakar, P. M. Hansen, and G. Burn-

ham, “A balanced scorecard for health services in afghanistan,” *Bulletin of the World Health Organization*, vol. 85, no. 2, pp. 146–151, 2007.

[68] E. Dale, “Performance-based payments, provider motivation and quality of care in afghanistan,” Ph.D. dissertation, 2014.

[69] M. Gagné and E. L. Deci, “Self-determination theory and work motivation,” *Journal of Organizational behavior*, vol. 26, no. 4, pp. 331–362, 2005.

[70] E. L. Deci and R. M. Ryan, “l9: Self-determination research: Reflections and future directions,” *Handbook of self-determination research*, p. 431, 2002.

[71] P. Glasziou, H. Buchan, C. D. Mar, J. Doust, M. Harris, R. Knight, A. Scott, I. A. Scott, and A. Stockwell, “When financial incentives do more good than harm: a checklist,” *Bmj*, vol. 5047, pp. 345–350, 2012.

[72] S. Woolhandler, D. Ariely, and D. U. Himmelstein, “Why pay for performance may be incompatible with quality improvement,” *Bmj*, vol. 345, no. 7870, p. e5015, 2012.

[73] C. F. Camerer, R. M. Hogarth, D. V. Budescu, and C. Eckel, “The effects of financial incentives in experiments: A review and capital-labor-production framework,” in *Elicitation of Preferences*. Springer, 1999, pp. 7–48.

[74] H. Patrick and T. A. Nicklas, “A review of family and social determinants of

childrens eating patterns and diet quality," *Journal of the American College of Nutrition*, vol. 24, no. 2, pp. 83–92, 2005.

[75] C. C. Jacques, J. McIntosh, S. Giovinazzi, T. D. Kirsch, T. Wilson, and J. Mitrani-Reiser, "Resilience of the canterbury hospital system to the 2011 christchurch earthquake," *Earthquake Spectra*, vol. 30, no. 1, pp. 533–554, 2014.

[76] N. Mimura, K. Yasuhara, S. Kawagoe, H. Yokoki, and S. Kazama, "Damage from the great east japan earthquake and tsunami-a quick report," *Mitigation and Adaptation Strategies for Global Change*, vol. 16, no. 7, pp. 803–818, 2011.

[77] B. Efron and R. Tibshirani, "An introduction to the bootstrap. chapman & hall/crc," 1998.

[78] P. A. G. A. Committee *et al.*, "Physical activity guidelines advisory committee report, 2008," *Washington, DC: US Department of Health and Human Services*, vol. 2008, pp. A1–H14, 2008.

[79] J. L. Gastwirth, "The estimation of the lorenz curve and gini index," *The Review of Economics and Statistics*, pp. 306–316, 1972.

# Vita

Sen Lin was born on April 1, 1989 in Liaocheng, China. In 2010, he received his Bachelor degree on Mechanical Engineering from Southwest Jiaotong University in China. After graduation he went to Changchun Institute of Optics, Fine Mechanics and Physics (CIOMP), Chinese Academy of Sciences. In CIOMP he studied the design and optimization of micro-electro-mechanical system. In August 2012, Sen Lin moved to Johns Hopkins University to purse a PhD degree in Civil Engineering. At first he joined Prof. James Guests group and worked on topology optimization, designed the best fluid diode using topology optimization. In 2014 he was switched to Prof. Tak Igusas group working on system science and its applications in the field of public health. To facilitate his research, Sen enrolled in several courses in the Department of Computer Science, which eventually led to a master degree. After graduation Sen will be working as a software engineer in California.